

RCA REVIEW

a technical journal

RADIO AND ELECTRONICS
RESEARCH • ENGINEERING

VOLUME XVII

SEPTEMBER 1956

NO. 3

RADIO CORPORATION OF AMERICA

DAVID SARNOFF, *Chairman of the Board*

FRANK M. FOLSOM, *President*

E. W. ENGSTROM, *Senior Executive Vice-President*

JOHN Q. CANNON, *Secretary*

ERNEST B. GORIN, *Vice-President and Treasurer*

RCA LABORATORIES

D. H. EWING, *Vice-President*

RCA REVIEW

C. C. FOSTER, *Manager*

C. H. VOSE, *Business Manager*

PRINTED IN U.S.A.

RCA REVIEW, published quarterly in March, June, September, and December by RCA Laboratories, Radio Corporation of America, Princeton, New Jersey. Entered as second class matter July 3, 1950 at the Post Office at Princeton, New Jersey, under the act of March 3, 1879. Subscription price in the United States and Canada; one year \$2.00, two years \$3.50, three years \$4.50; in other countries: one year \$2.40, two years \$4.30, three years \$5.70. Single copies in the United States, \$.75; in other countries, \$.85.

RCA REVIEW

a technical journal

RADIO AND ELECTRONICS
RESEARCH • ENGINEERING

Published quarterly by

RCA LABORATORIES

in cooperation with all subsidiaries and divisions of

RADIO CORPORATION OF AMERICA

VOLUME XVII

SEPTEMBER, 1956

NUMBER 3

CONTENTS

	PAGE
High-Resolution Flying-Spot Scanner for Graphic Arts Color Applications	313
L. SHAPIRO AND H. E. HAYNES	
A Magnetic Tape System for Recording and Reproducing Standard FCC Color Television Signals	330
H. F. OLSON, W. D. HOUGHTON, A. R. MORGAN, M. ARTZT, J. A. ZENEL, AND J. G. WOODWARD	
Fields In Imperfect Electromagnetic Anechoic Chambers	393
R. F. KOLAR	
Performance and Design of Low-Noise Guns for Traveling-Wave Tubes	410
R. C. KNECHTLI AND W. R. BEAM	
Image Orthicon for Pickup at Low Light Levels	425
A. A. ROTOW	
RCA TECHNICAL PAPERS	436
AUTHORS	438

© 1956 by Radio Corporation of America
All rights reserved

RCA REVIEW is regularly abstracted and indexed by *Industrial Arts Index Science Abstracts (I.E.E.-Brit.)*, *Electronic Engineering Master Index*, *Chemical Abstracts*, *Proc. I.R.E.*, and *Wireless Engineer*.

RCA REVIEW

BOARD OF EDITORS

Chairman

R. S. HOLMES
RCA Laboratories

M. C. BATSEL
Defense Electronic Products

G. L. BEERS
Radio Corporation of America

H. H. BEVERAGE
RCA Laboratories

G. H. BROWN
RCA Laboratories

I. F. BYRNES
Radiomarine Corporation of America

D. D. COLE
RCA Victor Television Division

O. E. DUNLAP, JR.
Radio Corporation of America

E. W. ENGSTROM
Radio Corporation of America

D. H. EWING
RCA Laboratories

A. N. GOLDSMITH
Consulting Engineer, RCA

A. L. HAMMERSCHMIDT
National Broadcasting Company, Inc.

O. B. HANSON
Radio Corporation of America

E. W. HEROLD
RCA Laboratories

C. B. JOLLIFFE
Radio Corporation of America

E. A. LAPORT
Radio Corporation of America

C. W. LATIMER
RCA Communications, Inc.

H. W. LEVERENZ
RCA Laboratories

G. F. MAEDEL
RCA Institutes, Inc.

H. B. MARTIN
Radiomarine Corporation of America

H. F. OLSON
RCA Laboratories

D. S. RAU
RCA Communications, Inc.

D. F. SCHMIT
Radio Corporation of America

S. W. SEELEY
RCA Laboratories

G. R. SHAW
Tube Division

L. A. SHOTLIFF
RCA International Division

A. W. VANCE
RCA Laboratories

I. WOLFF
RCA Laboratories

Secretary

C. C. FOSTER
RCA Laboratories

REPUBLICATION AND TRANSLATION

Original papers published herein may be referenced or abstracted without further authorization provided proper notation concerning authors and source is included. All rights of republication, including translation into foreign languages, are reserved by RCA Review. Requests for republication and translation privileges should be addressed to *The Manager*.

HIGH-RESOLUTION FLYING-SPOT SCANNER FOR GRAPHIC ARTS COLOR APPLICATIONS

BY

L. SHAPIRO AND H. E. HAYNES

RCA Commercial Electronic Products,
Camden, N. J.

Summary—There is described a high-resolution, slow-speed scanning and reproducing system developed to serve as input and output devices for an electronic computer which provides color correction in the production of half-tone plates for color printing. In addition to its extremely high resolving power, this system is notable for low image distortion, extreme time stability both geometrically and sensitometrically, uniformity of characteristics in different parts of the field, and precise control of tone rendition. Employing a special 10-inch kinescope, the scanner portion derives input information for the computer by simultaneously scanning three precisely registered color separation plates, requiring 12 minutes for a frame scan. Four images representing the required printing ink tone values (cyan, magenta, yellow, and black) are sequentially recorded photographically from a second identical kinescope. Over-all performance is such that on full-page pictures, prevailing requirements in high-quality magazine printing applications are satisfied.

This paper deals with the scanner and recorder, and includes a description of the equipment and some of the development problems encountered. The system as a whole, and particularly the computer, has been reported elsewhere.^{1,2}

INTRODUCTION

THE flying-spot scanner herein described was developed as part of a color correction project for the graphic arts.^{1,3} This activity involved the development of a system for the production of very-high-quality scanned color-corrected pictures. An abbreviated block diagram is shown in Figure 1 in which incoming information from a set of color separations is sensed by an optical system while computed color-corrected information is recorded in a camera. With a scanning speed of one frame in 12 minutes, three or four such consecutive frames are recorded as required to obtain the various necessary corrected ink pictures (cyan, magenta, yellow, and, where a four color process is

¹ L. Shapiro, "RCA Color Corrector for the Graphic Arts," presented at the Annual Conference of the Professional Group on Industrial Electronics of the Institute of Radio Engineers, Pittsburgh, Pa., September 30, 1954.

² H. E. Rose, "Electronic Computer for Color Printing," *Communications and Electronics*, May, 1955.

³ J. S. Rydz and V. L. Marquart, "Applications of the Neugebauer Equations to Electronic Color Correction," *Proceedings of the Technical Association of the Graphic Arts*, 1955.

used, black). These pictures are subsequently processed for production of final printing plates. A picture of the prototype color corrector is shown in Figure 2.

The above equipment required the development of a flying-spot scanner with the resolution and precision of high-quality graphic arts copy. This objective was substantially achieved.

The scanning system was designed for the simultaneous scanning, in register, of three color separations on glass plates. Desired resolu-

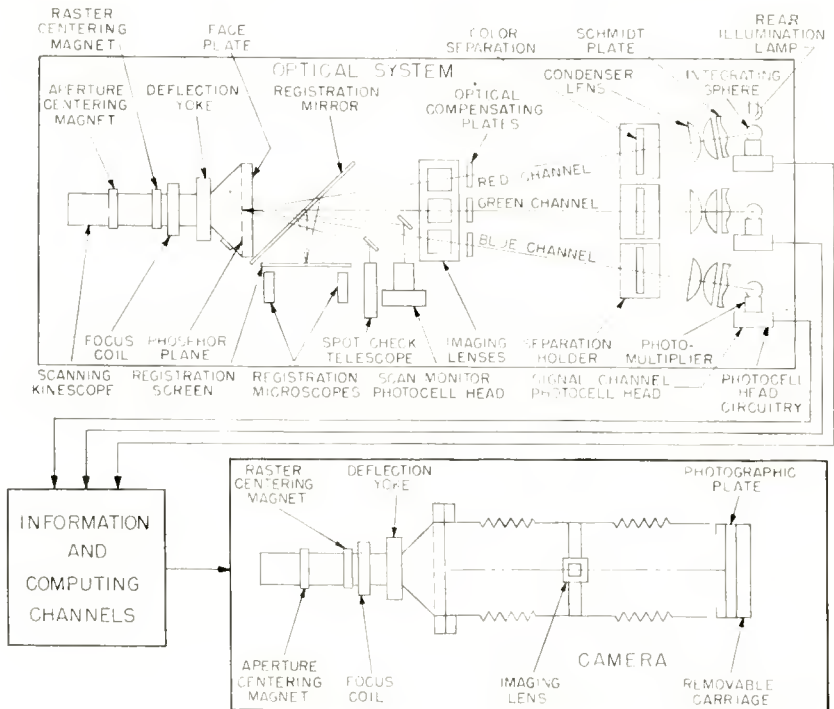


Fig. 1—Scanner-recorder block diagram.

tion was such that the structured image (halftone) process was to remain the limiting factor, this commonly being about 120 lines per inch. With the development of present photocomposing techniques involving the preparation, simultaneously, of several pictures on a single printing plate, as well as the very substantial market for large copy with intricate detail (calendars and maps), the upper limit of usable resolution rapidly reached the most optimistic "state-of-the-art" limitations. In addition, other exacting requirements of the industry

had to be met; smoothness and freedom from blemishes had to be achieved, and over-all geometric distortion produced by the entire scanning and reproducing system had to be very small. Quantitative values for these specifications are discussed below.

Referring again to Figure 1, the raster developed by the 10-inch flying-spot kinescope is imaged in registration by three matched symmetrical 16½-inch Goerz-Artar apochromat lenses on three separations. Transmitted light in each channel is collected by a condenser lens and integrating sphere and applied to the photosensitive surface of its

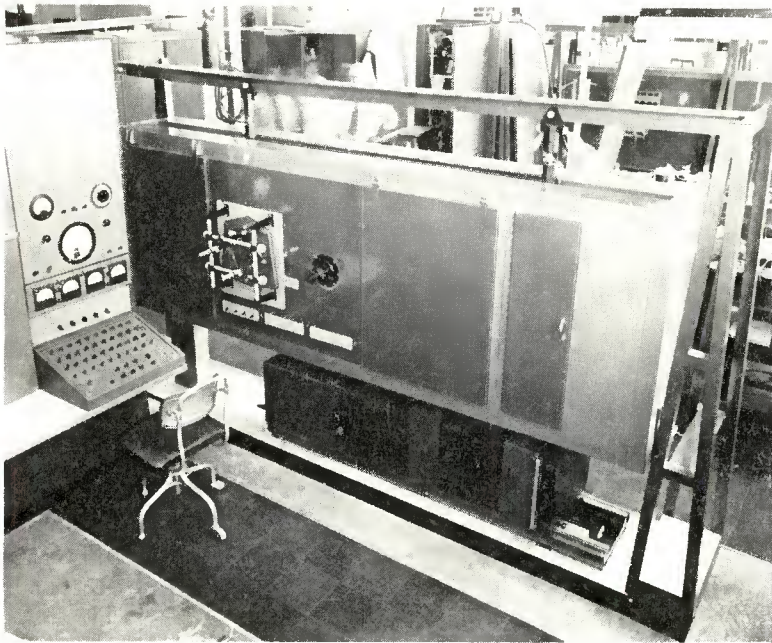


Fig. 2—Color corrector.

associated photomultiplier. Stabilization of scanning-spot intensity is achieved by means of a monitor photocell head and associated circuitry. The spot check telescope is for the purpose of viewing manual positioning of the scanning spot to specified picture areas for static studies. Two registration microscopes permit close adjustment of registration.

The lenses, which operate at unity magnification for the cancellation of geometrical distortion, represent, in accordance with our tests, the highest quality of available lenses for the over-all application. At

the same time, aside from the scanning process itself, they represent the greatest point of signal deterioration in the system. For reasons to be discussed later, the existing configuration, in which only a portion of the ordinarily usable field of each lens is utilized, was chosen. This restriction used up part of the margin in resolution which otherwise would have gone to the kinescope.

Resolution of the lenses was investigated with some care under the above conditions of operation. Based on an on-axis .0002-inch point source, the circle of confusion at $f/9.5$ was found to consist of a central area with a representative visible diameter of .0008 inch containing an estimated 80 per cent of the light and a single halo or first ring with a representative diameter of .0015 inch containing most of the remaining light. An on-axis sine-wave response factor for one of the same lenses (Goerz-Artar #777004) under the same conditions using a variable-density sine wave test film resulted in a value of 79 per cent at 2,000 lines in 5 inches and 62 per cent at 3,000 lines in 5 inches (the raster used is 5×7 inches). The corresponding equivalent passband,¹ N_c , is approximately 2,750.

It is noteworthy to mention composite performance data of the combined kinescope-lens system as taken through the center channel while scanning a bar pattern. Resolution over the major part of the raster area as observed with an oscilloscope at the output of the photocell head is approximately 30 per cent for 1,666 lines in 5 inches. Pictures taken in the camera were more conclusive. In this case, the information channel included two kinescopes and two imaging lenses as well as a very considerable amount of additional optical and electronic equipment. A substantial amount of resolution was obtained over most of the picture area for 1,430 lines* (in all orientations).

Since initial resolution met minimum requirements, neither focus modulation nor aperture correction was used in the prototypes.

DEVELOPMENT OF THE SCANNING MECHANISM

Kinescope

The kinescope for this project was developed by the RCA Tube Division at Lancaster, Pa. After a brief excursion into the double-crossover type of electron optics, the development took the form of continued refinement in design of the single-crossover type. Magnetic

¹ O. H. Schade, "Image Gradation, Graininess and Sharpness in Television and Motion Picture Systems," *J.S.M.P.T.E.*, Vol. 58, pp. 181-222, March, 1952.

* This figure includes, of course, degradation of resolution by the photographic emulsion as well as effects arising from the manner of film processing.

focus and deflection are employed. Particular attention was paid to accurate machining of critical parts in the electron gun and treatment of structures which might be subject to spurious emission. The P-11 phosphor was ball-milled for very small particle aggregate size and settled on the face plate with care to avoid pin holes, yellow spots, and other types of imperfections. The face plate itself was made of high-quality gray glass, one-half inch thick, flat to 20 fringes, and with a tight specification on "seeds," "stones," and opaque spots. Sine-wave aperture response data on these tubes was obtained by several experimental methods. While different approaches gave somewhat different results, as did different tube samples, it is safe to ascribe a typical N_c value of around 1,400 and a limiting resolution of about 5,500 to these tubes. The very low beam current required at the scanning speed involved is a large factor in making this performance possible.

Optical System

The basic optical system (Figure 1) initially utilized a conventional beam splitter to provide three-channel illumination, and dichroic mirrors to provide back illumination via an off-axis incandescent light in each channel. The latter technique is used to provide an image of the separations, either singly or composite, on the faceplate of the kinescope. This image is then viewed by means of the spot check telescope and associated mirror for observation of scanning spot manipulation, or, as will be discussed later, two registration microscopes for separation alignment purposes. Dichroic mirrors originally used allowed rear illumination to take place by designing these mirrors for reflection of an incandescent source while maintaining maximum transmission at the phosphor spectral light distribution.

The extremely efficient geometric integrating properties of the human eye, however, mitigated against attainment of satisfactory performance by the above system. The conventional beam splitter operates on the principle of simultaneous transmission and reflection at certain surfaces. Precision requirements necessitated use of stable, optically flat components throughout. For practical reasons, therefore, the beam splitter had to be made of thick glass plates. All transmitted light rays eventually met a glass-air interface on attempting to emerge from this glass plate. Residual reflection occurring at this latter interface resulted in the appearance of a spurious scanning spot in one of the channels. In actual practice, two of the three separations were finally scanned with one or more such spots. The net effect was to cause spurious displaced images or "ghosts" to appear on the final recorded picture.

A quantitative "ghost" specification is readily obtained. With the accepted minimum discernible density difference (for contiguous regions) of the human eye of .01 and a transmission ratio of 25:1, the minimum discernible transmission difference is .09 per cent.*

Since various density juxtapositions are possible such as a light ghost on a dark background or vice versa, it is necessary to consider the above requirement which, in the general case, would result in a minimum discernible ghost.

An extended investigation of the capabilities of known low reflectance coatings under conditions of field angles and spectral illumination encountered here led to the conclusion that the conventional type of beam splitter could not be used. As a result, the three-lens configuration of Figure 1 was developed. This system is inherently "ghost" free, but does not fully utilize the available field of any one of the imaging lenses.

Use of the dichroic mirrors brought to light another problem. Here, no "ghost" problem existed since the scanning spot had already passed through the separations. It is recalled, however, that the resulting modulation of the light in each channel (by passage through its respective separation) represents a particular tristimulus value such as red, green, or blue. From these values, the color correction equipment eventually computes the required percentages of colored printing inks to reproduce the original colors. An important point in color balance is the white end setup whereby proper tristimulus values are inserted into the equipment to maintain a correct gray scale throughout the neutral axis in the color solid. Once this adjustment has been made for any particular test point in the picture, it must hold for all parts of the raster. Very small spurious deviations of tristimulus values will displace this axis and insert color into an area where it does not belong. The human eye is extremely sensitive to such effects, especially at the "white" end of the gray scale. A small error in a tristimulus value may cause a complete color reversal in a pastel shade. In this connection, it is once again recalled that the color corrector was developed for graphic arts applications where the judgment and experience of art critics are applied to its pictures.

Dichroic mirrors were found to be too nonuniform in transmission-reflection characteristics to maintain required accuracy of information handling over their operating area—a requirement complicated by field angles involved. The optical system, therefore, was modified to provide rear illumination by physical movement of members. The present

* This value follows from the formula $D = \log (1/T)$ or $.01 = \log (1/1.023)$ and $.023/25 = .09$ per cent.

method is based on a swivel mechanism which rotates either photomultiplier or incandescent light into position as required.

Solution of the above problem focussed attention on the photomultipliers since here a similar problem arose on account of the nonuniform sensitivity over the photosensitive surface of these devices.⁵ During scanning, conditions were such that a "walking hot spot" operated over this photosensitive surface. The problem was attacked in two stages. First, integrating spheres were installed with the objective in mind that only the total amount of light flux entering the sphere, and not its space distribution, should influence the phototube output. Design limitations and efficiency requirements, however, made this method only partially successful; the problem was again reviewed.

Basic optical design is such as to image the aperture of the imaging lens on the photomultiplier photocathode. This procedure, theoretically, results in a stationary spot of essentially uniform intensity distribution on the photocathode. Such a mode of operation theoretically bypasses the nonuniform sensitivity problem. However, spherical aberration in the large condenser lenses* was causing spot movement as the raster was scanned—an inevitable situation with a simple-lens approach to the condenser problem.

An aspheric Schmidt-type corrector plate capable of removing spherical aberration from the condensers was designed and installed in each condenser-lens assembly. Integrating spheres are being retained for the time being, however, although indications are that accurate alignment of the condenser optics makes use of the integrating spheres unnecessary.

Operation of the optical system still revealed certain residual raster illumination variations. These nonuniformities could be ascribed to the following causes:

1. Differential "cosine fourth" effects in each channel and the inability of a single kinescope feedback loop to correct all channels simultaneously.
2. Limitations on the positioning of the light-sampling device of the above feedback loop. This device had to be placed somewhere before the separations to avoid confusing the feedback loop with picture information.

⁵ H. Edels and W. A. Gambling, "Spatial Variations of the Spectral Response of Photomultiplier Cathodes," *Jour. Sci. Instr.*, Vol. 31, p. 121, April, 1954.

* The condenser-lens assembly is based on two Bausch & Lomb 10½-inch diameter, 15-inch focal length lenses.

3. Possible mechanical tolerances and other problems in positioning the light sampling device which risked favoring one portion of the raster as against another.
4. Differential light absorption properties within each channel for different parts of the raster. A major offender in this respect is the condenser lens in which the scanning spot passes through four inches of glass at the center of the raster and only one-half inch at the edge.* The actual final illumination pattern was strongly suggestive of this latter condition.

Masking techniques were needed for correction of this final geometric illumination pattern. An investigation of photographic techniques resulted in development of a satisfactory optical mask incorporated in the condenser-lens Schmidt plate assembly.

Control of Intensity of Scanning Spot

For the reasons enumerated below, continuous control of scanning-spot intensity was found to be necessary:

1. Temperature variations affecting critical spacing in the kinescope electron gun, together with a rather long effective thermal time constant, result in major beam-current changes at fixed electrode voltages. The required high accuracy of information handling makes a "free running" spot intensity impracticable.
2. Normal electrical drifts are sufficient to cause significant changes in spot intensity. Maintenance of the minimum discernible density level (.01) indicates a required stability of approximately 1 volt at the 25-kilovolt level and 10 millivolts at the cathode or grid of the kinescope.
3. Phosphor variations such as graininess (actually aggregates of phosphor crystals), wedging, and discrete imperfections are significant.
4. Certain optical "cosine fourth" effects are significant.

Two methods were developed to stabilize the light intensity of the scanning spot. The first of these methods involved an all-electronic feedback loop which sampled the kinescope cathode current as a measure of light output. This method was capable of handling drifts due to items 1 and 2. It could not, however, handle light variations due to variations in phosphor efficiency, nor could it compensate for

* It is noted that the scanning spot (developed by the P-11 phosphor) is peaked at about 4600 angstroms—a wavelength region where glass absorption becomes appreciable.

purely optical effects. A second method was therefore developed involving an electro-optical feedback loop complete with monitoring photocell and light sampling device. This method was more powerful in that, in addition to items 1 and 2, it could compensate for 3 (except for actual pin holes), and it could compensate for a good deal of 4, depending upon the nature and location of the light sampling device.

The foregoing considerations pointed to the selection of the electro-optical feedback approach for use in the color correction prototypes. A schematic of the scanning system is shown in Figure 3. The light-intensity adjustment is made with 8R1. Phase-shifting network 8C2 and 8R9 compensates primarily for equivalent effects occurring at the phosphor plane due to finite light build-up and decay time. As viewed with an oscilloscope at the output of the monitoring photocell head, insertion of the feedback loop reduces the phosphor graininess signal by a factor of approximately 20, rendering it entirely invisible on the recorded picture.

Certain effects remained, however. The present kinescope face plates, while made of gray glass, are not coated. As a result, flare or spot "skirt" is appreciable. This flare pattern is a composite of the typical concentric ring type associated with the critical angle of reflection mechanism and a continuous distribution extending out from the spot proper.⁶ The first halo, which is $2\frac{3}{8}$ inches in diameter, encloses substantially the entire continuous skirt. Two additional halos are also visible.* A study of system performance, however, has indicated no appreciable effect on picture quality due to this condition.

Notes on Operation

One important aspect of operation still needed attention, however. Broadly speaking, it was the desirability of preserving the energy in the scanning spot as a small discrete bundle which sampled only the transmission characteristic of the picture element being scanned at the moment and then activated the photomultipliers to the exclusion of all spurious light sources. An important step in this direction was the elimination of spurious light paths. The interior of the optical system was coated with optical black and baffles were placed between adjacent channels. Light-tightness of the enclosure was ensured by installation of multiple light traps at all openings. Internal spurious sources were eliminated by adequate light shielding of thermionic tubes.

⁶ For a discussion of flare mechanisms, see F. J. Studer and D. A. Cusano, "Transparent Phosphor Coatings," *Jour. Opt. Soc. Amer.*, Vol. 45, pp. 493-494, July, 1955.

* This data was taken by exposing a photographic plate to a stationary spot for 12 minutes.

Of importance, too, was the very practical matter of optical defects and dirt. They could be classified either as permanent, such as defects in the kinescope faceplate or dust sealed into the condenser-lens assembly, or as removable, such as dust which rapidly collected on the kinescope faceplate due to electrostatic attraction. A further classification could be made in terms of the proximity of such dirt to a focal plane. For example, dirt particles on the kinescope faceplate and the condenser-lens assembly imaged directly on the final picture since, essentially, they modulated the scanning spot as picture information. In certain important cases, such dirt would defeat the purpose of the monitoring photocell heads by distinguishing between the optical transmission

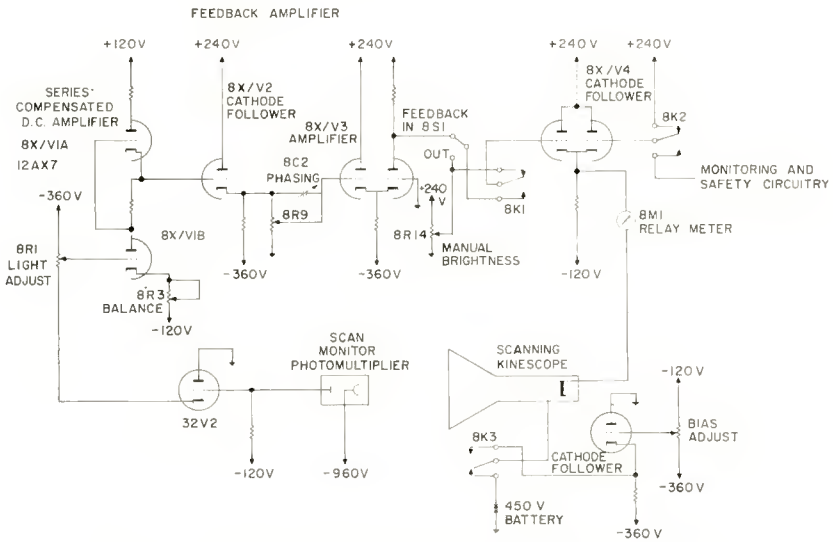


Fig. 3—Simplified scanning spot intensity control system.

axis of monitoring channel as against the axis of the signal channel. A speck of dirt on the kinescope faceplate would then cause its compensating burst of light to be displaced geometrically causing a peculiar double shadow for each such particle.

Dirt appearing at nonfocussed points in the optical system would cause no defined images, per se, but would contribute to unequal raster illumination and light scattering. Thus, the battle against dirt was one which, when waged constantly, paid dividends in affording continuous and reliable operation.

Registration and Physical Considerations

Registration is based on a three-point system. This method utilizes

a separation holder containing three accurately machined steel positioning pins against which the separation is spring loaded. Basic design is of the precision necessary to approach repeatable registration by registering plate holders rather than separations. With a registration specification of half a spot diameter (one thousandth of an inch) it is possible to register a new set of separations in 10 to 15 minutes.

Referring to Figure 1, registration is accomplished by insertion of a registration mirror into the optics at a point where all three channels converge. Back illumination lamps then image the separations onto a registration screen. Focal planes of the three aerial images are aligned to be coplanar with a grid pattern on this screen. Two registration microscopes are initially adjusted to facilitate rapid reiteration between two widely separated registration marks. All parts of the picture are checked, however, before registration is considered completed. Movement of imaging lenses and separation holders is accomplished by pushbutton operated motors in such a manner that various degrees of freedom (rotational and lateral) are decoupled. Details of the optical system are shown in Figures 4 and 5.

Physically, the optical system is based on a series of massive aluminum castings accurately positioned on four rigid steel rails. This structure inherently possesses a degree of thermal compensation.

A three-point suspension technique is employed for support of the entire optical system. The structure is suspended from two points overhead while a snubber stabilizes the system from below. All three points of support are heavily damped. The sheer weight of the suspended structure provides excellent protection from higher frequency vibration or shock components.

Extraction of Picture Information

Extraction of picture information from the optical system required design of an ultrastable photocell head with a frequency response extending from d-c to 15 kilocycles. Stability requirements here were more severe than anywhere else in the system. Whereas small drifts in scanning spot intensity would, to a first approximation, cause drifts along the neutral axis of the color solid, differential photocell head drifts would immediately insert color into a neutral region. Extensive investigation of simple cathode-follower operation following the 5819 photomultiplier, for example, indicated a cathode-follower instability unacceptable by a factor of about ten. The circuit finally chosen for this application is the three-stage feedback amplifier shown in Figure 6. Standard receiving-type tubes were used. C-1 and C-2 are phasing condensers and the output signal, at high voltage level, is developed across R-1.

An initial uneasiness about the gain stability of the photomultipliers proved to be unjustified. With maximum output current in the 1 or 2 microampere range, operation was below fatigue levels. No direct check was made on gain stability, but over-all system performance indicated that, except for occasional poor tubes, stability was maintained to at least better than 1 per cent and possibly was of the order of 1/10 of 1 per cent. It did prove suitable, however, to remove or redesign subsequent signal stages which might be upset by noise bursts.

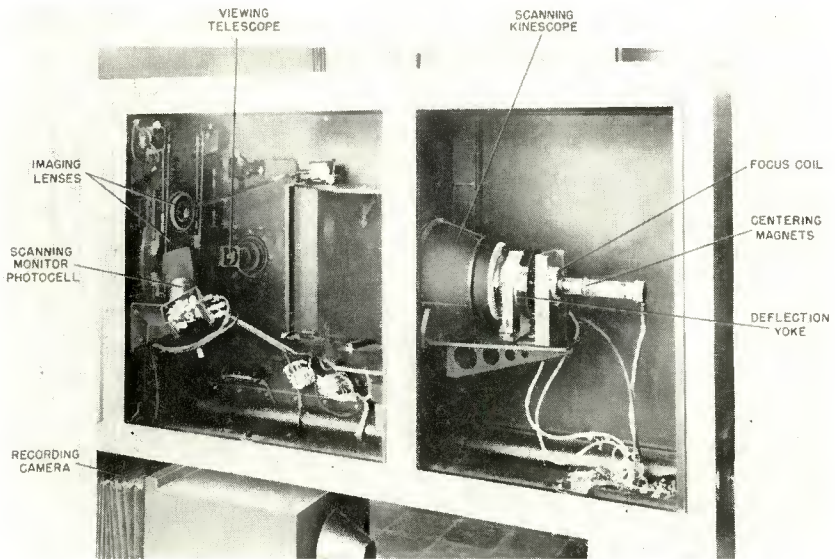


Fig. 4—Front end of optical enclosure, panels removed.

DEFLECTION SYSTEM

General Requirements

Development of an adequate deflection system constituted one of the major lines of endeavor of this project. The over-all raster-deflection requirement may be stated as follows:

$$\int_{\Delta t} \int_{\Delta s} L ds dt = K \quad (1)$$

where Δs is the nominal picture-element area (constant throughout the raster), Δt is the time of light emission for the particular picture element, and L is the light intensity. It is noted that this relationship

is, to a first approximation, that required to produce a uniform exposure density on the photographic plate in the camera. The constant-density photographic condition is met exactly if (as seen by the photographic

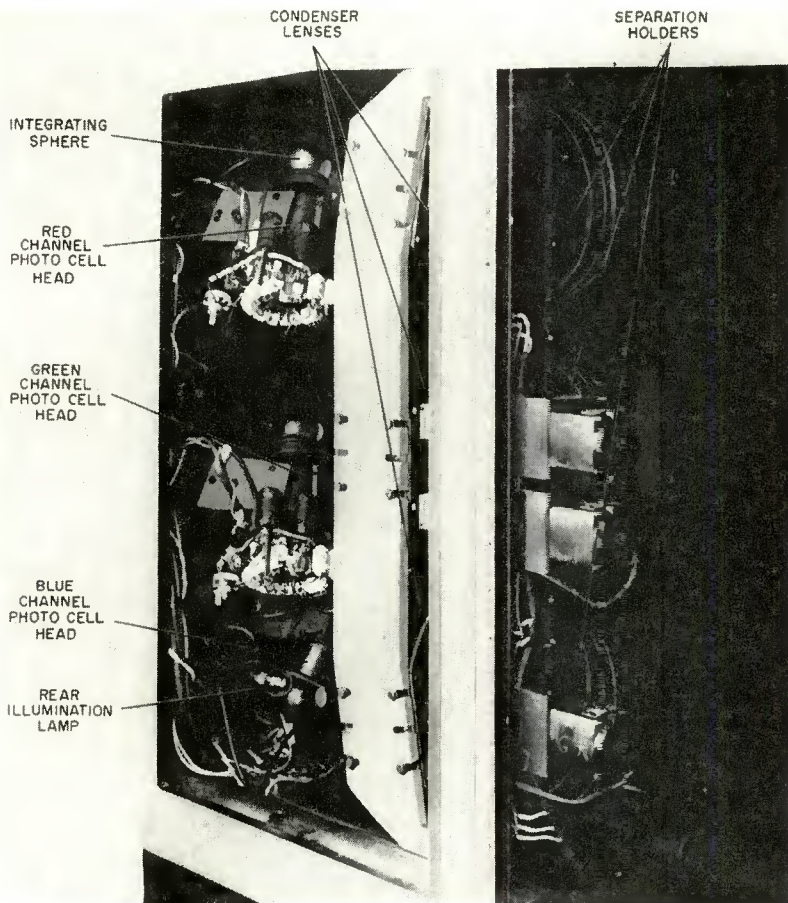


Fig. 5—Rear end of optical enclosure, panels removed.

emulsion) L and Δt are also constant everywhere on the raster.

With suitable line spacing,* these conditions would produce an almost continuous-tone plate, especially at higher light levels where the photographic "toe" is exceeded for a larger spot area.

In terms of a scanning-pattern relationship, Equation (1) would

* Rasters of from 2,500 to 3,000 scanning lines have been used, values in this range having been found to render the line structure substantially invisible. This agrees closely with a rule given by Schade that $N_e = 0.53 n_r$, N_e being the equivalent passband represented by the kinescope spot and n_r the number of scanning lines. Taking $N_e = 1,400$ as indicated previously for the tubes used, a value of $n_r = 2,700$ is derived.

be satisfied by the systematic exploration of the picture by a scanning spot of constant light intensity which moved along a path where line spacing and spot velocity were everywhere constant. More strictly, there must be a complete absence of velocity modulation. However, use of a spot of constant intensity may be considered as a convenient but not necessary condition. For example, a pincushion raster with appropriate spot-intensity modulation would also satisfy Equation (1).

Quantitative requirements for the establishment of adequate specifications were based on two factors:

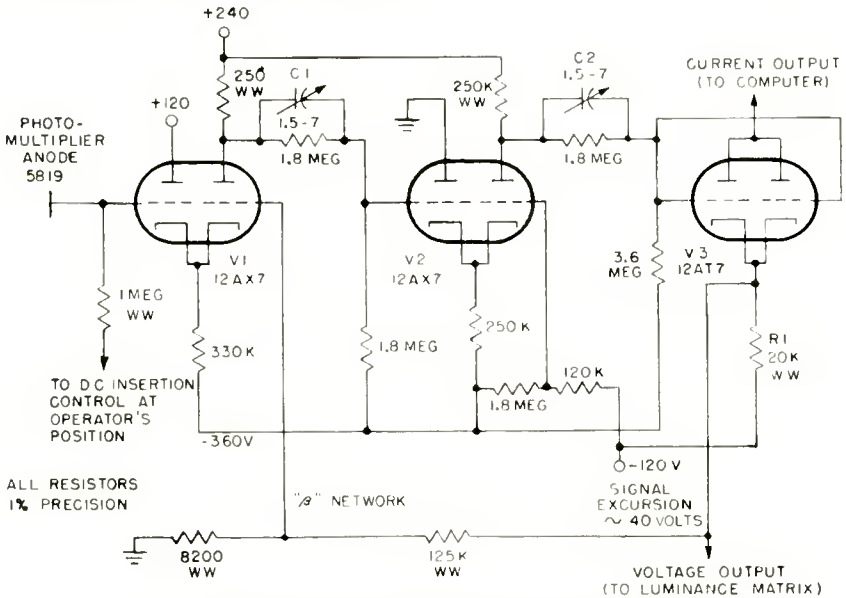


Fig. 6—Channel photocell head (condensed).

1. The extraordinary sensitivity of the human eye to geometrically correlated density-variation patterns.
2. Resultant colorimetric repercussions when color-corrected information is degraded by errors in picture densities.

Effects of item 1, above, were instantly recognizable on the output pictures. Effects of item 2, however, were not usually obviously noticeable until actual proofing took place—a process rather expensive in time and money. Density distortions of this latter nature were revealed, however, by sensitometric measurements.

Engineering effort first gravitated to removal of raster imperfections associated with item 1, since this requirement was in the nature of a *sine qua non*.

Review of the basic raster requirement of Equation (1) indicated that over-all permissible variation in K was that which would be recorded as less than a .01 density difference geometric pattern.* As previously indicated, this set an outer limit of less than .1 per cent transmission value on such variations. Since a spot of substantially constant intensity was generally used, this reduced the scanning pattern to a matter of precise line spacing and very uniform spot movement. Easiest of attainment was the spot of constant intensity. Use of feedback methods together with effective noise suppression, stable circuitry, and power supplies readily provided such a spot.

Velocity modulation was quite another matter, representing a problem in testing as well as in design. Since, for certain reasons of over-all stability, the horizontal repetition rate was synchronized with the 60-cycle power frequency (at a 17:1 ratio), velocity modulation at this frequency appeared as vertical striations across the picture. However, this venetian-blind effect proved amenable to sustained conventional clean-up techniques. Vertical deflection was more difficult. Here, very small circuit movements, such as resulted from normal thermal drifts, wreaked havoc with the picture. A single misplaced line, such as that due to a noise pulse, gave a horizontal streak. With approximately 2,500 lines over a deflection coil voltage swing of 120 volts, this meant a line for each 50 millivolts of deflection. Permissible displacement before appearance of a visible streak was not quantitatively measured. Computation for a .01 density difference streak visibility is, of course, contingent on some assumed light distribution. Experience indicated that individual line spacing variations must be held to approximately 5 or 10 per cent. Required precision, then, is of the order of a few millivolts, or the equivalent line movement that would take place near the raster edge due to a few volts change at the 25-kilovolt ultor voltage.

Circuitry

The vertical deflection circuit is shown in Figure 7. The function generator is comprised of V1-3. V1 is a two-stage constant-current source which develops a positively going voltage at the upper plate of C-1 during the scanning cycle. V1, in turn, secures its plate voltage from V2 which is a constant-phase, unity-gain amplifier, cathode modulated by the deflection signal via cathode follower V3. In this manner, a constant voltage is maintained across the constant current source, V1. R-2 and C-2 are very high precision components developing a half minute time constant which filters the output signal and reduces the

* The definition of a geometric pattern as used here is primarily psychophysical. It is a pattern such as would be seized upon most easily by the recognition mechanism of the brain.

effect of thermal drift of the cathode follower. R-1 adjusts sweep time.

The deflection coil driving circuit consists of V4-7. V6 and V7 comprise a two-stage very high variational impedance source which supplies current either to cathode follower V5 or to the vertical deflection coils depending upon the signal appearing at the grid of V5. In this manner, current in the deflection coils is able to reverse smoothly with no necessity for push-pull or push-push balancing. It may be noted in passing that the six 5687 tubes comprising the cathode follower have a combined g_m of approximately 130,000 micromhos.

The foregoing current amplifier (V5, 6, 7) is driven by V4 which is a balanced bridge type of feedback circuit. The voltage signal

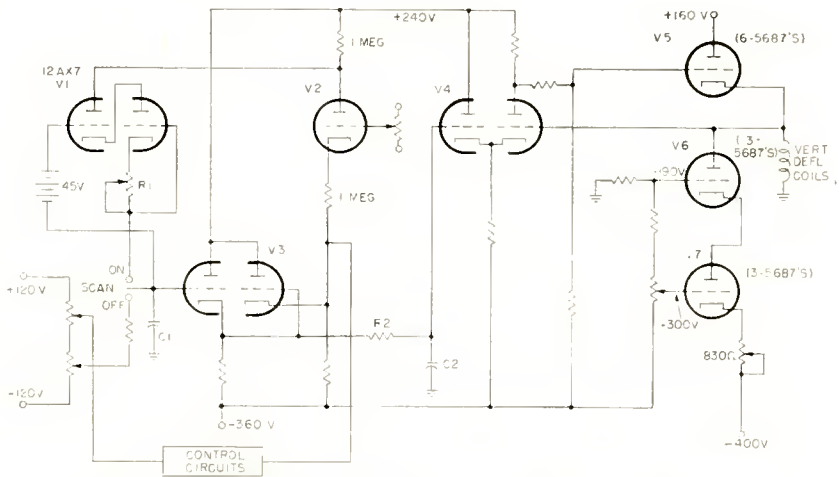


Fig. 7—Simplified schematic of vertical deflection circuit.

appearing at the vertical deflection coils is continuously sampled and compared with the output of the vertical function generator (V1, 2, 3). Any variations produce an error voltage which is then applied to V5 for correction.

The scanning spot must also be capable of being held stationary with great precision. Since illumination and color correction computing are set up at particular picture or test patch areas on the color separations, a "walking" spot would cause difficulty on fine picture detail and, in some cases, for normal emulsion or test patch graininess. As far as possible, a defocused spot is used for averaging effects.

Considerations of Raster Geometry

There are two rasters of importance in the system. The first of these is the actual scanning-line configuration on the recorded plate.

Due to the excellence of the optics, this scanning-line configuration is essentially that developed at the kinescope faceplate. This is the raster that must be free of velocity modulation and which, when unmodulated, must record a photographic plate of constant density.

The second raster is the resultant of the combined scanning and recording rasters. This is the raster which records a scanned geometric pattern with geometric accuracy. Extreme care was taken with this latter raster in order to achieve this condition. In addition to series operation of deflection yokes and focus coils, both yokes and focus coils are of the precision type and positioned with great care. Present performance of this raster on a 5×7 inch test square indicates an accuracy to within $1/64$ inch at all points. Neither raster magnets nor deflection modulation are used, but these methods are being held in abeyance should it prove desirable at some future time to improve this degree of precision.

To maintain resolution of picture detail in the final proof, the set of four successively scanned corrected plates must register with each other to within a fraction of a thousandth of an inch at all points. This condition is achieved by series operation of deflection yokes and focus coils. No discernible misregistration is present.

CONCLUSION

Pictures of graphic arts quality have been produced by the prototype equipment since the Fall of 1954. Recently proofed pictures, in particular, have been quite favorably evaluated by critics within the graphic arts industry. Resolution-wise and smoothness-wise, these pictures are substantially indistinguishable from purely photographically processed products. The blank, or constant density, recording raster is quite uniform to the eye, showing variations over wide areas of only the order of .01 density difference. Except for scanning lines, visible only by microscope, the raster cannot be recognized as the product of a scanning. One of these equipments is now being installed in the plant of a major printing firm for field test and operation.

ACKNOWLEDGMENTS

Acknowledgment is gratefully made to the many individuals who contributed to the successful conclusion of the engineering effort involved. Of particular importance were the contributions of K. E. Andrews in the optical design, J. G. Lee in the mechanical design, and J. S. Rydz in the final stages of performance refinement. Acknowledgment is also made to A. J. Walsh, senior technician, for his invaluable assistance throughout the entire period of development.

A MAGNETIC TAPE SYSTEM FOR RECORDING AND REPRODUCING STANDARD FCC COLOR TELEVISION SIGNALS

BY

HARRY F. OLSON, W. D. HOUGHTON, A. R. MORGAN,
M. ARTZT, J. A. ZENEL, AND J. G. WOODWARD

RCA Laboratories,
Princeton, N. J.

Summary—A system¹ for recording and reproducing television signals by means of magnetic tape was described and demonstrated in December 1953. Developments since that time include: a reduction in tape speed from 30 to 20 feet per second, an increase in resolution by the use of improved heads and the addition of a fifth channel for carrying the combined highs, recording and reproducing a complete composite FCC color signal, an improved servo system for maintaining constant equivalent tape speed in recording and reproducing the television signal. Two systems have been developed for reproducing the audio signal employing two different modulation means, namely, two carrier amplitude modulation, and frequency modulation. The five parts of their paper outline the general principles of a magnetic tape system for recording and reproducing a standard FCC color television signal.

Part I — General Considerations

BY

HARRY F. OLSON

INTRODUCTION

RECORDING AND REPRODUCING BY MEANS OF MAGNETIC TAPE

THE magnetic storage of information has been known for over a half century. However, it is only within the last decade that theories, techniques, and materials have been developed which make it possible to record, store, and reproduce relatively large amounts of information by means of a system employing magnetic tape. The magnetic tape consists of a plastic base coated with a layer of iron oxide, as shown in Figure 1. One of the important characteristics of the magnetic coating is the hysteresis loop of the material shown in Figure 2. B is the magnetic induction in gaussses. H is the magnetizing force in oersteds. The point on the characteristic where $H = 0$ represents the intrinsic coercive force. The point on the characteristic

¹H. F. Olson, W. D. Houghton, A. R. Morgan, J. Zenel, M. Artzt, J. G. Woodward, and J. T. Fischer, "A System for Recording and Reproducing Television Signals," *RCA Review*, Vol. XV, p. 3, March, 1954.

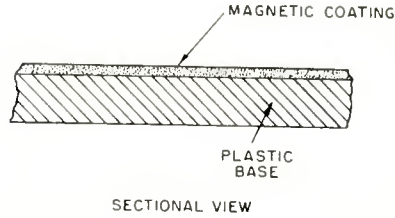


Fig. 1—Sectional view of magnetic recording tape.

where $B - H = 0$ represents the retentivity. The magnetic material used for the coating must exhibit a rectangular type of hysteresis loop in order to provide the magnetic retentivity required to store information in a permanent form. A typical hysteresis loop for the coating on magnetic tape is shown in Figure 2.

The signal is recorded and reproduced from magnetic tape by means of an electromagnetic head, shown schematically in Figure 3. The application of a voltage to the coil of the head leads to the production of a magnetomotive force in the magnetic circuit which in turn magnetizes elements of the tape in proportion to the voltage which is applied. The signal stored on the tape is in the form of a series of longitudinal permanent magnets. In reproduction, the tape is moved past the head. When one of the magnetized portions of the tape passes over the air gap of the head, a magnetic flux is generated in the head which leads to the induction of an electromotive force in the coil.

In any recording and reproducing system, the object is to store as much information as possible. This information may be recorded

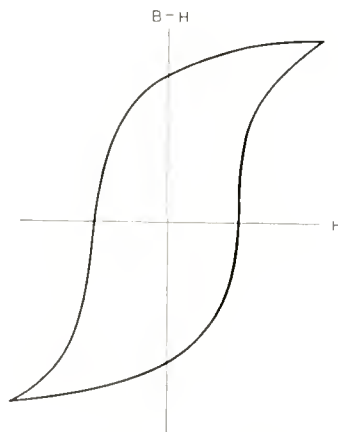


Fig. 2—Typical B-H characteristic of the iron oxide coating on magnetic tape.

and reproduced in many different ways. For example, it may be desirable to record and reproduce with a wide frequency range and a relatively small signal-to-noise ratio. A system with these characteristics would be useful in the recording of television signals. On the other hand, it may be desirable to record with a large ratio of signal-to-noise and a relatively narrow frequency range. A system with these characteristics would be useful for the reproduction of sound. These bandwidth and signal-to-noise considerations may be illustrated by the use of the generalized recording and reproducing systems shown in Figure 4. The recording system consists of an information source, which contains both signal and noise, and a recorder which adds noise when the record is recorded. The reproducing system consists of the record which contains both signal and noise, the reproducer which adds noise to the signal when it is reproduced, and the information receiver or

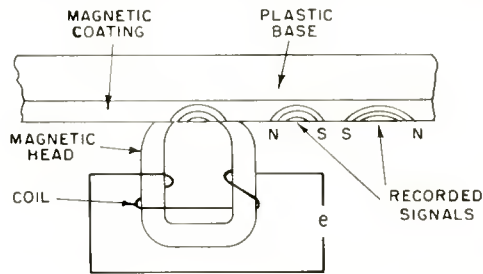


Fig. 3—Diagram depicting the magnetic tape recording and reproducing process.

ultimate destination of the information. The quantity of information² which may be transmitted can be expressed by

$$Q = Bt \log \left(1 + \frac{p}{N} \right) \quad (1)$$

where Q = quantity of information,
 t = time of transmission,
 B = frequency bandwidth,
 p = signal power, and
 N = noise power.

From Equation (1), it will be seen that bandwidth, time, and signal-to-noise are interdependent. From data relating to signal and noise

²C. E. Shannon and W. Weaver, *The Mathematical Theory of Communication*, University of Illinois Press, 1949.

obtained in the audio frequency band, it appeared that the recording of television signals would be possible. Development work on new forms of magnetic recording and reproducing heads proved that signals having the bandwidth required for television could be recorded and reproduced. Closely allied with this development of the heads, an over-all system for the recording and reproducing of television signals from magnetic tape was developed. This development culminated in a system for recording and reproducing television signals in both color and black-and-white. This system was demonstrated to the public in December, 1953.

THE SYSTEM

The original system employed a simultaneous color recording and

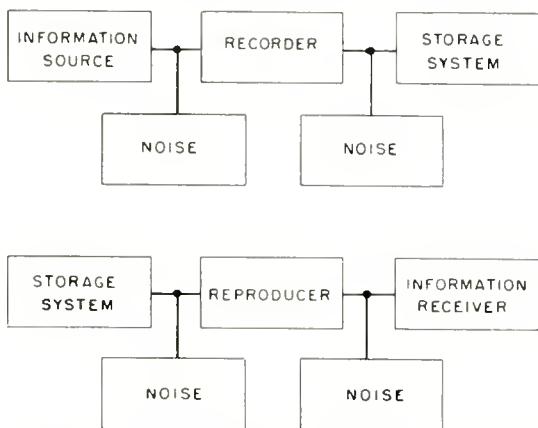


Fig. 4—Diagram of a generalized recording and reproducing system consisting of a recording section and a reproducing section.

reproducing system. The development since that time has included work directed primarily towards recording and reproducing a composite color signal. Magnetic tape systems, for recording and reproducing color television signals are shown in Figures 5 and 6 respectively. A photograph of the complete system is shown in Figure 7. A photograph of the tape transport mechanism and magnetic head system is shown in Figure 8.

Referring to the recording system of Figure 5, it will be seen that the composite color signal is decoded into the green, red, and blue video signals and the synchronizing signal. The red, blue, and green video signals are recorded with bandwidth of 1.5 megacycles in three separate channels. The combined high-frequency video channel containing the combined high-frequency responses of the red, blue, and green

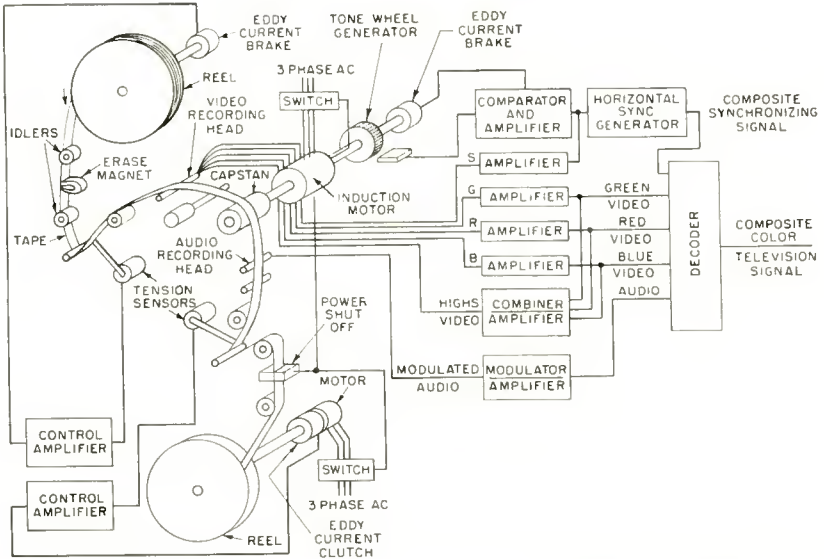


Fig. 5—Schematic arrangement of the apparatus for recording standard FCC color television signals.

video signals from 1.5 to 3.5 megacycles is recorded in a fourth channel. The horizontal synchronizing signal is recorded on a fifth channel. The signals in these channels are recorded on the tape by means of a quintuplet head. The sound is recorded on two amplitude-modulated carriers at about 80 and 150 kilocycles. The sound has also been re-

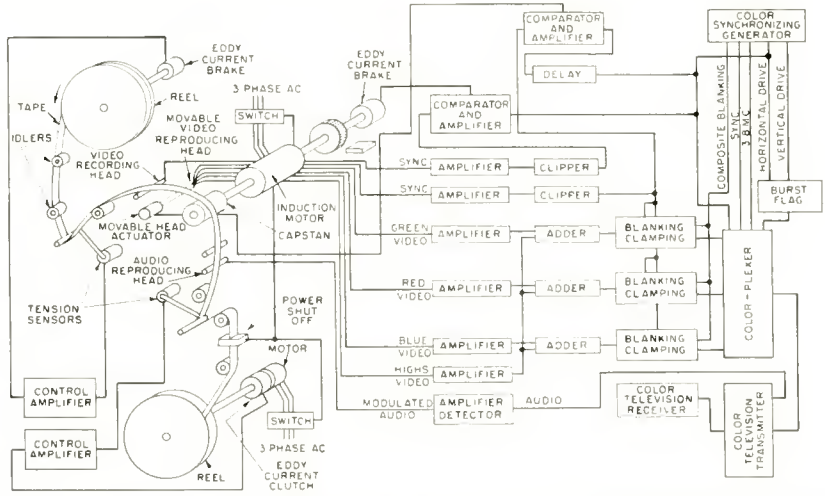


Fig. 6—Schematic arrangement of the apparatus for reproducing standard FCC color television signals.

corded on a frequency-modulated carrier at 90 kilocycles. Thus, it will be seen that the complete television signal is recorded by means of six channels on seven magnetic tracks on the tape. The rotational speed of the capstan is maintained at constant value in recording by means of a servo system consisting of a tone wheel alternator, eddy current brake, horizontal drive generator, electronic comparator, and amplifier. The tone wheel signal is compared with the horizontal synchronizing

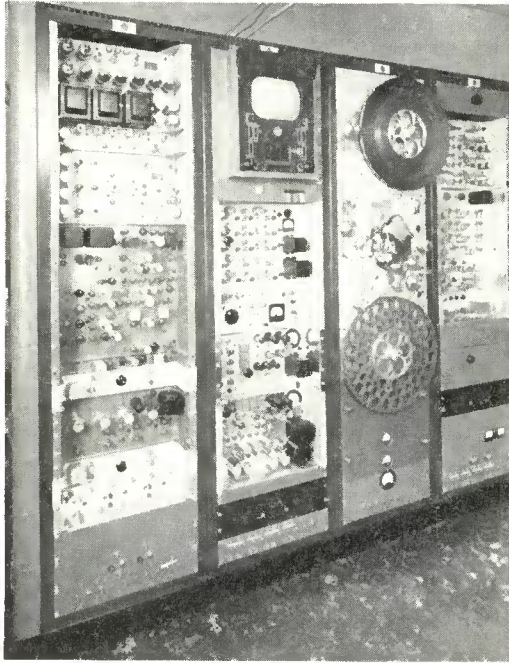


Fig. 7—Complete video recording and reproducing system. From left to right the racks contain the following: #1—Decoding and encoding equipment. #2—Line monitor, video recording equalizer, audio recorder, and velocity servo control equipment. #3—Tape transport equipment (recording and reproducing amplifiers in panel below upper tape reel). #4—Blanking inserter, video reproducing amplifiers, sync amplifiers and audio reproducing equipment.

signal from the local synchronizing generator and the difference between these two signals is applied to an induction brake. If the phase of the tone wheel output leads or lags the horizontal synchronizing signal, the braking will be decreased or increased until the two signals are in phase. In this manner, constant angular speed of the capstan is maintained in recording within the accuracy of the servo and the machined parts. As a result, the speed of the tape at the capstan will be constant within the same limits. To insure constant tape tension

required to maintain constant speed and pressure of the tape on the heads, electronic servo systems are used in the driving system of the supply and take-up reels. The take-up reel employs an electronic system, sensor, and motor-clutch drive which maintains constant tension in the tape to the take-up reel. The supply reel employs an electronic system, sensor and eddy current brake which provides a constant tension in the tape from the supply reel.

The system for reproducing the television signals recorded on the tape is shown in Figure 6. The red, blue, and green video signals, the combined high-frequency video signals, and the horizontal synchronizing signal are reproduced by the movable reproducing head. The

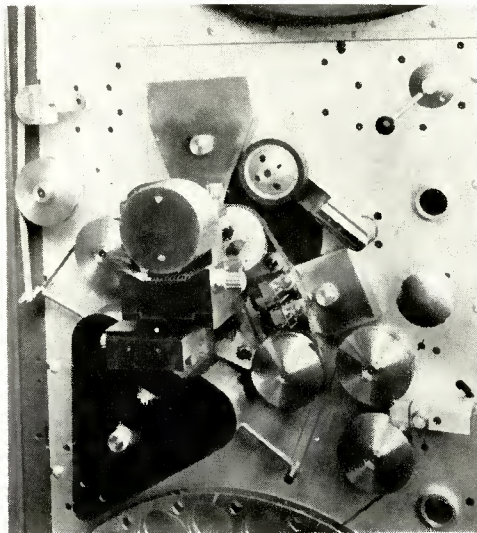


Fig. 8—Close-up view of the tape transport mechanism and magnetic head systems.

horizontal synchronizing signal is also reproduced by the fixed recording head. The reproduced synchronizing signal is amplified and compared with the local horizontal synchronizing signal obtained from a signal generator. The difference between these two signals is fed to the brake. If the phase of the tape output leads or lags the horizontal drive obtained from the local signal generator, the braking will be decreased or increased until the two signals are in phase. In this manner there is maintained a constant phase relationship between the horizontal synchronizing signal obtained from the tape and the horizontal synchronizing signal obtained from the local synchronizing generator within the accuracy of the electronic and servo systems. Since the mass

of the motor system is relatively large, it is difficult to maintain a constant phase relationship with the accuracy required. A deviation is manifested as a jitter of the picture since the synchronizing signal from the synchronizing generator is used as the synchronizing signal. Variation of the phase relationship between the horizontal synchronizing signal from the tape and the horizontal synchronizing signal from the local signal generator is reduced by means of a movable head. Since the video signals are also obtained from the same head, these signals will also be corrected with respect to phase. The output of the horizontal synchronizing signal from the tape is compared with the horizontal synchronizing signal from the local synchronizing generator and the difference applied to the movable head. The movable head acts to reduce the phase difference to a minimum. The red, blue, green, and combined high video signals reproduced by the magnetic head are amplified and fed to separate blanking amplifiers. Clamping amplifiers are employed to maintain the low-frequency response. The combined high-frequency video signal output is mixed with the red, blue, and green video signals. These are fed to the colorplexer where the composite television signal is produced. The horizontal and vertical synchronizing signals and color burst signals are obtained from the local generator. Since the phase of the video signals are maintained exceedingly accurately with respect to the local synchronizing signals, blanking and the insertion of new synchronizing signals are possible. Thus, the composite color television signal meets the FCC specifications. In reproduction, the modulated carrier signals carrying the audio information are demodulated and an audio signal corresponding to the original audio signal is thereby recovered.

The remainder of the paper provides detailed information on the components of the complete system. This system has been on field test at the National Broadcasting Company, New York, N. Y., since April, 1955.

To demonstrate that the system could record and reproduce a standard FCC color television signal, the following test was made. In connection with the dedication of the new Research Center of the Minnesota Mining and Manufacturing Company, three programs were recorded on magnetic tape several days preceding the dedication. On May 12 and 13, 1955, the programs were reproduced at the National Broadcasting Company in New York and transmitted by microwave circuits of the American Telephone and Telegraph Company to a television transmitter at St. Paul, Minnesota. The output of the transmitter was picked up and reproduced on standard color-television receivers in the auditorium of the new Research Center. This was the

first time that a television program recorded on magnetic tape had been reproduced and sent over a complete chain of standard television facilities.

In this connection, television programs originating in California and other remote parts have been recorded in New York and reproduced at some later time.

The performance of the system as described in the remainder of the paper represents a good average. It does not, however, represent the ultimate possibilities of performance with this type of equipment. For example, under controlled conditions, usable signals well over 4 megacycles have been recorded and reproduced, audio systems having a signal-to-noise ratio of 60 decibels and imperceptible distortion may be realized, and practically noise-free conditions have been obtained with some magnetic tapes.

Part II — Electronic System

BY

W. D. HOUGHTON

INTRODUCTION

THIS part concerns the electronic portion of the color television tape system that is presently undergoing field testing at the National Broadcasting Company in New York City.

In order to provide a background for the information which follows, reference is first made to the simultaneous color tape system that was publically demonstrated in 1953.¹ As it was demonstrated, this system operated with a tape speed of 30 feet per second and four minutes of program were recorded on each 17-inch reel of tape. The color information was recorded in the form of three simultaneous video signals representing the red, green, and blue color components. These video signals, together with the composite synchronizing pulses, were recorded on four separate tracks on the tape by a special, four-element video recording head. The audio was recorded on a fifth track by a separate audio unit designed for the higher tape speed.

In the reproducing portion of the system, the four signals from the video reproducing head were coupled to special processing amplifiers. These amplifiers corrected the signals so as to re-create the 3 wide-band color components. The corrected signals, from the processing amplifiers, were then coupled to the video and sync inputs of simultaneous viewing units for demonstration purposes.

REQUIREMENT FOR FCC COLOR SIGNAL

Although the 1953 demonstrations were proof that magnetic tape could be used as a storage medium for both black-and-white and color television signals, several problems still remained. The most important of these was the production of a composite color signal suitable for distribution by commercial facilities.

As a first observation, it would seem that having once produced the simultaneous color components, it would be a relatively simple task to produce a composite color signal. However, further investigation reveals that more is required than merely connecting the separate color signals to the inputs of a standard color television encoder. The reason for this is that a color encoder also requires a color carrier, a burst flag, horizontal drive, and composite synchronizing pulses. Furthermore, the resulting composite color signal must meet the specifications set up by the FCC.³ These standards require that the color carrier and sync signals must bear an interlaced relation and that the carrier must meet the requirements of a 10-cycle frequency stability with a rate of change of frequency no greater than 1/10 cycle per second per second.

Present color television systems meet these requirements because the timing of all signals including the simultaneous video is under the direct control of a common color synchronizing generator.

THE TAPE VELOCITY PRINCIPLE

When a color synchronizing generator is used as the timing unit in a video tape system, a time lock must be maintained between the video signals reproduced from the tape and the synchronizing pulses from the sync generator. In the present system this is accomplished by a servo control unit which operates to vary the tape velocity in a manner such that the vertical and horizontal blanking periods in the reproduced tape signals coincide with the vertical and horizontal pulses from the color synchronizing generator.

Since the tape transport mechanism is the subject of Part III, it will not be discussed in great detail here. However, some of its characteristics will be given to show how it fits into the operation of the complete system.

The transport mechanism performs two basic operations. The first is that of maintaining constant tape velocity during the recording operation so that the video signals are properly recorded on the tape. The second is that of controlling tape velocity during reproduction so as to maintain an essentially fixed time relation between the sync reproduced from the tape and the sync from the color sync generator.

³ "Final Color Television Decision, adopted December 17, 1953," *Television Digest*, December 17, 1953.

Since the sync is recorded with a fixed time difference relative to the picture information, the video components are reproduced as phase-locked signals relative to the sync generator pulses. This arrangement permits the use of standard color processing equipment and also permits the video tape system to be used in conjunction with other commercial color television apparatus. Furthermore, normal video operating techniques such as fading, super imposition and lap dissolve can be employed.

The use of standard color encoding equipment insures the production of a composite color signal that meets the interlace and stability requirements stipulated by the FCC. Any undesired variations in the tape velocity cannot affect the color saturation, hue, or burst stability. Instead, they will result only in a horizontal movement of the reproduced picture within the scanning raster. When these variations are kept small, and at a relatively low frequency, the resulting picture movement becomes comparable to that observed in present film reproductions.

In the present equipment, when the vertical and equalizing pulses are recorded on the same track with the horizontal sync, they tend to interfere with the operation of the servo control unit. Therefore, presently, only the horizontal pulses are recorded on the sync track, and vertical framing is made as a manual adjustment. After the vertical framing is established, the picture remains automatically framed by the action of the servo control unit. This is described in detail in Part III.

THE MAGNETIC ELEMENTS

The record and reproduce heads, including their construction, operation, biasing, and frequency response are described in detail in Part IV. However, some of the characteristics obtained at tape speeds of 20 feet per second will be given to show the operation of the system. These are: the maximum undistorted low-frequency output is obtained with a d-c bias current of approximately 2.5 milliamperes; the maximum high-frequency output is obtained when the recording bias current is reduced to less than 0.5 milliampere; the maximum output over the video band is obtained when the record signal current is maintained essentially constant with frequency and the bias current is raised as an approximate inverse function with frequency. With a constant signal current input of 1 milliampere, and a constant d-c bias of 2 milliamperes, the maximum output occurs in the frequency range between 70 and 150 kilocycles. For these conditions, the output at 1.5 megacycles is approximately 40 decibels below the maximum and the 400-cycle output is down approximately 35 decibels. When the d-c bias is reduced to less than 0.5 milliampere, the 1.5-megacycle

output rises to approximately 17 decibels below the maximum output value.

This indicates that a bias of 2 milliamperes will result in a usable frequency range extending from approximately 400 cycles to 1.5 megacycles, and a bias of less than .5 milliampere is required for the frequency range above 1.5 megacycles.

HIGH-FREQUENCY CHANNEL

The condition of different bias values for the maximum signal output in the two frequency ranges was combined with the "mixed highs"⁴ principle of color television to provide an increase in the storage time on a reel of tape.

In color television systems it is common practice to mix the high-frequency portions of the separate color signals to form what has become known as the mixed-highs component. This technique has been incorporated in the color tape system by recording the mixed highs on a separate track on the tape by an additional element in the recording head. This element is then supplied a lower value of bias current than that required by elements used to record the low-frequency components. This results in an increase in the high-frequency signal-to-noise output in the over-all system.

Because the 1953 demonstration equipment operated at tape speeds of 30 feet per second, a satisfactory signal-to-noise could be obtained by using a compromise value of bias current to record the signals on a full wide-band bias, and the complication of adding the additional head elements was avoided. However, in the present equipment where a longer operating time is obtained by reducing the tape velocity, the increase in signal-to-noise becomes appreciable with the use of the additional elements.

In the system as it is now operating, the separate color signals are limited to frequency bands extending to 1.5 megacycles, and the high-frequency channel carries the combined frequencies above 1.5 megacycles.

SYSTEM OPERATION

As shown in the block diagrams of Figures 9 and 10, the complete color tape system operates between single 75-ohm input and output lines. In the recording section, as shown in Figure 9, the composite color signal, from the input feed, is coupled to a decoder unit. This unit recovers the three primary color components, red, green, and blue, together with the composite synchronizing pulses. These signals are then coupled to the recording section where they are applied to the

⁴ A. V. Bedford, "Mixed Highs in Color Television," *Proc I.R.E.*, Vol. 38, p. 1003, September, 1950.

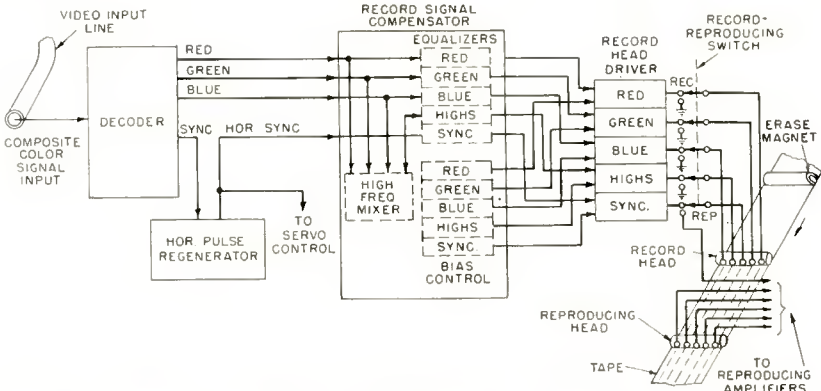


Fig. 9—Diagram showing electronic elements used in recording video signals on magnetic tape.

tape on 5 separate tracks as: low-frequency red, low-frequency blue, low-frequency green, mixed highs, and sync.

As shown in Figure 10, the 5 separate signals are recovered from the tape by a 5-element reproduce head. They are then combined, in the reproducing equipment, to form a composite color signal on the 75-ohm output line.

Parts III, IV, and V describe the operation of each of the various components shown in Figures 9 and 10.

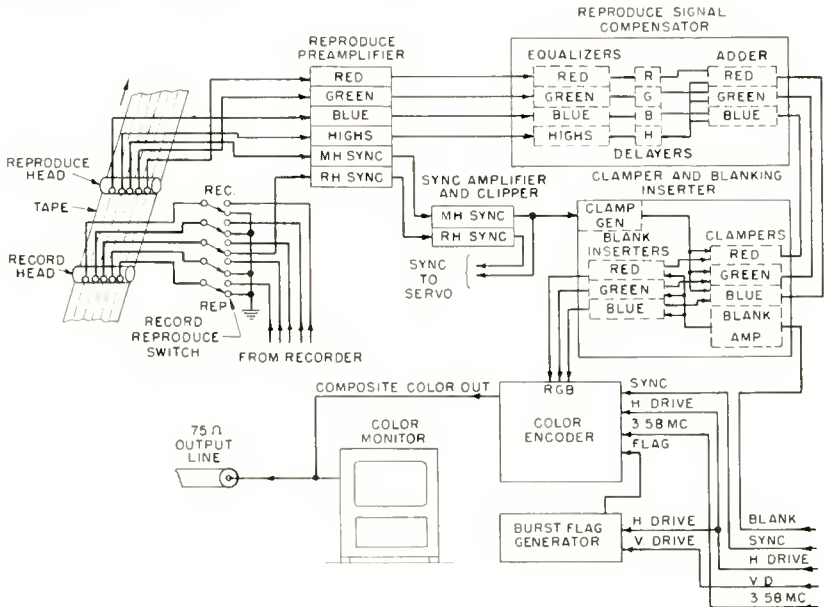


Fig. 10—Diagram showing electronic elements used in reproducing video signals from magnetic tape.

RECORDING SECTION

The block diagram of Figure 9 shows the various elements used during the recording operation.

Decoder

As shown in Figure 9, a composite signal from the video input line is coupled to the decoder. This unit is similar to the video portion of a standard color television receiver. That is, it contains the oscillator, color hold, color detectors, and matrix circuits necessary to recover the red, green, blue, and sync components from the composite color signal. The composite sync is coupled to a horizontal pulse regenerator and the separate color signals are coupled to the video inputs of a signal compensator unit.

Horizontal Pulse Regenerator

The horizontal pulse regenerator is used to separate the horizontal sync information from the composite sync pulse signal. This unit also reduces the effects of any noise which might be introduced by the transmission path between the signal source and the recording equipment.

Basically, the regenerator consists of a highly stable LC reactance-controlled oscillator that is locked to the incoming pulses by conventional automatic-frequency-control circuits. The oscillator drives a series of pulse-forming networks to produce an output pulse which is similar to the horizontal drive pulse from a standard sync generator. This unit also contains a feedback gating network. In operation, this gate network opens shortly before the expected arrival time of a horizontal pulse and closes shortly after the pulse. This action prevents the equalizing pulses and any noise occurring between the horizontal pulses from reaching the phase-detecting networks of the automatic-frequency-control section. The pulse regenerator is used to insure that the best possible sync pulses are recorded on the tape.

Record Signal Compensator

The record signal compensator performs three separate functions, namely, high-frequency mixing, signal processing, and bias control. The high-frequency mixer selects the frequencies above 1.5 megacycles from each of the separate color signals and combines them to form a single high-frequency monochrome signal. The bias control section provides a means for independently controlling the bias in each recording head element. Basically, this section contains 5 separate potentiometers across a bias voltage source and a milliammeter which can be switched to measure the bias current in each record head element.

The equalizers are used to modify the signal so that a maximum of information, with the desired phase characteristic, is recorded on the tape. The four sections, red, green, blue, and sync, are all identical in construction and operate in the frequency range below 1.5 megacycles, while the highs section is built to operate in the frequency band above 1.5 megacycles.

Head Driving Amplifier

The 5 video and 5 bias signals from the recording compensator are coupled to a 5-channel record-head driver unit as shown in Figure 9. The record-head driver is made as a separate unit so that it can be placed in close proximity to the recording head to reduce stray capacitance effects. The 5 amplifiers are made identical in construction and wideband in operation. Each channel contains a single pentode amplifier operating in a circuit designed to provide a high impedance relative to the head element for all frequencies in the video band. With this arrangement, a constant input voltage will result in an essentially constant head current for all frequencies encountered. Each channel also contains a separate RL circuit for adding the d-c bias current to the recording head element. In order to provide wide-band connecting links between the compensator and the driver, 1000-ohm connecting cables are used.

REPRODUCING SYSTEM

As shown in Figure 9, there are three magnetically active elements located along the tape path. The first is an erase magnet which removes any previous recordings by completely saturating the magnetic material on the tape. The second is the 5-element record head which places the information on the tape in the form of 5 parallel tracks. The third is a reproducing head which produces 5 separate output signals in response to the information recorded on the tape. During the recording operation, the reproduce head, and the associated electronic equipment, can be used as a monitor pickup to check the quality of the recording as it is being made.

When tapes are to be reproduced, the erase magnet is physically removed from the tape path and the record-reproduce switch is set to the reproduce position. With the switch in this position, all record-head sections except the sync unit are connected to ground to insure against any undesired recording. As explained later, the sync channel is not grounded because, in delayed playback operation, it is used to reproduce sync pulses for the tape-velocity control equipment.

Reproducing Preamplifier

As shown in Figure 10, the 5 signals from the reproduce head and

the sync signal from the record head are coupled to a 6-channel reproducing amplifier. Since this amplifier must be located close to the reproducing head to keep stray capacitance to a minimum, and the record amplifier must be located close to the record head for the same reason, both units are mounted on the same panel in the tape transport rack. Mounting the amplifiers in the transport rack solves the lead capacitance problem, but at the same time it introduces the additional problems of microphonics due to vibration and feed-through from the record driver to the reproduce preamplifier. The problem of microphonics was solved by shock mounting the preamplifiers and the feed-through was eliminated by extensive shielding of both the circuits and the interconnecting head leads. Each preamplifier channel contains a cascode type wide-band video circuit employing two type 417A triodes. The gain per channel is approximately 24 decibels and the input noise is approximately 15 microvolts.

The 4 video signals from the preamplifier are coupled to the reproducing compensator and the two sync signals are coupled to a two-channel sync amplifier and clipper, as shown in Figure 10.

Reproducing Compensator

The reproducing compensator performs three separate operations. One is the equalization of the red, green, blue, and mixed highs signals. The second is the time positioning of the three color signals. The third is the addition of the high frequencies to each of the separate color signals.

The timing units are actually 3 tapped delay lines inserted between the equalizers and the mixers. These provide a means for correcting the timing errors introduced by slight misalignments of the record and reproduce heads or by unequal phase delays of the different equalizing channels. In operation, the variable delay lines are adjusted to obtain exact registry between the mixed highs and each of the separate color signals.

The time-corrected color signals and the monochrome high-frequency signal are connected to three adding networks as shown. These units merely add the high frequencies to each of the separate color components to form 3 wide-band video signals. The three color signals, from the compensator output are coupled to the inputs of a blanking and clamping inserter as shown in Figure 10.

Clamper and Blanking Inserter

The clamper and blanking inserter performs two separate functions. One is the restoration of low-frequency components by gated clamp networks, and the other is the removal of tape noise and spurious sig-

nals for the time interval during which sync and color burst information is later added by the encoder.

Since the d-c and low-frequency restoration action of gated clamps is a well known video operation,^{5, 6} and it is beyond the scope of this paper to cover the details, it will merely be said that these units are designed to restore frequencies below approximately 400 cycles. The 400-cycle frequency is chosen since it is the lowest frequency where adequate tape signal to amplifier noise is presently obtained. Furthermore, this value is within the restoration range of gated clamp networks. It should be noted that the clamp keying pulses are obtained from the tape instead of from the local color sync generator. This is done to insure against the introduction of false information which might result from any time variations between the clamp pulses and the video signals.

The blanking inserter is used to introduce the sync generator blanking pulses in to the reproduced tape signals. Since the blanking pulses are correctly timed relative to the sync and color burst signals, tape noise and spurious signals will be gated out and, therefore, they will not interfere with the color synchronizing information that is inserted by the encoder.

In normal operation, the blanking does not affect the picture portion of the signal because the transport operates to maintain a coincidence between the blanking periods of the tape signals and the blanking pulses from the color sync generator. Thus, the added blanking merely cleans up the blanking area of the reproduced signals. Any time variations due to changes in tape velocity may cause a slight clipping of the edges of the reproduce picture, but if the variations are small, this effect becomes negligible.

The clamped and blanked signals from the blanking inserter are coupled directly to the simultaneous color camera inputs of a standard color encoder, as shown. The encoder is also fed horizontal drive, 3:58 megacycles, and sync components obtained directly from the station color synchronizing generator. The burst flag signal for the encoder is obtained from a standard burst flag generator which also operates from the sync generator drive pulses.

It can now be seen that with this arrangement the composite color signal produced at the output of the encoder contains color carrier and burst signals which meet the stability requirements set by the FCC. Furthermore, the correct interlace condition is maintained between the sync pulses and the color carrier. Thus, when the com-

⁵ K. R. Wendt, "Television DC Component," *RCA Review*, Vol. IX, p. 85, March, 1948.

⁶ S. Doba and J. W. Rieke, "Clampers in Video Transmission," *Transactions of the A.I.E.E.*, Vol. 69, p. 477, 1950.

posite signal is coupled to a suitable television transmitter, any commercial color receiver can be used to display the reproduced tape pictures. The only defects which the tape system can introduce are: loss in resolution, which may be due to incorrect adjustment or head alignment; slight horizontal picture displacement due to small irregularities in tape velocity; and incorrect color balance due to improper gain settings in the separate reproducing amplifiers. Such difficulties are also encountered in various film systems where separate amplifiers carry the different color signals and mechanical devices move the film.

A video-fed color receiver is used to monitor the signals as they are fed out on a standard 75 ohm video line for normal distribution.

The photograph of Figure 7 shows the four racks of video tape equipment. Counting from left to right: rack 1 contains the decoder, encoder, and horizontal pulse regenerator; rack 2 contain a video line monitor, the video recording compensator, the audio recording equipment, and the transport velocity control apparatus; rack 3 contains the tape transport, the supply and take-up reels, the reel control units, and the record and reproducing amplifiers; rack 4 contains the blanking inserter, the reproducing compensator, the sync clippers, and the audio reproducing equipment. This rack also contains a switch panel which permits switching from tape to direct signals for alignment purposes and a test pulse switch to permit the recording and reproduction of a test pulse for setting up and testing purposes.

Figure 11 shows, from left to right, the input monitor, the power supply rack, the tape rewinding rack, and the output color monitor.

The top chassis shown in Figure 12 is a close-up view of the recording compensator unit. The large knob at the left is the main input gain control. This drives a 3-gang potentiometer to vary the input amplitude of the three color signals. The meter and switch at the right are used to check the bias current in each of the recording head elements. The 5 separate channels are arranged horizontally on the panel. Reading from the top, they are: blue, red, green, highs, and sync. The high gain and low gain knobs, in the center, control the equalization, and the gain knobs at the right provide a means for differentially controlling the record signal amplitudes. The toggle switch labeled "BW-COLOR" is used to tie all color channel inputs together for black-and-white recording. This is also used in the setting up adjustments.

The panel at the top of Figure 12 is the switching panel for the video line monitor and the chassis at the bottom is the audio recording equipment.

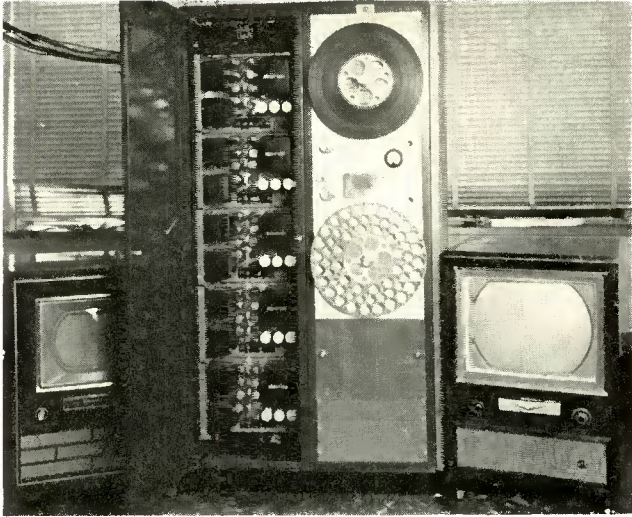


Fig. 11—Left to right—input color monitor, power supply rack, tape re-winder, output color monitor.

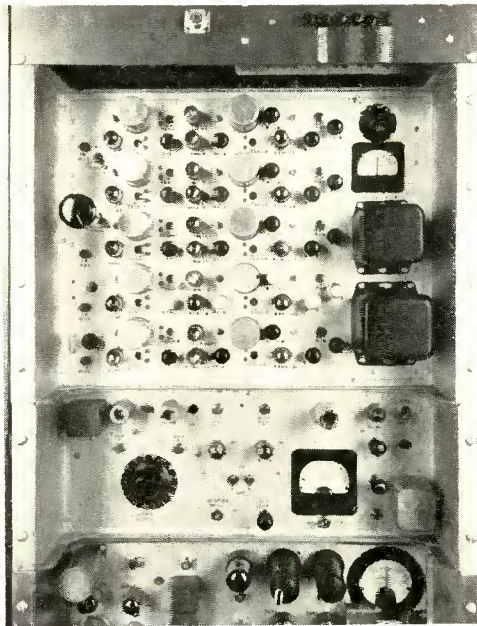


Fig. 12—Top to bottom—line monitor switch panel, recording equalizer, audio recorder, and part of servo control unit.

Figure 13 shows the blanking inserter at the top and the reproducing compensator at the bottom.

The 4 channels, red, green, blue, and highs, are arranged horizontally on the compensator chassis. The 3 large knobs at the top of the compensator chassis control the variable delay circuits. The 4 left-hand knobs are the individual input gain controls. From left to right, the next two knobs in each channel control the low- and high-frequency equalizing. The 4 right-hand knobs are the color balancing and high-frequency adding adjustments.

The large knob at the left in the blanking inserter controls the gain in all channels by means of a ganged potentiometer. The mono-

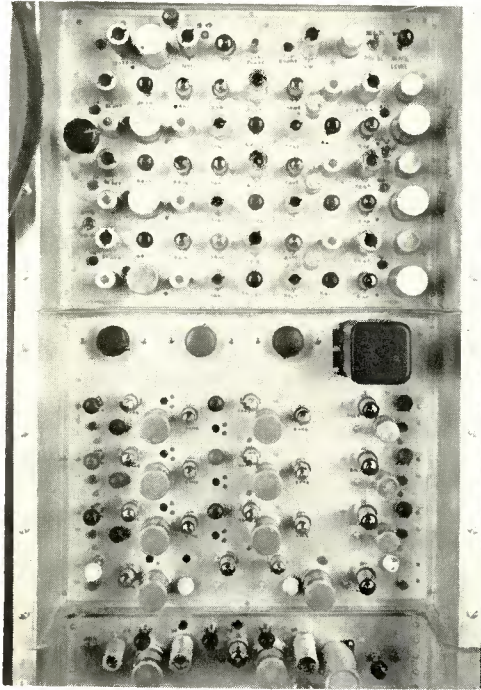


Fig. 13—Top to bottom—blanking inserter, reproduce equalizer, and part of sync pulse amplifier and clipper unit.

color switch at the left ties all inputs together for black-and-white reproduction. This is also used when setting the color balance and background controls in the blanking inserter.

OPERATIONAL CHARACTERISTICS

The foregoing has shown how the various electronic components operate in the system for producing a composite color television signal from the information reproduced from magnetic tape.

A brief outline of some of the operational characteristics of the system follows:

Tape speed is 20 feet per second;

12 to 15 minutes of program, depending upon thickness of tape used, are contained on each 20-inch diameter reel of 1/2-inch tape;

The video amplifying and equalizing unit contains 75 tubes and the blanking inserter unit contains 38 tubes;

Approximately 35 decibels of low-frequency boost and 38 decibels of high-frequency peaking are incorporated in the reproducing equipment;

The average useful head life is approximately 100 hours;

A single tape can be erased and re-used at least 100 times without any perceptible deterioration;

Print-through does not appear to be a problem. Tapes have been stored as long as several months without noticeable print-through;

The total power drain of the complete system is approximately 3 kilowatts;

The total plate current is supplied by five 300-volt regulated power supplies, and two 300-volt units supply the negative bias voltages;

Approximately 15 seconds is required for the start-up and framing operations;

Test patterns with resolution of at least 250 lines can be recorded and reproduced;

Tape breakage does not appear to be a problem. In several months of operation no accidental tape breakages were encountered.

ACKNOWLEDGMENT

The writer wishes to express his appreciation for the assistance of John T. Fischer and Robert E. Morey of RCA Laboratories, and Dudley Goodale, R. A. Lafferty, Lloyd Clark, and John Schroeder of the National Broadcasting Company for their active participation in the development and field testing of this equipment.

Part III—The Tape Transport Mechanism

BY

A. R. MORGAN AND M. ARTZT

Section 1—Tape Velocity Control Servomechanisms

Introduction

IN THE recording and reproduction of television signals on magnetic tape, distortion of the signal can result from irregularities of tape motion during recording and reproduction. This form of

distortion results in an extraneous variation in frequency or phase of the components of the reproduced signal. The distortion is usually observed as extraneous horizontal motion of, or in, the reproduced television picture. If the tape motion irregularities occur at a slow rate, the picture will move as a whole. If the irregularities occur at a rapid rate, the effect is noticed as a waviness within the picture.

This paper outlines the development of a tape transport mechanism with the best performance that available techniques of design and construction will permit.

THE PROBLEM

The specifications for the performance of the transport mechanism must be derived from considerations of the video electronic portion of the system, and the over-all performance that is required. The basic principle of the video electronic system as described in Part II requires a tape motion that will produce a definite time relationship between the reproduced video signals and a local color synchronizing signal. The horizontal and vertical blanking intervals of the reproduced video signal are required to coincide with the horizontal and vertical synchronizing pulses, respectively, in the local color synchronizing signal.

It is evident that the horizontal coincidence is the primary problem for the tape transport mechanism. The horizontal jitter of the reproduced picture is a direct measure of the accuracy of the horizontal coincidence. The vertical coincidence is important, but once established, is maintained by the horizontal coincidence.

It is of interest to estimate the accuracy of coincidence required between the horizontal synchronizing pulses. The inaccuracies of coincidence appear, as stated above, as horizontal displacements in the reproduced picture on the television kinescope.

It would seem natural to compare the performance required of the tape equipment with the performance of commercial photographic motion picture equipment. The 16 millimeter motion picture performance appears to be acceptable in television installations, so the displacements that occur in a 16 millimeter projected picture can serve as an estimate for the performance of the tape transport mechanism. It can be shown^{7, 8} that the effective frame displacement of a 16-millimeter film corresponds to approximately \pm one sixteenth inch in a picture the size of one found on a 21-inch television receiver.

⁷A. C. Robertson, "Dimensions of 16 MM Film in Exchanges," *Jour. S.M.P.T.E.*, Vol. 57, p. 401, November, 1951.

⁸J. G. Streiffert, "The Radial-Tooth, Variable-Pitch Sprocket," *Jour. S.M.P.T.E.*, Vol. 57, p. 529, December, 1951.

This horizontal displacement corresponds to approximately $\pm \frac{1}{5}$ of a microsecond displacement of the reproduced horizontal synchronizing pulses with respect to the station horizontal synchronizing pulses. At a tape speed of 20 feet per second, the specified displacement corresponds to a tape displacement of approximately 50 millionths of an inch. In the language of the sound recording art, the displacement limit would correspond to approximately 0.004 per cent "wow" at a 30-cycle rate. This figure is at least an order of magnitude beyond the accepted performance of professional sound recording and reproducing machines.

Whether or not this variation is acceptable must be determined by subjective observations. There can be no doubt, however, that the problem of controlling the horizontal stability to the degree indicated above is a critical one.

THE APPROACH

Reproducing Tape Transport

Early in the approach to the problem it was realized that the success of the magnetic tape system would depend, in large part, on the horizontal stability of the reproduced picture. It was decided, therefore, to concentrate on the horizontal stability to the near exclusion of the vertical problem. This decision allows the tape transport specification to be restated in terms of the horizontal synchronizing pulses alone. The tape transport mechanism must function to maintain coincidence between the local and the reproduced horizontal synchronizing pulses, as shown in Figure 14.

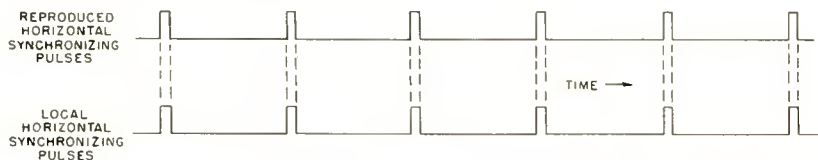


Fig. 14—The necessary relationship between reproduced and local synchronizing signals.

It is important to realize that a constant speed mechanism will not provide the necessary performance. It must be assumed that the recorded tape will contain irregularities that will require a complementary motion of the tape if the reproduced pulses are to have the desired relationship to the station pulses. In other words, the mechanism must be capable of rapid changes in speed. As an example, consider what the mechanism would be required to do with the discontinuity resulting from a haphazard splice made in a previously recorded tape.



Fig. 15—Basic servomechanism.

A servomechanism in which the station synchronizing pulses are the input function and the reproduced synchronizing pulses are the output function would solve the problem. A block diagram for the basic servomechanism is shown in Figure 15. In this arrangement the error detector is a device that delivers a signal proportional to the difference of the input and output functions. For the present problem, the error would be the lack of coincidence between the two sets of synchronizing pulses. The controller includes that portion of the servomechanism which converts the error signal to a force that is used to drive the controlled mechanism. The controlled mechanism is that portion of the system which generates the output function. Here the controlled mechanism is that which transports the tape over the recording and reproducing heads. The basic servomechanism is a feedback arrangement and is, of course, arranged so that the feedback is negative.

The next step is the selection of the components that will combine to make up the servomechanism. A discussion of this process of selection is beyond the scope of this paper. Instead, the final choice of components with the salient reasons for the choice are given.

It was first decided to obtain the power for driving the controlled mechanism directly from the 60-cycle line. This choice obviated the need for a high-power amplifier in the controller. The motor could then best be controlled by means of a variable mechanical load.

With this broad concept, the servomechanism selected for the reproducing operation became as shown in Figure 16. The dotted rectangles indicate the basic division of the servomechanism.

The controlled mechanism is made up with a three-phase induction motor and a directly coupled capstan. The three-phase motor was selected because of its inherent freedom from torque ripple. The controller is a combination of an amplifier and an eddy current brake or

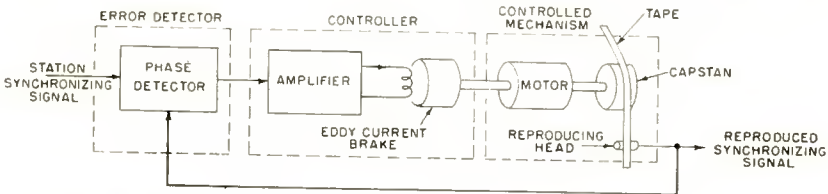


Fig. 16—Practical servomechanism for the reproducing operation.

drag cup. The eddy current brake was selected because it provides a mechanical load that is smooth and rapidly changeable by means of a relatively small electric current. In fact, the ratio of mechanical power absorption to applied electrical power in a representative eddy current brake has been found to be better than 10 to 1. There is no mechanical wear in the eddy current brake so that excellent stability with time can be expected. The amplifier portion of the controller is a direct-current amplifier, and careful attention must be given to drift or extraneous signals generated within the amplifier.

The error detector is required to determine the lack of coincidence between the two synchronizing signals. This type of detector is better known as a phase detector. In the selection of a phase detector, it was decided to apply pulse techniques for the sake of simplicity of construction.

Theoretically, the servomechanism as outlined in Figures 15 and 16 can reduce the error of coincidence between the two synchronizing signals regardless of the cause of the error. The causes of error can be irregularities in tape speed during recording, irregularities introduced during the storage of a recorded tape, and various irregularities encountered by the reproducing servomechanism (such as power variations, tape tension variations, etc.).

Recording Tape Transport

Obviously it is desirable to minimize or avoid the introduction of irregularities wherever possible. Irregularities of tape speed during recording should be minimized if for no other reason than to avoid overloading of the reproducing servomechanism.

For practical reasons it is desirable that a single tape transport mechanism be capable either of recording or of reproducing a reel of tape. It is, therefore, necessary to examine the reproducing servomechanism to determine what changes will be required to obtain a desirable recording performance.

To control the tape speed during recording, it is necessary to obtain a signal which is indicative of any irregularity in the tape speed. There appears to be no practical method by which the instantaneous speed of unrecorded tape can be determined with the desired accuracy. The best practical procedure is to control the speed of the capstan and accept whatever irregularities may occur between the capstan and tape motions. In this procedure variations in capstan speed, due to power and tape tension variations, will be reduced.

The necessary signal for indicating irregularities in the capstan speed can be derived from a magnetic tone generator attached to the capstan shaft. If a tone generator is added to the controlled mechanism

of the reproducing servomechanism and a few wiring changes are made, it becomes the recording servomechanism as shown in Figure 17. The operation of the recording servomechanism is essentially the same as that of the reproducing servomechanism with the exception that during recording the capstan speed is the output function.

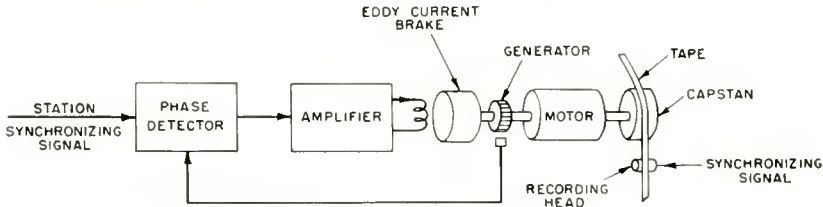


Fig. 17—Practical servomechanism for the recording operation.

The tape transport mechanisms as outlined above are subject to the practical limitations of servomechanisms. Most servomechanisms can reduce but not eliminate the error. Only certain amounts and rates of error corrections can be achieved if a stable system is to be realized. The speed of response of a servomechanism is usually limited, in large part, by the inertia of the moving system.

The Moving Head

Because of the above limitations, some additional means for operating on the tape motion is desirable.

Basically, it is the relative velocity between the tape and the reproducing head which must be controlled to produce the desired relationship between the reproduced and the station synchronizing pulses. It is evident that this relative velocity can be controlled by moving the tape, by moving the head, or by moving both the tape and the head.

Thus far, only control of the motion of the tape over a stationary head has been considered. Theoretically, it would appear that a similar result could be obtained by controlling the motion of a head along a stationary tape. The practical difficulties of such a procedure will not be discussed. Instead, a combination of the two procedures will be considered.

If the movable reproducing head is considered as an adjunct to the tape transport mechanism, the moving head and its associated apparatus constitutes a separate servomechanism which is required to correct only the residual irregularities resulting from the tape transport servomechanism. Such a system is shown in Figure 18.

This servomechanism is similar in principle to the servomechanism adopted for transporting the tape. The major difference is in the

electromechanical portions of the controller and controlled mechanisms. The configuration of the motor and mode of motion of the head were selected to complement the configuration of the head. The head is cylindrical in shape and the reproducing gaps are located on the periphery of the cylinder, parallel to the axis of the cylinder. It is desirable that the motion of the movable head introduce a minimum of disturbance into the actual motion of the tape; such is the case if a cylindrical head is rotated about its axis. The desired motion of the gap along the length of the tape is also obtained by a rotational motion of the head. The movable head moving system becomes, therefore, a rotational vibrating system.

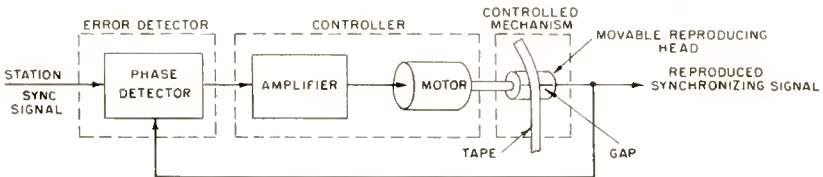


Fig. 18—Basic movable head servomechanism.

It is desirable that the vibrating system have a single degree of freedom; consequently, a rigidly coupled motor and moving head structure with a single centering compliance has been employed as the basic vibrating system. The final arrangement is shown schematically in Figure 19. The motor used to drive the movable head is a balanced magnetic driving unit.⁹ The armature is coupled to the moving head by means of a rigid nonmagnetic shaft. The shaft is pivoted on its axis by two knife-edge bearings. Two rubber pads are held in compression against the shaft. These rubber pads serve the double purpose of holding the knife edge bearings in contact and of supplying the compliance for holding the motor armature central between the motor pole pieces. The arrangement shown in Figure 19 allows a current in the motor driving coils to rotate the reproducing head about its central axis.

Complete Recording-Reproducing Tape Transport Mechanism

In the final over-all arrangement of the tape transport mechanism, it is necessary to consider the practical aspects of combining the servomechanisms, switching between recording and reproducing operation, and combining the tape transport with the video electronic system. A satisfactory arrangement is shown schematically in Figure 20.

⁹ H. F. Olson, *Dynamical Analogies*, D. Van Nostrand, 1943, p. 134.

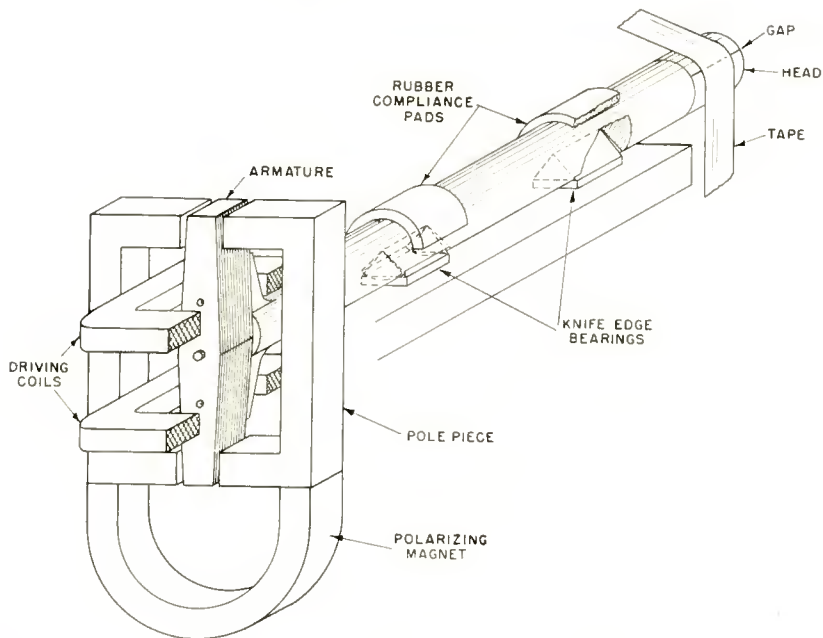


Fig. 19—Movable head mechanical system.

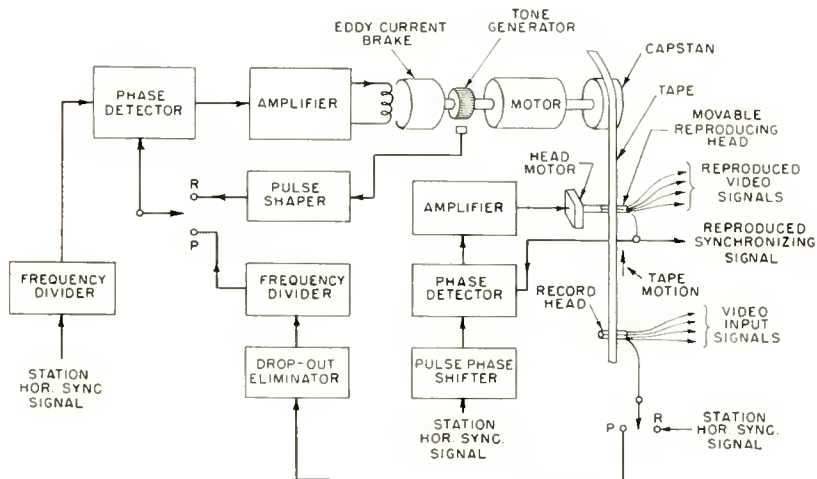


Fig. 20—Schematic arrangement of servomechanisms for recording--reproducing operations.

The recording operation will be described first. The several double-throw switches are thrown to the recording, or "R," position. The input signals are then connected to the recording head, and the tone generator is connected into the tape transporting servomechanism. There are several practical aspects of the capstan drive which must be considered. It is impractical to construct a tone generator for a frequency as high as the horizontal synchronizing pulse rate. Since a phase detector can most easily compare signals of the same frequency or pulse rate, it is desirable to derive a lower pulse rate reference signal for the capstan servomechanism. This lower frequency or pulse rate signal is derived from the horizontal synchronizing pulses by means of a counter type of frequency divider. This type of frequency divider has the advantage of delivering a signal which has a definite and constant time relationship with the divider input pulses. For recording purposes, therefore, a frequency divider is inserted between the source of the horizontal synchronizing pulses and the tape transport phase detector, as shown in Figure 20. Because the phase detector is designed to operate on pulses, a pulse shaper is required to convert the near sine-wave shape of the tone generator signal to a rectangular pulse.

In the reproducing operation, the tape transport will be considered first. The several double-throw switches are thrown to the reproduce, or "P" (for playback), position. Since the tape transport and moving head servomechanisms are to be operated as separate assemblies, a separate reproducing head is required for the tape transport servomechanism. The recording head is available for this purpose during tape reproduction. In fact, it is a desirable safety precaution to switch the recording head away from the input signals during the reproducing operation. A switch is provided, therefore, to connect the synchronizing pulse channel of the recording head to the tape transporting servomechanism during the reproducing operation.

Again the problem of pulse rates supplied to the capstan phase detector arises; the reproduced pulses from the recording head do not agree in frequency with the pulses from the first-described frequency divider. For reasons that are too lengthy to discuss here, it was decided to employ a second frequency divider, identical to the first, to solve the problem.

Tape-reproduced signals are subject to momentary losses of signal due to flaws in the tape coating. These flaws appear to be present, to a varying degree, in all tapes. The effect of the flaws on the signal is now commonly called a "drop-out." The effect of a drop-out on the tape transporting mechanism is rather severe. The frequency divider is

particularly vulnerable to drop-outs. Since the frequency divider functions by counting pulses, a missing pulse will delay the operation of the divider and produce a jump in the phase of the output signal. The effect is the same as if the tape were momentarily stopped during its normal motion. The servomechanism will behave accordingly and introduce a severe irregularity into the motion of the tape. Since it appears, at present, that little can be done to prevent the occurrence of drop-outs, a way must be found to supply the missing pulses during a drop-out. A method for supplying the missing pulses has been found in the form of an oscillator which is tightly locked to the reproduced synchronizing pulses. During a drop-out the oscillator supplies the missing pulses. The accuracy in timing of the oscillator-supplied pulses during a drop-out is dependent on the drift of the oscillator. Fortunately, the duration of the usual drop-out is very short; a stable oscillator does not, therefore, have time to drift a significant amount. One requirement of the oscillator is that it must be capable of following and passing on the phase or timing information contained in the reproduced synchronizing pulses. The drop-out eliminator is placed between the recording head and the frequency divider, as shown in Figure 20.

During the recording operation, it is desirable to monitor the newly recorded tracks so that proper adjustments of the recording facilities can be made. This combination of recording with monitoring has been named "simultaneous playback" or "immediate playback." It requires that the reproducing head follow the recording head as encountered by the tape.

The spacing between the reproducing head and the recording head is important. For the tape reproducing operation (switches at "P" in Figure 20), the tape transport servomechanism establishes a substantially constant phase relationship between the station horizontal synchronizing signal and the reproduced synchronizing signal from the recording head. Suppose for the moment that the movable reproducing head is stationary. The reproduced synchronizing signal from the movable head then has similarly constant phase relationship with the station synchronizing signal. The average phase relationship between the station pulses and movable head pulses is dependent on the spacing between the movable head and the recording head. Consequently, the spacing must be adjustable to obtain the desired average phase relationship. The desired phase relationship is obtained for integral wavelength spacings between the heads. In order to minimize the effects of storage changes in dimension of a recorded tape, it is

important that the distance between the two heads be the minimum that physical dimensions will allow.

When the proper movable head position has been established, the movable head servomechanism is placed in operation. For proper operation of the servomechanism it is necessary to consider the phase relationship between the two signals that will be applied to the movable head phase detector. It is preferable that the phase detector operate in the central region of its linear range. For most phase detectors, it is found that the central region of the linear range corresponds to an appreciable phase displacement between the input signals. For this reason, a variable pulse delay or phase shifting network is inserted between the station synchronizing signal source and the movable head phase detector, as shown in Figure 20. This permits the pulse requirements at the output of the movable head to be at variance with the preferred phase requirements at the phase detector.

The station horizontal synchronizing pulses supplied to the various parts of the tape transport mechanism must meet rigid requirements. These pulses "provide the goal," or "show the way," for the servomechanism. They should, therefore, be an accurate representation of the desired performance of the tape transport.

It will be recalled that a decision was made to reduce the tape transport problem to a consideration of the horizontal synchronizing pulses alone. It has been assumed that these pulses are continuous, and the tape transport system was designed accordingly. The station horizontal synchronizing pulses must be free of any extraneous timing irregularities.

In applications of the magnetic tape system where the color synchronizing pulse generator is available, the horizontal drive output of the generator is adequate as a source of horizontal synchronizing pulses for the tape transport mechanism. If the color synchronizing pulse generator is not available, as is the case in remote pickup operations, the horizontal synchronizing pulses must be derived from the color television signal. The composite synchronizing signal is not satisfactory since the vertical equalizing pulses interfere with the operation of the tape transport system servomechanisms. In fact, a concerted effort is required to eliminate any semblance of the vertical pulse in the derived horizontal pulses.

Another problem in the over-all arrangement of the tape transport mechanism is the attainment of vertical coincidence between the reproduced signals and the station synchronizing signal. In the present equipment, vertical coincidence is obtained manually. At the start of reproducing a reel of tape, the capstan motor is turned on and

the capstan servomechanism is disabled. This allows the tape to be transported at an improper velocity so that the reproduced signals will "crawl" with respect to the station synchronizing signal. One needs only to watch the reproduced picture until it is "framed," indicating the proper coincidence, and then snap the servomechanism into operation. As has been stated previously, the horizontal pulses assume control and maintain the complete coincidence.

MECHANICAL DESIGN

Tape Transport Mechanism.

The mechanical design of the tape transport components calls for extreme attention to any detail that might introduce irregularities in the transport performance. Since longitudinal tape displacements of tens of microinches cause serious picture jitter, the full import of precision in the machine work can be appreciated.

The eddy current brake is a major item in the capstan drive mechanism and, as shown later, is also important in the reel drive units. Figure 21 is a photograph of the brake components. On the

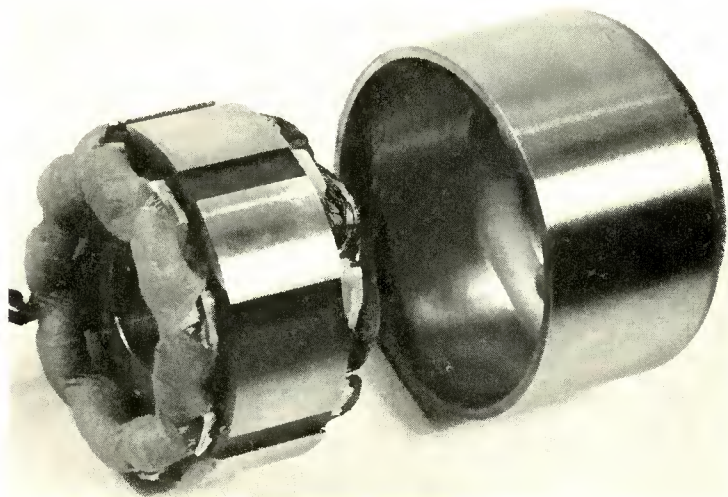


Fig. 21—Eddy-current brake components.

left is the field structure which is an eight-pole laminated steel core with interspersed windings. The windings are arranged to provide alternate north and south magnetic poles around the core. The eddy current brake cup, on the right, is a soft steel cup with a thin layer of copper on its inner cylindrical surface. In operation, the cup surrounds the field structure and the copper layer becomes the primary carrier of the eddy currents. The copper layer must, therefore, be

uniform in thickness and in conductivity. The thickness is maintained by accurate machine work and the conductivity by care in plating the copper on the steel cup.

The capstan spindle is shown in Figure 22. For comparison the movable head spindle is also shown. As the extreme left of the capstan spindle the tone generator rotor may be seen. Next to the right is the cup portion of the eddy current brake. To the right of the eddy current brake cup is the motor armature. Finally at the extreme right is the capstan roller.

In the construction of the capstan spindle, the primary concern was with the dynamic balance of the assembly, and with any form of run-out of the various cylindrical surfaces.

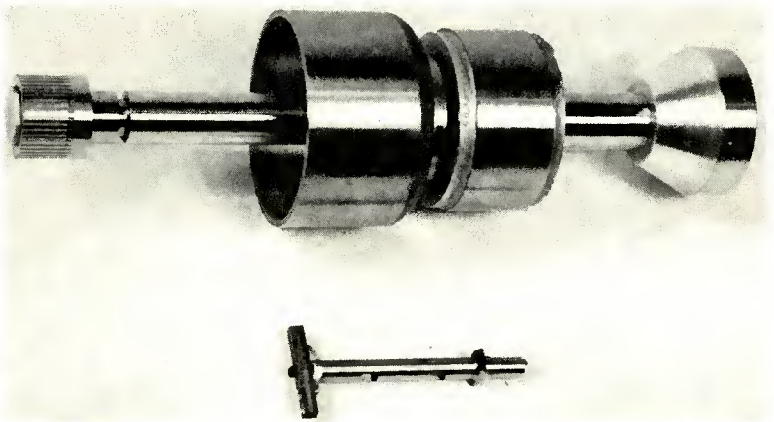


Fig. 22—Capstan spindle (above) and the movable head spindle (below).

The tone generator rotor has a large number of teeth that rotate in a magnetic stator, thus generating a signal, the frequency of which is indicative of the rotor speed. Obviously, if there is to be a true correspondence between the frequency and the speed, the teeth must be uniformly spaced around the rotor. The shape of the teeth is not important, but they must all be identical.

The eddy current brake cup makes up a large part of the inertia of the capstan spindle. It is necessary, therefore, to insure that the cup has accurate dynamic balance.

The motor armature was obtained from a commercial three-phase motor. An independent balancing procedure was applied to the armature for a dual purpose. First, it resulted in the desired balance condition, and second, it provided a check on possible physical flaws in the armature.

The capstan roller has a subtle importance in its relation to the

spindle. All of the care spent on the rest of the spindle is lost if the capstan roller periphery has run-out in the complete tape transport assembly. In other words, the capstan periphery must be absolutely concentric with the spindle bearing surfaces.

There are two capstan spindle bearings, one between the tone generator and the eddy current brake cup, and the other between the motor armature and the capstan roller. These bearings determine the accuracy with which the capstan spindle turns about its axis. Resort was made to the techniques applied to low-clearance precision grinding spindles. A self-aligning sleeve bearing with forced lubrication was adopted.

The final consideration in the design of the capstan spindle is rigidity of the structure. Compliance in the spindle shaft can allow relative motion between the capstan roller and the tone generator. Compliances between the various components of the spindle complicate the stability considerations in the associated servomechanism. It is desirable, therefore, to reduce the shaft compliances to an insignificant value.

Movable Head Mechanism

As shown in Figure 22, the movable head spindle consists of a motor armature on the left coupled by means of a shaft to the magnetic reproducing head on the right. The motor armature is a laminated steel structure, shaped to minimize its moment of inertia. The coupling shaft is nonmagnetic stainless steel to minimize the magnetic coupling between the motor and the reproducing head. The reproducing head is fastened to the coupling shaft in an easily demountable fashion, thus facilitating replacement of the head.

In the movable head spindle it is important that adequate stiffness be built into the coupling shaft. Any resonances in the structure must be at frequencies well above the expected operating frequency ranges of the movable head servomechanism.

In connection with the speeds of response of the tape transport servomechanism and the movable head servomechanism, it is interesting to compare the two structures shown in Figure 22. There can be little doubt that the moments of inertia of the two structures will be vastly different. One can easily visualize the possibility of higher speeds of response with the movable head system than with the capstan system. Indeed, that was the original surmise in adding the movable head system to the tape transport mechanism.

Complete Tape Transport Mechanism.

The mechanical arrangement of the complete tape transport mech-

seen centrally in the photograph. This structure has been named "the video head turret." The turret provides for a number of independent adjustments of the position of either video head. Lateral across the tape and turning within the tape wrap are set-leave adjustments for either head. Azimuth adjustment is set-leave for the record head, but is readily available for finger tip adjustment on the reproduce head. Finger tip adjustment is provided for the spacing between the record and reproduce head. The tape wrap angle on the video heads is adjustable by raising or lowering the whole structure.

The capstan roller (with hexagonal nut) is seen just to the right of the video head turret.

The pressure roller and arm is located above and to the right of the capstan roller. The pressure roller is a rubber-tired roller which is lowered to press the tape in contact with the capstan. This roller must, of course, be particularly free of run-out. The rubber tire must be very uniform in density and compliance. The axis of the pressure roller must be accurately parallel to the capstan axis, otherwise the tape will skew at the pressure point. Adjustments have been provided to allow accurate orientation of the pressure roller bearing axis.

The audio record and reproduce heads are seen to the right and below the capstan roller. Both audio heads have independent adjustments in position as described for the video heads. The audio head turret is simpler in construction, partly because both heads are stationary and partly because the audio head position adjustment is not so critical and set-leave adjustments are satisfactory.

ACKNOWLEDGMENT

Credit is due to George Kasyk for his contribution to the design of the mechanical parts of the present system.

Section 2—Reel Control Systems and Motor Regulators

INTRODUCTION

The preceding description of the transport mechanism dealt largely with synchronizing the capstan and tape to the horizontal drive signal of the television system. The effectiveness of this synchronizing system will depend on the relationship of its built-in accuracy to any changes in loading or drive torque. This may be stated in another way—that as the work required of the synchronizing system is reduced, the accuracy will increase.

In the mechanism under consideration, changes in loading are avoided as far as possible, by regulating the tension of the tape so

as to be constant. Changes in drive are also avoided by regulating the three-phase supply to the capstan motor. If both of these regulators performed without error, there would be no work for the synchronizing system after it had established its lock-in position with respect to the television synchronizing generator, and the system would come to a steady-state value depending on the steady load involved.

An additional reason for regulating tape tension on the input side of the capstan is that the tape has some resilience. Changes in tension will, therefore, have the same effect as moving the video heads or changing the tape velocity. This will be reflected in accuracy of phase comparison and synchronization.

REEL SERVOMECHANISM SYSTEM

Two different systems have been developed for controlling tape tension. Both are described, and equipments of both types have been used. Each has advantages and disadvantages, and a direct answer as to which is the better cannot be given at this time.

The tape is unwound from a reel which has some form of variable braking action applied, and after passing over the video heads, is pulled by the capstan at a fixed speed of 20 feet per second. From the output side of the capstan it passes over the sound head, and is then wound up on a motor driven take-up reel. A full reel of tape rotates at about 230 r.p.m. for a tape speed of 20 feet per second and an empty reel with $8\frac{1}{2}$ inch diameter core rotates at about 540 r.p.m.

The reels are slowly but constantly changing their speeds between these two limits, and at the same time are changing in weights and rotational energies. For a constant tension in the supply side of the capstan, the braking torque applied to the reel must be directly proportional to the radius of the tape roll at that instant. Likewise, the torque of the motor on the take-up reel must be directly proportional to the radius at any instant.

The reels have been made as light as possible by using magnesium hubs and side plates so as to reduce the stored kinetic energy and improve the tension control action. In addition, rather large hubs have been used so as to limit the ratio of maximum to minimum speed. This is a safety measure as well as a means of reducing the range of control required. If the core were reduced to 4 inches, the increase in tape storage would be 17 per cent, but the maximum reel speed would increase from 540 to 1150 r.p.m. A 20-inch disc rotating at this speed would be too dangerous to leave open and unprotected.

The side plates of the reel are separate from the hub, and it has been found that a properly wound roll is self supporting and can be

handled, stored and placed on the supply shaft without spilling. However, side plates are used on the take-up spindle as a safety measure in case of tape breakage or other accidents while running.

SENSING CONTROL OF TENSION

The most obvious method of controlling tension on either reel is to pull the tape over a sensing arm which is spring biased so as to indicate by position the tension in the tape. Error signals generated by this arm will indicate plus or minus errors in tension from the center position. These signals may then be used to increase or decrease tension and thus restore the arm to its mid-position. This is the method used in the present equipment.

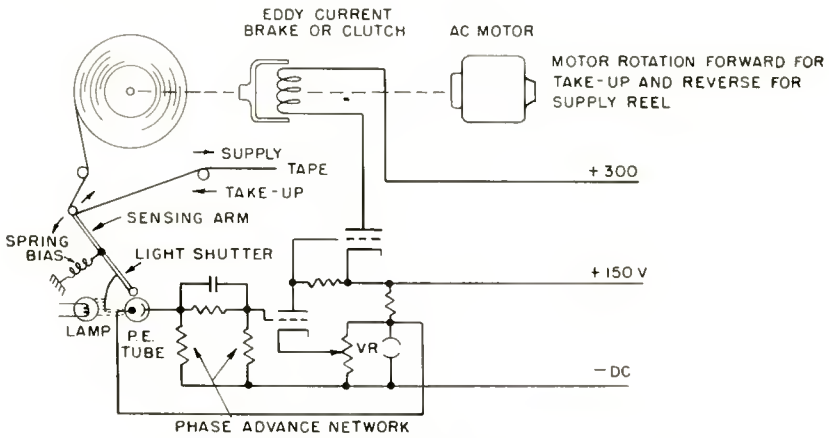


Fig. 24—Optical sensing of tape tension.

Such a system is shown in Figure 24, and the same mechanism and circuit is used for either braking the supply reel or driving the take-up reel. For take-up action, the stator windings of the eddy current brake are motor driven in the same direction as the tape so the eddy current brake acts as a clutch to supply the variable take-up torque. For the supply reel, the stator is either motor driven in the reverse direction or blocked, and the eddy current cup acts as a brake.

Mechanically, each reel drive consists of a free running reel shaft to which is attached an eddy current cup similar to that used for braking the capstan motor. The electromagnetic field structure is mounted on the shaft of a three-phase induction motor so that it can rotate separately inside the cup, and the coil leads are brought out to slip rings.

Several types of sensing arms have been tried; one of the most

satisfactory uses optical indication of arm position. The arms are of very light stainless steel tubing pivoted on ball bearings, and holding a tape slide at the end. Travel is limited to about 3 inches of motion at the end by rubber bumpers, and the arm is spring loaded to one end of its travel. A shutter or light vane is attached to the arm near its pivot and moves into or out of the light path between a low wattage pilot lamp and a photocell. The photocell output current then varies with angular position of the sensing arm, and is at mid value when the arm is in its center operating position.

A two-stage d-c amplifier is connected between the phototube signal output and the brake or clutch coils. This amplifier has one high-gain voltage amplifier stage and an output stage capable of supplying a maximum of at least 200 milliamperes into the brake coils. The last but not least important part of the circuit is a phase advancing network connected between the photocell output and the amplifier input. This circuit allows a higher over-all feedback gain to be used without hunting, and thus increases the accuracy with which the arm position is maintained.

In operation, the spring loading of the sensing arm is set to the value for correct tension in the tape when it is in mid-range. The gain of the d-c amplifier is then increased to the maximum usable value without causing hunting, and the over-all feedback then tends to maintain the arm in its center position. The angle of phase advance in the anti-hunting network is also adjusted for the greatest stability of operation. In the system as used here, the tape tension is maintained to considerably less than 1 per cent error over the entire speed changes of the reels. Tension on the supply reel side of the capstan is the more critical because the video heads are located here. Take-up tension is usually set somewhat higher than supply tension, and thus actually aids the capstan motor a small amount.

The sensing arms provide resilience between the reels and the capstan. This resilience has been found necessary to prevent the tape from being pulled off the capstan or occasionally broken under transient conditions. This is especially true during the rather violent transient of starting. There are unavoidable differences in inertia of reels and capstan and also differences in transient response which can rapidly change the length of free tape between the two. Thus transients tend to tighten the tape or build up an uncontrolled free loop. The limits of arm movement must be sufficient to take care of such transients, and the arm must also be light enough to follow all tape movements exactly and never let the tap out of control even momentarily.

From this reasoning it also follows that the acceleration of the take-up reel must be at least as rapid as the acceleration of the capstan motor in starting, or it will not take up the tape as fast as it is being delivered. This is the reason for using a high torque motor and clutch on the take-up system, even though under actual running conditions only about 1/30 horse power is required. In the interest of uniformity of parts, the same machine was first used for the supply reel brake, though its full power was never required in this service. Later the reversed motor was eliminated and only the brake was used with magnetic coils stationary.

CONSTANT POWER REGULATION OF TENSION

A second method of regulating tension in the tape is to take advantage of the fact that the tape speed is constant, and if its tension is also constant, then the power supplied into or out of the tape will be some fixed value. Any type of regulator on the supply reel brake which makes this brake absorb a constant mechanical power at all speeds will be regulating the tape to a constant tension. Similarly, any regulator on the take-up motor which forces this motor to deliver a constant mechanical power output at all speeds will also be regulating the take-up tension. A system using standard d-c shunt motors has been devised which performs these functions.

The supply reel brake shown in Figure 25 is the simpler of the two methods. The reel is mounted on the shaft of a d-c motor which is used as a generator supplying power into a resistance load. The voltage supplied to this resistive load is compared with a standard d-c voltage, in the form of a tap across a glow-tube regulator, and a high-gain amplifier uses this error voltage to control the field current of the generator and maintain the generator voltage constant. With a fixed load resistor, this also establishes the generator load current at a constant value, and thus the generator becomes a constant power

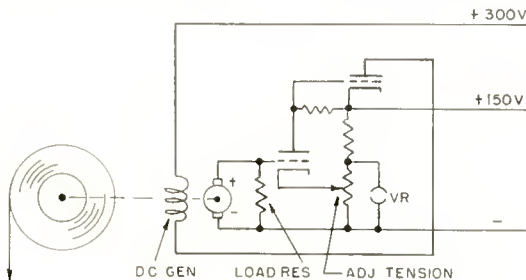


Fig. 25—Constant power supply-reel brake.

absorber or brake. The internal resistance of the armature and brushes form part of the generator load, so the machine should be chosen for low armature and brush resistance. Even then there will be a slow decrease in load as the machine windings warm up and increase in resistance. As long as this is a slow and smooth change, no bad effects can be noticed. Rapid changes, such as might be caused by erratic brush contacts must be carefully avoided by a regular cleaning of commutator and brushes.

This type of brake load has no sensing arm, and therefore does not introduce resilience in the tape path from reel to capstan. However, in operation it was soon found that a spring-mounted tape guide was necessary to supply the quick take up or release of tape that is required in snubbing out a transient.

The take-up motor drive, as shown in Figure 26, is similar to the supply reel system except that here power is fed into the d-c machine instead of being drawn from it. Both current and voltage fed to the armature are regulated to fixed values so that the mechanical power output is constant. A current regulator is connected in series with the armature and holds the armature current to some fixed value whether the motor is stalled or running at any speed over a wide range. The voltage as read by a meter across the brushes will then be the sum of the generated back EMF of the motor and the IR drop of the armature current flowing through the armature and brush resistance. This second voltage is constant since the current is held constant, so the meter reading would be the back EMF plus a fixed voltage. Now a second feedback circuit is added that is almost identical to that used for field control of the generator brake circuit. This feedback controls the motor field to maintain a constant brush to brush voltage on the armature, and thereby make the back EMF of the motor constant.

Since the mechanical power output of a d-c motor is the product of

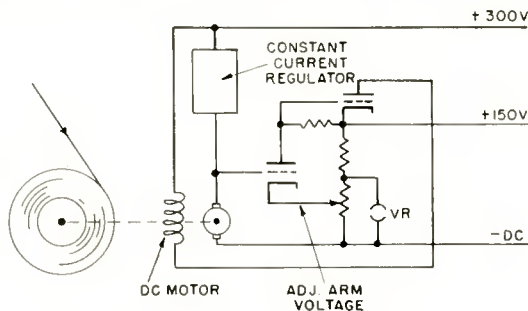


Fig. 26—Constant power take-up reel motor.

back EMF and armature current, the motor will have a constant power output at any speed over the regulating range. The field is automatically adjusted to hold this condition as the speed changes during windup.

On this side of the capstan the resilience of the tape path is not too important, so the equipment using this particular take-up does not have extra resilience added.

AUTOMATIC START AND STOP FEATURES

Starting and stopping the complete transport system involves a rather complicated system of contactors set for various times of closing or opening. Only a few of the main features can be mentioned here.

The capstan motor is started through series resistors to limit its acceleration to a value the take-up reel motor can meet. After a time delay of approximately 3 seconds these resistors are shorted out and brake synchronizing applied to the capstan. About 3 or 4 seconds later all servos have settled down to normal running conditions.

Stopping can be initiated by push button or by a tape indicator. A small lamp and photocell indicator is placed in the tape path near the take-up reel. As long as tape is in the machine the cell is dark, and a stop relay remains in a non-operate position. When the tape is missing, the phototube receives light and trips this stop relay. This indicator is shown on the lower right of Figure 8.

In stopping, the capstan motor and its control brake are first turned off, and the drive motor of the supply reel brake is turned off to allow this empty reel to coast to a stop. At the same time the drive motor of the take-up reel is "plugged" or switched to reverse to stop the reel quickly. A rotation direction feeler riding this reel shaft turns off the motor when the reel passes through zero speed and starts to reverse. The depressor on the capstan is lifted by hand, and the machine is ready to rethread.

REGULATION OF CAPSTAN MOTOR SUPPLY

In addition to the other regulators, a regulator for the three-phase supply to the capstan motor has been provided. A three-phase induction motor is used because such a motor has zero torque ripple when both line and motor are perfectly balanced in voltage and phase angles.

It can be shown that an unbalance in voltage only of one phase of the line will produce a torque ripple of approximately the same percentage as the voltage unbalance. If the voltages are held constant and the 120° angles unbalanced, the torque ripple produced will be

nearly twice the percentage of angular unbalance. Therefore, angular balance in the motor supply is in effect twice as important as voltage balance.

One solution to the problem was found in using a motor-alternator set to supply capstan only. Here a three-phase synchronous motor is used to drive a three-phase synchronous alternator and the net result is that any angular or voltage unbalances in the power line is mechanically averaged into all three phases of the alternator. A perfect angular and voltage balance can thus be maintained. This has proved a satisfactory solution to the problem, but is bulky and noisy, and therefore an electronic regulator is still desirable.

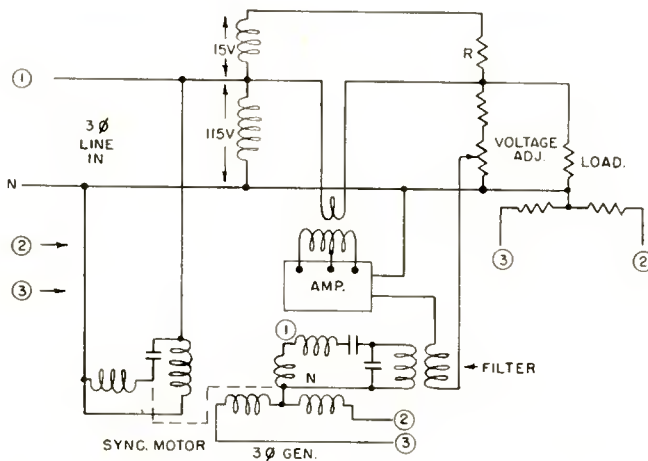


Fig. 27—Three-phase voltage and waveform regulator.

One form of regulator, which holds both voltage and angular balance, is shown in Figure 27. This regulator also filters out higher harmonics to leave practically pure 60-cycle output. Basically, each line to neutral load is fed by a bridge circuit. The voltage is stepped up 15 volts or so and then dropped by approximately the same amount by a series resistor. If the input voltage and output are then exactly the same, there will be zero voltage across the secondary of the line-in to line-out transformer which is the output transformer of the regulating amplifier.

A standard a-c voltage is now developed in a manner described later that is pure in waveshape, constant in amplitude, and in-phase with phase 1 of the three-phase line. This standard voltage is subtracted from the regulator output to obtain an error signal that will

represent in voltage, phase, and harmonic content the amount by which the output fails to meet this standard. A feedback amplifier then supplies this error voltage to the regulator output at such a polarity as to cancel the error and tend to make the difference zero. The net result is that the output is made to agree with the standard to within a small fraction of 1 per cent, and this is a dynamic comparison with a high speed of response at all times during each cycle. The response time is practically instantaneous with respect to 60 cycles.

In a three-phase regulator, three identical single-phase units are used, but the standards of comparison for phases 2 and 3 are derived from phase 1 so that their phase angles can be accurately set at 120° and 240° from phase 1. The angles of the power line may then wander over a number of degrees from true balance while the regulated outputs are held at the fixed separation angles of the standard. This requires the amplifiers to deliver both in-phase and reactive power to the loads, but this is automatically accomplished in the feedback system. The only requirement is that the output stage be capable of supplying the sum of in-phase and reactive power by which the required output differs from that supplied directly by the line. An output stage for each phase having output capabilities of 10 per cent of the load power of each phase will give a very wide control range.

Several types of three-phase standards have been used. One form consists of a 60-cycle oscillator of very pure wave form and auto-gain control for amplitude constancy. This is locked in phase with phase 1 and $\pm 120^\circ$ phase networks are used to obtain phase 2 and phase 3 standards. Another consists of using a 1/100 horse power synchronous motor driving a small, permanent-magnet field, three-phase alternator. This second method has proved the simplest and most accurate.

In performance, a regulator has been designed to supply the 250 watts required by the capstan motor. This regulator holds line-to-neutral voltages at 120 volts $\pm .25$ per cent and line-to-line voltages at 208 volts $\pm .25$ per cent over the range of 120 ± 15 volts change on any or all 3 lines. Under any combination of input voltages indicated above, and no load to full load on all or any single phase, the total harmonic content of the output of any phase is less than 0.3 per cent, and maximum observable transient response time less than $\frac{1}{4}$ cycle.

Section III—Performance and Conclusions

PERFORMANCE

Performance of the complete tape transport mechanism is best

judged by observations of the reproduced picture on a television receiver. The results of observations on a 21-inch television receiver are described in the following paragraphs.

The result of irregularities in the tape motion were seen as a waviness in the vertical lines of the picture. This waviness has been observed to range from barely perceptible to a peak-to-peak amplitude of approximately $\pm 1/16$ inch. The shape of the waviness appeared to range from a periodic 120-cycle wave to a random shape having frequency components as high as several thousand cycles. As might be expected, the higher frequency components were very small in amplitude.

There appears to be a definite relationship between the picture waviness and the condition of the tape as it passes through the mechanism. Occasionally a section of tape has been observed to have a serpentine or curved shape along its length. The attempt to guide such a tape in a straight line through the mechanism results in serious "picking" at the guide roller flanges, and even though guided, the curved tape will skew over the magnetic heads. Such a condition causes serious waviness in the reproduced pictures. Other sections of tape have been encountered where odd coating surface conditions have caused what appears to be a stickiness between the tape and the magnetic heads. This effect results in a large amount of a random waviness of the picture.

The playing time of a full 20-inch reel of tape, with a tape speed of 20 feet per second, is dependent on the thickness of tape. The popular $1\frac{1}{2}$ mil based tape gives a playing time of approximately 8 minutes. The advent of Mylar* has permitted the manufacture of thinner tapes. With $\frac{3}{4}$ mil based Mylar tape a playing time of 15 minutes per reel of tape is obtained. A full reel weighs approximately 7 pounds.

The starting time of the tape transport mechanism is about 6 seconds to the instant that the capstan servomechanism "locks up." Some additional time must be taken to manually establish the vertical framing. This additional time is partly dependent on the skill of the operator, but is usually about 8 to 9 seconds. In other words, approximately 15 seconds are required to place the tape transport in proper operation.

CONCLUSIONS

With regard to the effects of irregularities in tape motion, it is

* Registered trade-mark of E. I. duPont de Nemours & Company, Wilmington, Del.

concluded that the present tape transport mechanism will reproduce a television picture, the steadiness of which will compare favorably with that of studio motion picture equipments. It is concluded further that the best available techniques of design and construction must be applied to the tape transport if satisfactory performance is to be obtained.

Part IV — The Magnetic Head*

BY

J. A. ZENEL

BASIC REQUIREMENTS FOR A VIDEO HEAD

WHEN work on the magnetic head was begun, the goal was the development of a head which would permit the direct, wide-band recording of television signals on magnetic tape. A new head was necessary because of the obvious futility of attempting to record video by extending the range of audio equipment. Since current-day audio equipment contains heads which are representative of the state of the magnetic recording art at the time the development was begun, the discussion that follows is based on the performance of such equipment.¹⁰

As is generally known, the upper frequency limit of an audio recorder, at a given tape speed, is primarily determined by the resolution capabilities of the magnetic head. The maximum information that audio magnetic heads can resolve is about 2,000 cycles per lineal inch. This means that an audio recorder has to be run at a tape speed of about 8 inches per second if response at 16,000 cycles per second is desired. Now if an attempt were to be made to record frequencies beyond 3 megacycles per second, a tape speed 200 times greater—1,600 inches per second, or about 90 miles per hour—would be necessary. The first requirement for a video head, therefore, is that it must be able to resolve five to ten times as much per lineal inch if the tape speed of the video recorder is to be kept within reasonable bounds.

Thus far, only the resolving ability of the audio head has been considered. Since this ability is a function only of the geometry of the head, the electrical behavior must be separately taken into account. Some audio heads could probably be used up to about 100,000 cycles

* This part contains the essential portion of a thesis submitted in partial fulfillment of the requirements for the degree of Master of Science in Engineering from Princeton University, 1956.

¹⁰ S. J. Begun, *Magnetic Recording*, Murray Hill Books, 1949.

with higher tape speeds. This upper limit is determined by electrical losses of various kinds within the audio head—losses which bear no direct relation to the resolving ability. But since video signals include frequencies beyond 3 megacycles, the second requirement for a video head becomes apparent; it must be able to perform, from an electrical viewpoint, over the entire video range. In specific terms, it must present a reasonable impedance from about 400 cycles to about 3.5 megacycles, a span of about 13 octaves, compared to the 8 octaves within the audio range. It must be free of resonances within this range, and energy losses must be small so that the head will not be physically damaged.

The two requirements so far discussed are basic to the problem of direct video recording. In the course of the work, it was discovered that the high-frequency performance of a given record head varies as a function of bias. The present system overcomes this difficulty by providing separate tracks for the low-frequency and high-frequency components of the television signal. Hence, another requirement must be satisfied: the elemental video head must be of such design that a number of these elements can be built into a single package. This entailed new difficulties, such as keeping all the gaps in line, making all the elements equally sensitive, etc.

The over-all system imposes other requirements, but since they are of secondary importance, they need not be considered here.

DEVELOPMENT OF THE VIDEO HEAD

In general, the resolution of a magnetic head depends on the gap length. It was found possible to devise a head having an extremely short gap structure in which the shunt area—the area of contact between the pole faces—was very small. The resulting head proved sensitive enough to provide the desired resolution. The structure devised showed promise of satisfying not only the two basic requirements, namely, more resolution and wider frequency range, but also of being adaptable to multiple-element construction. The basic structure, even when incorporated in a multiple head, provided the performance necessary for recording and reproducing signals at frequencies covering most of the video spectrum at a tape speed of 20 feet per second.

ELECTRICAL PERFORMANCE OF THE VIDEO HEAD

The video head, in its present state of development, can record and reproduce more than 15,000 cycles per lineal inch. The upper frequency limit is about 3,500,000 cycles per second, at a tape speed of 20 feet per second.

Figure 28 shows the response of the head when used with a tape moving at 20 feet per second. Curve A, which extends from about 400 cycles to about 1.5 megacycles, was taken at fixed operating conditions; the bias and signal were adjusted for best response at 1,000 cycles. Curve A represents the available output at the lower frequencies under practical operating conditions. However, under such conditions, the high-frequency response suffers. Curve B was also taken at fixed operating conditions; bias and signal were adjusted for best response at 1 megacycle. (Curve B was not plotted below 1 megacycle because distortion, caused by using no bias while operating over a large part of the dynamic range of the tape, becomes excessive.) Curve B repre-

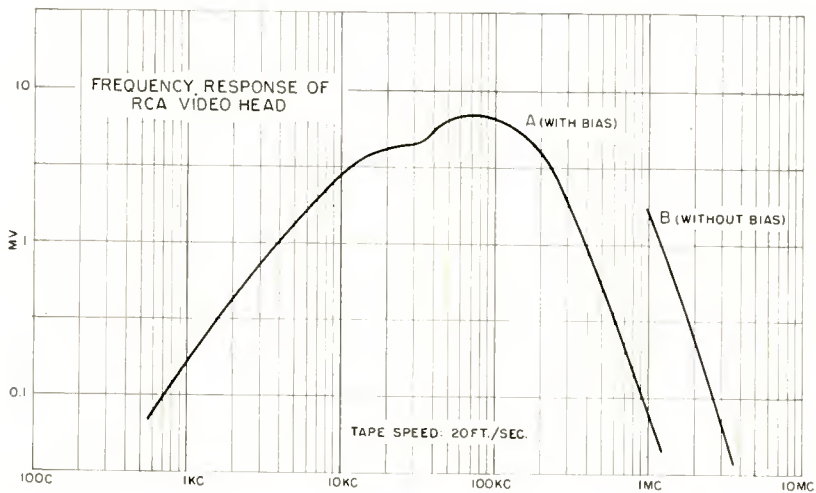


Fig. 28—Frequency response at a tape speed of twenty feet per second.

sents the output available at the higher frequencies under practical operating conditions. These two curves, therefore, represent the output that can be obtained at either end of the band. These curves were taken with the same head doing the recording and reproducing; a slight loss, no more than two or three decibels, will result if a different head of comparable quality does the reproducing.

In the video recording system, separate elements record low-frequency signals, as shown in Curve A, and high-frequency signals, as shown in Curve B. When the system is used for recording color television signals, four elements are used; three elements for the low-frequency components of the three colors, and one element for the combined high-frequency components. When the system is used for

recording black-and-white television signals, only two elements are used.

Since there is no observable null in either of these curves, no positive statement about gap width can be made. However, since the information density represented by the high end of Curve B is about 15,000 cycles per lineal inch, the gap length can be deduced from this as being no greater than one wavelength, or about 7×10^{-5} inch.

The resolution capabilities of the head are shown more graphically in Figure 29. One horizontal line across the kinescope face, as represented by the video waveform drawn above the television set, occupies .015 inch along the tape. By way of comparison, a penny is approxi-

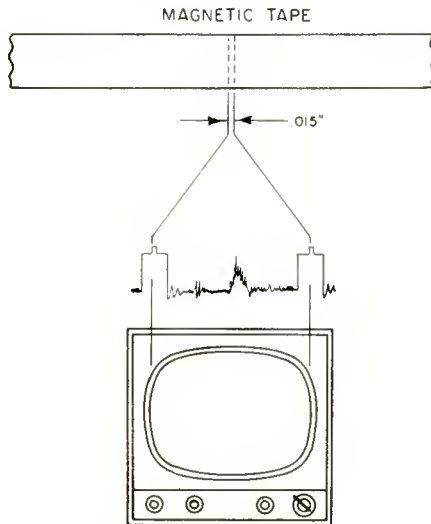


Fig. 29—Dimension involved in recording one horizontal line.

mately .060 inch thick, or four times the length of one line on the tape.

Some of the system considerations involving bias are shown in Figure 30. Magnetic tape, as is generally known, exhibits the non-linearity which is characteristic of all magnetic materials. In contrast with audio practice, a d-c bias, instead of a-c bias, is used to "linearize" the operating characteristic.

The method of operation is as follows. Before the tape is brought into contact with the recording head, it is passed through a strong field (supplied by a permanent magnet) which saturates the tape. This saturation accomplishes two things; it obliterates anything which is already recorded on the tape, and it also "conditions" the tape for the next operation.

Figure 30(a) shows a typical hysteresis curve for magnetic tape. When the tape passes through a saturating field, it is taken along the curve to point 1. When the tape leaves the field, it retains a value of B shown by B_1 on the curve. This is the condition of the tape when it is ready for the record head.

Figure 30(b) is an operating curve derived from Figure 30(a). Every negative value of H on the hysteresis curve determines a value

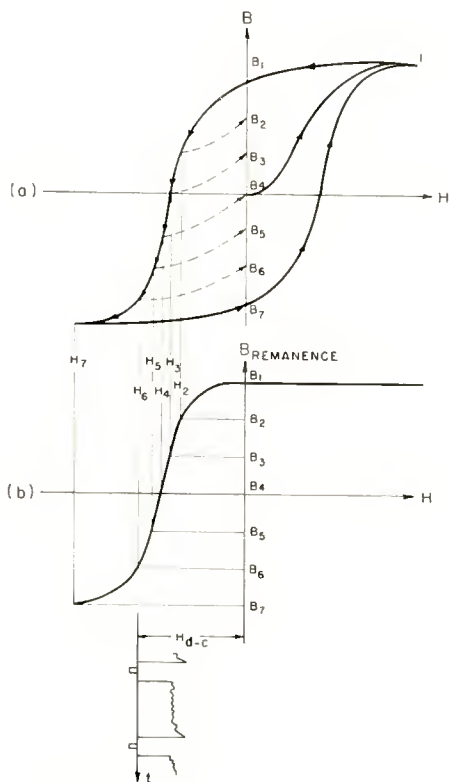


Fig. 30—D-C bias method of operation.

of $B_{\text{remanence}}$, and this information is re-plotted in a more convenient form in the lower figure.

The value of bias represented by H_{d-c} provides good low-frequency response with the low-frequency record head. A separate head using almost no bias is used to provide the required high-frequency response.

The impedance versus frequency characteristic of the head is shown in Figure 31. The impedance, as well as the frequency, has been

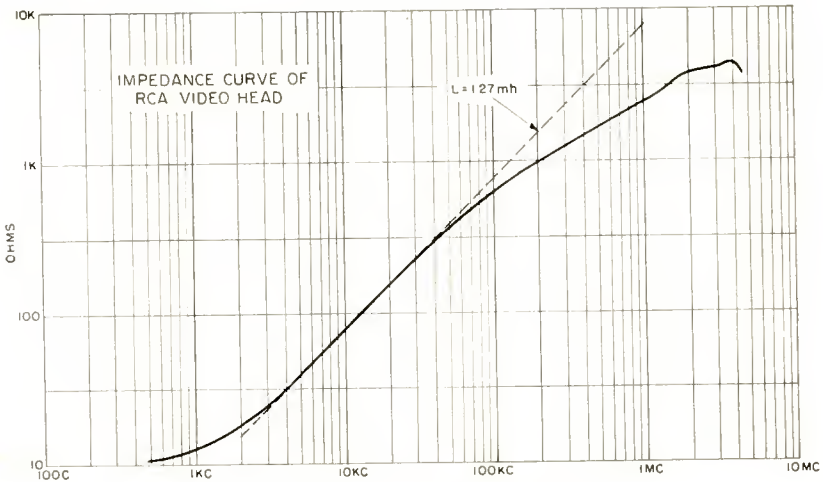


Fig. 31—Impedance characteristic.

plotted on a logarithmic scale. The dotted line shows how the impedance of the head would behave if it were primarily inductive, based on the inductance of the head at 10,000 cycles. The diminishing permeability of the metallic core as the frequency is increased permits the use of a relatively high-impedance coil without resonance troubles.

PHYSICAL STRUCTURE OF THE VIDEO HEAD

A photograph of a complete five-element head is shown in Figure 32. Two leads are brought out from each element, making a total of ten leads which are connected to the plug, as shown.

Figure 33 is a sketch of the basic element. The pole-face structure uses no separator between the pole faces; the faces are in intimate contact. Thus the "gap," which in conventional magnetic heads consists of an actual nonmagnetic spacer, is only a concept in this unit.



Fig. 32—Complete five-element head.

The head may be assembled in various ways. In a preferred method, a pair of coils are threaded with several strips of Hymu 80*. The ends of the strips are pressed and held together by two half-cylinders made of stainless steel. The ends of the strips then become the pole faces. The entire assembly is bonded together with a casting resin.

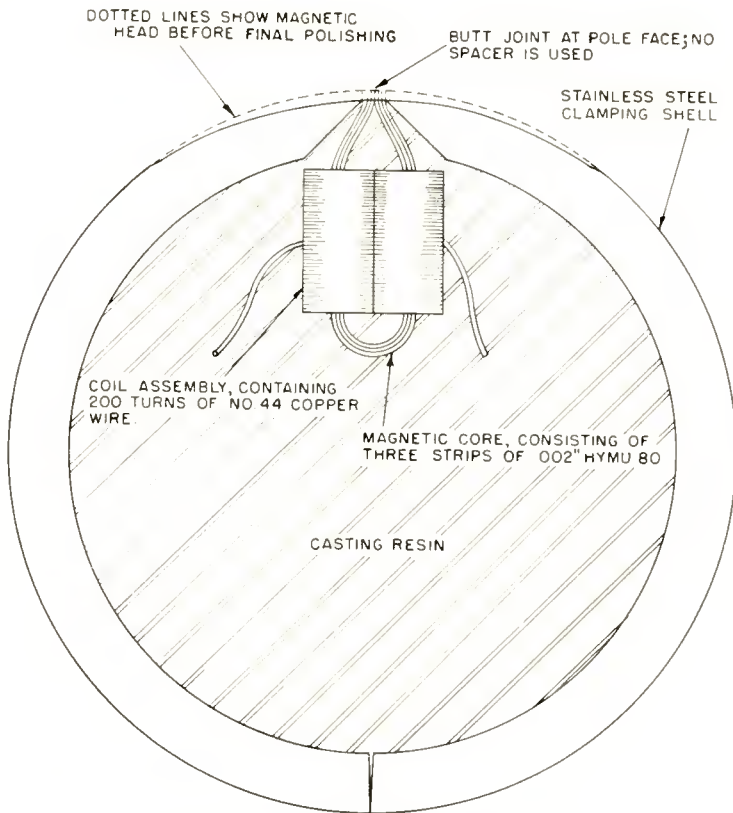


Fig. 33—Sketch of the basic element.

The manner in which the small shunt area between the pole faces is obtained can now be seen. When the two half-cylinders press the two ends of the core together, the area of contact between these ends is about .005 inch in depth. These ends, or pole faces, are carefully cut down until the depth is about .001 inch, at which time the pole faces are virtual knife edges in contact with each other. The head then performs as has been described.

* Registered trade-mark of the Carpenter Steel Company, Reading, Pa.

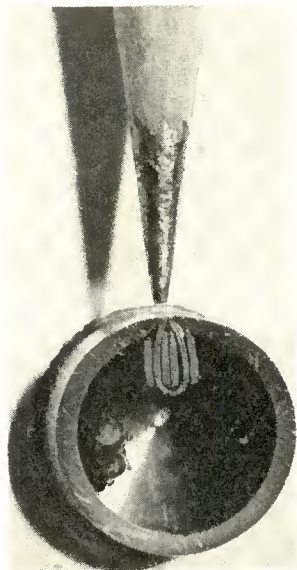


Fig. 34—Sectional photograph of the basic element.

With the aforementioned materials, an average head life of about 150 hours may be expected when the heads are used with a tape speed of 20 feet per second.

Figure 34 is a photograph of the basic element. The photograph shows a head which was sliced so that its interior would be clearly visible. The point of a pencil is also shown for size comparison.

Another cross section is shown in Figure 35. A multiple-element head was sliced along the long axis such that the five separate elements would be visible. The cross talk between the separate elements is negligible.

Figure 36 shows the track layout on the tape. If the magnetic

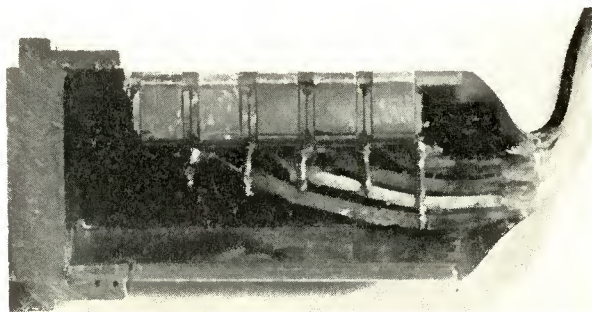


Fig. 35—Sectional photograph through the long axis of a five-element head.

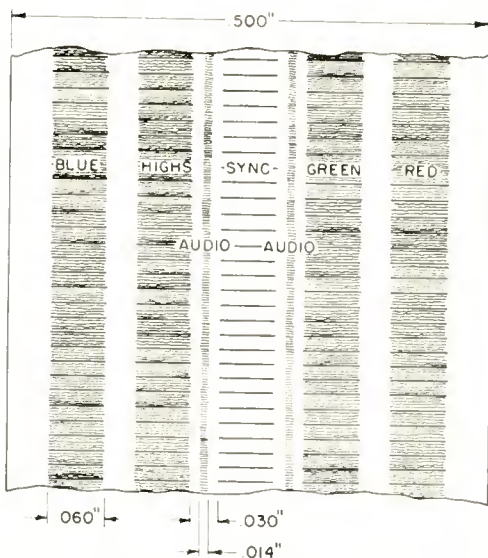


Fig. 36—Track layout on the magnetic tape.

information could be made visible, the tape would look something like the sketch shown. The sound tracks, which are also shown, are recorded by separate, two-element heads, built very much like video heads.

CONCLUSIONS

The video head, as developed by the RCA Laboratories, has proven itself in extensive experimental video recording. In addition, its successful use has established the feasibility of wide-band video recording.

ACKNOWLEDGMENT

I wish to acknowledge my indebtedness to Adolph R. Morgan, with whose cooperation some of the early work was carried out, and to Benjamin Kulley and Walter Dimitruk, who solved many of the mechanical problems.

Part V — Audio Systems

By

J. G. WOODWARD

INTRODUCTION

IT IS accepted and expected practice in television systems to provide an audio channel to convey sound information from the pickup location to the ultimate viewing location. This audio chan-

nel must pass through the television tape recorder when this recorder is used for storing and reproducing video signals. The obvious way to record the audio simultaneously with the video signal and to maintain synchronism between the two is to record the audio on the same magnetic tape used for the video signal. The techniques for recording audio frequencies on magnetic tape have been highly developed during recent years, and one might expect the addition of an audio channel to the television tape recording system to be a routine matter. However, the special system requirements of the video channels impose several conditions on the audio channel which are not ordinarily encountered in audio tape recorders. Because of the exceedingly great difficulties attending useful tape recording and reproduction of video signals, the audio design must accept and build around the special conditions necessarily set for it by the video system. These conditions and the ways in which they influence the design and operation of an audio system are described.

SYSTEM REQUIREMENTS AND ARRANGEMENT

The principle audio-system factors which are determined by operation of the video system in the television tape recorder are:

1. Tape speed.
2. Method of erasing and biasing.
3. Recording-track location and width.

A tape speed of 20 feet per second is used in the television tape recorder. This is 32 times faster than the 7.5 inches per second frequently used in high-quality audio tape machines.

In the television tape recorder the tape is erased as it passes over a permanent magnet prior to passage over the video and the audio recording heads. Corresponding to this d-c erasure technique is a d-c biasing technique, wherein a direct current is superimposed on the varying signal current in each recording head, to place the operating point at an optimum location on the magnetic recording characteristic. This is in contrast with the customary high-frequency erasing and biasing technique used in high-quality audio tape recorders.

Figure 36 shows how the tape area is budgeted among the audio and the several video channels. The audio is recorded on two .014-inch tracks situated in the gaps between the video sync track and the tracks for the mixed-highs and the green signals. The .008-inch guard bands separating the audio from the video tracks have been found sufficient to prevent cross talk when the heads are properly aligned. The two tracks are recorded by two identical head units connected in series. The two audio tracks together give a total track

width of .028 inch, which is considerably less than the $\frac{1}{8}$ -inch and $\frac{1}{4}$ -inch tracks employed in conventional audio recorders. The effect of the narrower track is to reduce the signal-to-noise ratio. While space is available on the tape for as many as four .014-inch audio tracks, the small increase in signal-to-noise ratio achieved by going from two to four tracks does not warrant the added complexity and cost of the heads.

While several other types of recording and playback heads have been tested, the audio heads currently used in the television tape recording equipment are similar in construction and performance to the video heads described in Part IV. A typical unequalized record-playback response characteristic is shown in Figure 37 for a 20-feet-per-second tape speed.

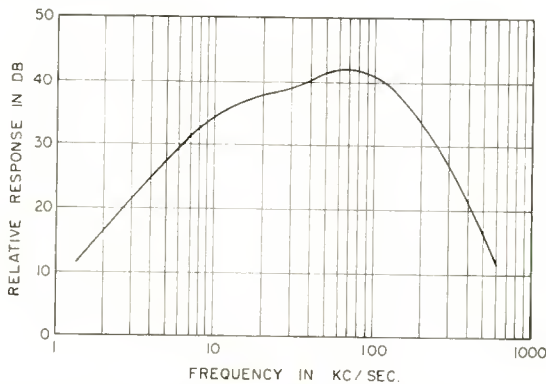


Fig. 37—Unequalized record-playback response characteristic of audio heads with a 20-feet-per-second tape speed.

The audio recording and playback heads are located on the output side of the driving capstan; that is, the tape passes over the audio heads immediately after leaving the capstan. The location of the audio heads is shown in relation to the other components of the tape-transport system in Figure 23.

While the foregoing factors influence the performance of the audio system, several methods of audio recording may be considered for use. These methods have various capabilities and limitations, and the choice of one rather than another will be based largely on economic considerations and on the performance criteria for a particular application.

DIRECT RECORDING

In direct recording the audio is recorded directly on the tape as an audio-frequency signal. It is the method used in all conventional

audio tape recorders and is capable of yielding excellent results in well-designed equipment. It suffers a great disadvantage in the television tape recorder, however, since the high tape speed gives a greatly increased output noise voltage in playback without a comparable increase in the audio signal. While some improvement might be expected if heads having longer gaps were used, such heads would be susceptible to low-frequency cross talk between the audio and the video tracks. The performance obtained with direct-recording techniques is likely to be marginal or unacceptable for most applications of the television tape recorder. Some type of recording method employing a modulated carrier appears more promising and appropriate for use in the high-tape-speed device.

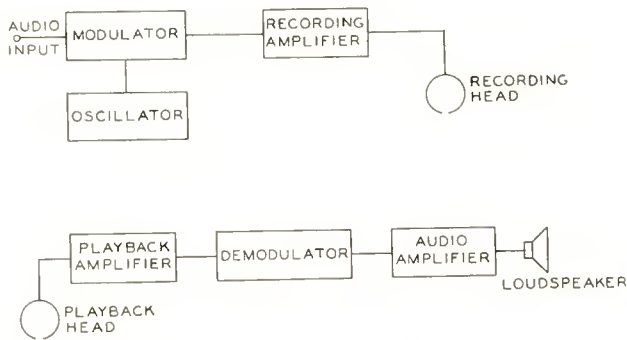


Fig. 38—Block diagram of a simple, AM-carrier audio-recording system.

AM-CARRIER RECORDING

In amplitude-modulated-carrier recording, a high-frequency signal is recorded on and reproduced from the tape. The audio signal passes through the tape system as an amplitude modulation of this high-frequency carrier. After reproduction from the tape, the modulated carrier is amplified and demodulated to recover the audio signal. A block diagram of the simple AM-carrier system is shown in Figure 38. Two factors must be considered in choosing the carrier. First, the carrier should have a frequency well above the audio range to simplify the filtering problem in demodulation. Second, the carrier frequency should be in the neighborhood of the maximum response of the head-tape system. In the record-playback characteristic, shown in Figure 37, the response maximum is quite broad and is centered near 80 kilocycles. Carrier frequencies between 50 and 150 kilocycles have been found to work well.

The AM-carrier method of audio recording has the advantage of

simplicity of electronic circuitry. It also has a basic limitation which precludes its use in some applications. The limitation resides in the characteristics of the oxide coating of the tape. The peak carrier level which may be recorded on the tape is determined by the magnetic characteristic of the coating. If too high a level is recorded, the audio output signal is distorted as the oxide approaches magnetic saturation on carrier modulation peaks. The lowest useful recorded level is determined by the noise modulation of the carrier caused by magnetic and surface irregularities of the tape coating. Thus, a compromise must be made between the signal-to-noise ratio and the distortion of high-level audio. With tape coatings now available a typical compromise gives a 34-decibel signal-to-noise ratio and about 3 per cent r.m.s. total harmonic distortion for a 100 per cent modulated carrier and an 8-kilocycle audio bandwidth. The signal-to-noise ratio is lower when worn or otherwise inferior tape is used. For some applications, particularly with a more restricted audio bandwidth, the simple AM-carrier recording method might be considered acceptable. For a high-quality audio system having a wide dynamic and frequency range it is not acceptable.

TWO-CARRIER AM RECORDING

A significant improvement in the signal-to-noise ratio of the AM-carrier audio-recording system may be achieved by the use of two carriers as follows: Two carriers of different frequency are amplitude modulated by the same audio signal. After modulation, the two carrier signals are combined and are recorded by the same recording head on the same track on the tape. In playback, the two carriers are separated and amplified in tuned amplifiers and are demodulated separately. Thus, each carrier yields an audio signal independently of the other carrier. Noise reduction is accomplished by modulating the two carriers out of phase and also reversing the phase of the demodulators. When this is done, and when the audio output signals from the two carriers are added, the desired audio signals combine in phase, while any undesired output noise voltages due to modulation of both carriers in passing through the tape system combine out of phase, and totally or partially cancel. A block diagram of the two-carrier noise-reduction recording system is shown in Figure 39.

The carrier frequencies should be sufficiently close together to insure both carriers being similarly affected by noise modulation on the tape, but should be sufficiently different to allow convenient separation of the two by tuned circuits in the playback amplifier. Also, the carrier frequencies should be adjusted relative to one another to make any beats between the carriers and/or their low-order harmonics

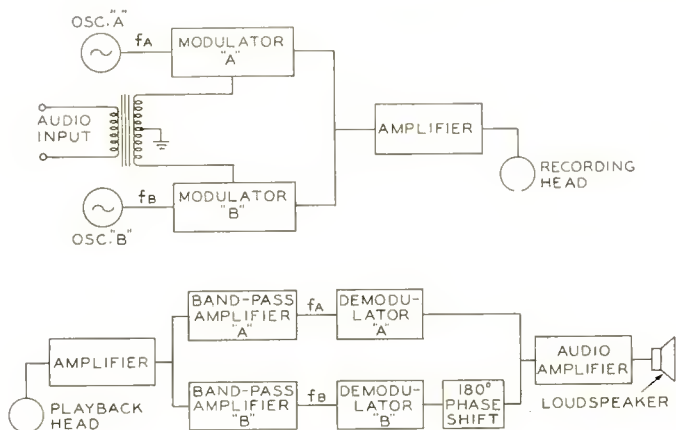


Fig. 39—Block diagram of a two-carrier, AM-carrier audio-recording system.

lie above the audio frequency range. Carrier frequencies of 88 and 141 kilocycles have been used satisfactorily.

The effectiveness of the two-carrier system in reducing noise is illustrated in Figure 40 which shows oscilloscope traces of the noise in the audio output of the playback amplifier while a tape recorded with unmodulated carriers is being reproduced. The upper trace was

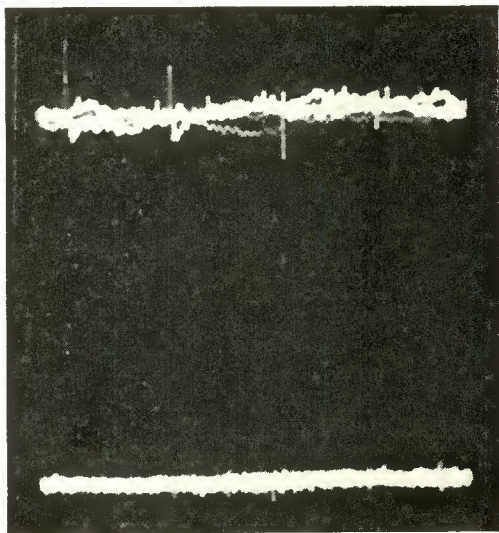


Fig. 40—Noise-reduction with two-carrier, AM recording. Upper: Audio-noise output with a single, unmodulated carrier. Lower: Audio-noise output with two unmodulated carriers adjusted for noise cancellation.

made with only a single carrier operating. Both low-frequency noise and high-frequency spikes are evident. The lower trace in Figure 40 was made with two carriers operating and adjusted for maximum noise cancellation. All of the low-frequency noise and most of the high-frequency noise has been eliminated. Measurements show an increase of as much as 8 decibels in signal-to-noise ratio resulting from the use of the second carrier.

With the two-carrier system the basic limitation is again the oxide coating of the tape, and again the compromise must be made between high-level-audio distortion due to magnetic saturation, and noise due to magnetic and surface irregularities in the tape coating. A typical compromise gives a 42 decibel signal-to-noise ratio and about 3 per cent r.m.s total harmonic distortion for 100 per cent modulated carriers and an 8-kilocycle audio bandwidth. Audio of this quality is acceptable in many, but not all, applications.

FM-CARRIER RECORDING

As pointed out above, the minimum attainable noise level in amplitude-modulated-carrier recording is determined by tape-coating irregularities modulating the carrier. This difficulty may be overcome in a frequency-modulated-carrier system in which any amplitude modulation of the carrier is removed by limiting prior to demodulation. Furthermore, with a *wide-deviation* FM system the greater utilization of available bandwidth, as compared to an AM system, will permit a greater signal-to-noise ratio. That these expectations may be realized, with some restrictions, is borne out by our tests as well as by the tests of other investigators.^{11, 12}

An FM-carrier system may be designed so that its operation is, in fact, practically independent of the magnetic and surface characteristics of the tape coating. The limitations of FM recording are found elsewhere. The maximum dynamic range which may be used is determined by the frequency deviation. The maximum deviation, in turn, is determined either by the available bandwidth of the recording-playback system, or by the frequency range over which adequate linearity may be maintained in the modulator and demodulator circuits. In the television tape recorder, the circuit linearity is the limiting factor at present. The maximum signal-to-noise ratio attainable with FM recording is limited by variations in the tape speed. Any change

¹¹ W. T. Selsted, "A Low-Noise FM Recording System," *Jour. Audio Eng. Soc.*, 1, p. 213, April, 1953.

¹² J. T. Mullin, "Video Magnetic Tape Recorder," *Tele-Tech*, Vol. 13, p. 77, May, 1954.

in tape speed as the tape passes over the recording and playback heads causes a corresponding change in the carrier frequency. This results in a noise voltage at the demodulator output. The signal-to-noise ratio, the frequency deviation of the modulated carrier, and the variation in tape speed are interrelated. This interrelationship is shown graphically in Figure 41.

In Figure 41 the ordinate is the signal-to-noise ratio expressed in decibels, assuming that the noise is entirely that due to tape-speed variations. The abscissa is the percentage variation of the tape speed about its mean value during recording or during playback. In preparing this chart it is assumed that tape-speed fluctuations occur in

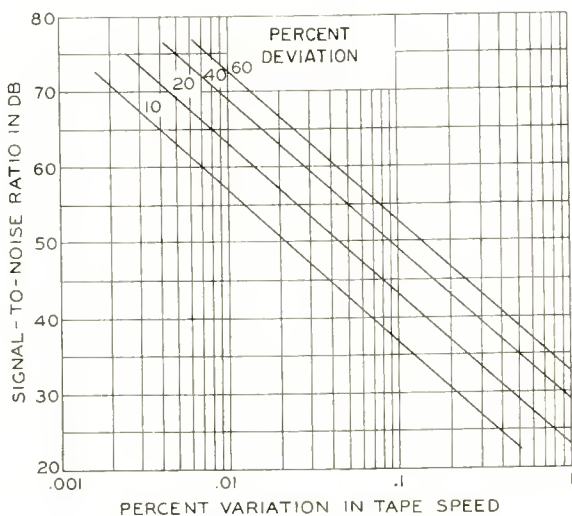


Fig. 41—Relation between tape-speed variation, carrier-frequency deviation by desired audio signal, and the resulting signal-to-noise ratio.

recording as well as in playback, that the recording fluctuations are equal in magnitude to the playback fluctuations, and that recording and playback fluctuations combine in a random manner to give the resultant noise output. The parameter of the lines plotted in Figure 41 is the percentage frequency deviation of the carrier produced by the desired audio signal. An example will illustrate the use of Figure 41 and will indicate the practical reality of the limitation imposed by tape-speed fluctuations.

Assume that the maximum levels of the audio modulating signal produce a carrier frequency deviation of ± 25 kilocycles about a mean frequency of 89 kilocycles. The percentage deviation is $(25/89)$

$\times 100 = 28.2$ per cent peak, or $28.2 \times .707 = 20$ per cent r.m.s. If an audio output level 50 decibels above the noise level is required, what is the maximum speed variation which can be tolerated? In Figure 41 the line for the 20 per cent frequency deviation has, at the ordinate of 50 decibels, an abscissa value of .045 per cent.

Let us now consider some of the techniques used in the FM-carrier recording system. A block diagram of this system is shown in Figure 42. The audio input goes through an amplifier-modulator stage and is used to frequency modulate the oscillator. The modulated oscillator signal passes through a limiter, is amplified and is fed to the recording head. The current in the recording head is, therefore, a frequency-modulated rectangular wave train.

If the rectangular wave passed through the recording and reproducing process without distortion, the output of the playback head would be a series of alternate positive and negative spikes, correspond-

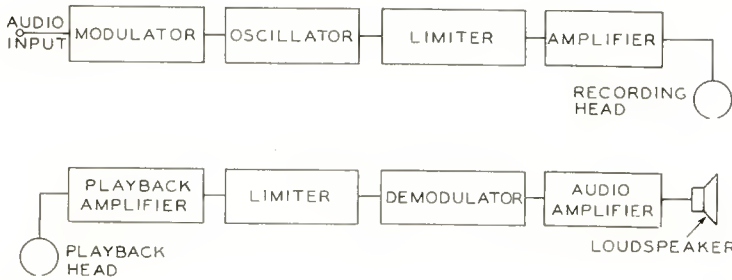


Fig. 42—Block diagram of an FM-carrier audio-recording system.

ing to differentiation of the rectangular wave. This is true because the voltage generated by the playback head is proportional to the time rate of change of flux passing from the tape through the magnetic circuit of the head. With a mean carrier frequency of 90 kilocycles, it would be necessary to transmit unattenuated all harmonics of 90 kilocycles up to at least 1 megacycle in order to achieve the type of reproduced waveform described. The record-playback response characteristic of the system, as depicted in Figure 37, shows that the higher harmonics of the 90-kilocycle rectangular wave are greatly attenuated. As a result, the voltage output of the playback head is very nearly sinusoidal. The high-frequency content could be restored by equalization, as is done in the video channels, but it is simpler to take the sinusoidal voltage and amplify and limit it in the playback amplifier to make a frequency-modulated rectangular wave which is identical to that originally fed to the recording head. This newly formed rectangular

wave is then demodulated to recover the audio. The audio output of the demodulator is amplified and fed to a loudspeaker or to an audio-program line.

The frequency deviation and linearity of the FM system appear to depend on the effort one is willing to expend on the design and adjustment of the modulator and demodulator circuits. A deviation of ± 40 per cent peak with an over-all r.m.s. total harmonic distortion less than 1 per cent is readily attainable, and values of deviation as high as ± 60 per cent have been reported. When testing the FM-carrier system in the television tape recorder, a 90-kilocycle mean carrier frequency was used, and a signal-to-noise ratio of 52 decibels was realized with a 15-kilocycle audio bandwidth. Since the tape speed varies less than .025 per cent at the audio heads, (this is without the benefit of a movable head as used in video playback) the considerations discussed above indicate that, with improved circuitry, a somewhat greater signal-to-noise ratio may be expected.

CONCLUSIONS

Several audio-recording methods have been considered for use in television tape recording systems. The basic limitations of each method have been shown, and typical performance data have been given. In direct recording and in AM-carrier recording the dynamic range as well as the linearity is limited by the magnetic and surface properties of the tape coating. In an FM-carrier system the noise level is determined by variation in tape speed, while the linearity and dynamic range are limited by the electronic circuitry. The information presented for the various audio systems permits a choice of system based on the audio-quality specifications for a particular application and on the specifications of the tape-transport system. The data given are based on the characteristics of existing tape coatings and on known circuitry. Therefore, any significant improvement in tape coatings and in circuitry in the future may affect the choice of audio system.

FIELDS IN IMPERFECT ELECTROMAGNETIC ANECHOIC CHAMBERS*

BY

ROBERT F. KOLAR

RCA Victor Television Division,
Camden, N. J.

Summary—The performance of an electromagnetic anechoic chamber can be predicted from the results of transmission line measurements on small samples of the wall absorbing material. Since the calculation of the field within a room is a near-field problem, the customary Fraunhofer or Fresnel approximations of Kirchhoff's equation cannot be used. However, the problem can be solved fairly accurately if the room is sufficiently large. The calculations have been checked by measurements made in front of a twelve-foot-square wall covered with the absorbing material and with an aluminum sheet.

INTRODUCTION

AN IDEAL anechoic chamber would be a room having walls which absorb all the incident energy. Although a perfect broadband wall covering is at present physically unrealizable, materials can be developed which absorb more than 98 per cent of the incident electromagnetic energy. In the past, anechoic chambers have been designed in an empirical manner. A variety of measurements were made on absorbing materials in order to select the absorber which shows the most promise, and a chamber was then constructed and its performance measured. Since the material for the lining of anechoic rooms suitable for low frequencies is expensive, it is felt that an adequate theory is needed which will be capable of predicting the performance of such a chamber on the basis of measurements on small samples of absorbing material. The purpose of this paper is to relate the reflection coefficient of absorbers, as determined by measurements on small samples, to the performance of a completed room.

TRANSMISSION-LINE MEASUREMENTS

A parallel-plate transmission line can be used to secure data on small samples of absorbing material. Standard slotted-line measuring techniques are used to determine the reflection coefficient of the material.

The justification for using transmission-line measurements to predict the free-space performance of an absorber is obtained by draw-

* This paper was presented in partial fulfillment for the requirements of a Masters Degree at the University of Pennsylvania.

ing an analogy between the transmission-line problem and that of free space. An infinitely long transmission line is self-terminating in the same manner as infinite space if the same propagating mode exists in each case. Furthermore, a finite line is self-terminating if the dissipation along the line causes all reflected waves to arrive at the point of measurement with a magnitude too small to be detected. When a section of lossless line (analogous to a section of space) is connected to a section of highly dissipative line (analogous to the chamber lining) such that no electrical discontinuity exists at the junction, the lossy section will serve as a termination for the dissipationless line. This means that the room lining will terminate the space within the chamber. Since the lossy material terminates the plane wave between the plates of a given line, it will terminate any other size line and therefore will terminate the space in the room.¹⁻³ Using this analogy, measurements can be made on small absorber samples and the results will provide data from which the performance of a larger room can be computed.

EFFECT OF FINITE WALL SIZE

The walls of the chamber will be of finite size. It will be assumed that only first-order reflections need be considered because if the material absorbs 98 per cent of the energy of each incident wave, only 0.04 per cent, a negligible amount, will be reflected at the second incidence. Each wall will be considered individually and the effects of each will be added vectorially in order to determine the combined effect of all the walls. The usual image theory based on an infinite reflector size cannot be used to predict the field within a room with finite-sized walls.

COORDINATE SYSTEM

The system of coordinates to be used in this paper will be the right-hand set shown in Figure 1. The analysis will be based on the response to a short dipole placed in the center of the room and linearly polarized in the x direction. The probe antenna will also be a dipole polarized in the same direction. Any cross polarization component will be neglected. The length of the cubical room will be taken as $2d$, as is shown by Figure 2. The field will be computed along the z axis of the room, which passes through the center of the room and is normal

¹ E. C. Jordan, *Electromagnetic Waves and Radiating Systems*, Prentice-Hall, Inc., New York, 1950, pp. 147, 216.

² John K. Kraus, *Antennas*, McGraw-Hill Book Company, Inc., New York, 1950, p. 360.

³ C. L. Andrews, "Diffraction Pattern In A Circular Aperture Measured In The Microwave Region," *Jour. Appl. Phys.*, Vol. 21, p. 761, August, 1950.

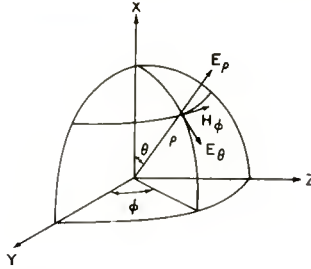


Fig. 1—Coordinate system.

to wall *ABCD*. When the room is in use, both the source and the probe are to be located on the *z* axis. In order to determine the total field along the *z* axis of the room, it is necessary to compute the energy reflected along this axis due to wall *ABCD* and that due to wall *ABFG*.

FIELD EQUATIONS

The fields of an infinitesimal dipole may be written^{1,5}

$$E_{\theta} = \frac{P_0}{4\pi\epsilon} \left[\frac{1}{\rho^3} + \frac{i\beta}{\rho^2} - \frac{\beta^2}{\rho} \right] \sin \theta \exp(-i\beta\rho), \tag{1}$$

$$E_{\phi} = \frac{P_0}{2\pi\epsilon} \left[\frac{1}{\rho^3} + \frac{i\beta}{\rho^2} \right] \cos \theta \exp(-i\beta\rho), \tag{2}$$

$$H_{\phi} = \frac{i\omega P_0}{4\pi} \left[\frac{1}{\rho^2} + \frac{i\beta}{\rho} \right] \sin \theta \exp(-i\beta\rho), \tag{3}$$

where ρ is the distance from the center of the dipole to a specified field

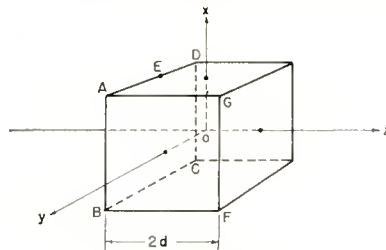


Fig. 2—Cubic room.

¹ S. A. Schelkunoff, *Electromagnetic Waves*, D. Van Nostrand Co., Inc., New York, N. Y., 1943.

⁵ S. Silver, *Microwave Antenna Theory and Design*, McGraw-Hill Book Company, Inc., New York, 1949, p. 93, chapters 5, 6.

point, $\beta = 2\pi/\lambda$, $P_0 = Il/i\omega$, θ and ϕ are as shown in Figure 1; λ is the wavelength. I is the moment of the source, ω is the angular frequency, and ϵ is the dielectric constant of the medium. The time factor $\exp(i\omega t)$ is to be understood present throughout this discussion.

The radial component of the electric field at the surface of the wall $ABCD$ will have its maximum value at the center of the wall, point E , where $\theta = 45^\circ$ and $\cos \theta = 1/\sqrt{2}$ in a cubical room. This value will be

$$E_{\rho_{\max}} = \frac{i P_0 \beta}{2\sqrt{2}\epsilon\pi\rho^2} \exp(-i\beta\rho) \quad (4)$$

from Equation (1) where ρ^{-3} term has been neglected. The component of this vector in the x direction, which is the direction in which the probe antenna is polarized, is again proportional to $\cos \theta$, resulting in a value of

$$E_{\rho_x} = \frac{i P_0 \beta}{4\pi\epsilon\rho^2} \exp(-i\beta\rho), \quad (5)$$

which is the maximum value of the component of the radial field in the x direction within the room.

The magnitude of this term is equal to the maximum value of the ρ^{-2} term in Equation (1). Thus, if the terms in ρ^{-2} and ρ^{-3} are much smaller than the ρ^{-1} term in Equation (1), the radial field is negligible. Furthermore, if the anechoic chamber is used for antenna-pattern measurements, the radial component need not be considered since it is general practice to orient the probe antenna such that only the tangential component of the field, E_θ , excites currents in it. Also, in this problem, both the probe and the source are to be located on the z axis where the radial term is zero since $\theta = 90^\circ$.

SIZE OF ROOM

The purpose of an anechoic chamber is to make it possible to obtain free-space radiation data indoors. Since radiation problems are only concerned with the radiation, or ρ^{-1} term in Equation (1), the induction (ρ^{-2}) and electrostatic (ρ^{-3}) terms must be small enough to be neglected for the measurements to be correct. Therefore, it will be necessary to construct the room large enough to allow the source to be placed far enough from the point of measurement so that the higher-order terms in ρ can be neglected.

If the error introduced by neglecting the induction term is less than one per cent of the total tangential field, the higher-order terms may be considered negligible. Since only the magnitude of the field can be measured, we may write the equation

$$\frac{\left[\frac{\beta^4}{\rho^2} + \frac{\beta^2}{\rho^4} \right]^{1/2} - \frac{\beta^2}{\rho}}{\left[\frac{\beta^4}{\rho^2} + \frac{\beta^2}{\rho^4} \right]^{1/2}} \leq 0.01 \tag{6}$$

for the fractional error in neglecting the ρ^{-2} term in Equation (1), where the ρ^{-3} term has been omitted. Using the identity $(1 + x)^{1/2} = 1 + \frac{x}{2} + \dots$ where $x = \frac{1}{\beta^2 \rho^2}$, it is found that $\rho \geq 1.12 \lambda$ in order for the error to be less than one per cent when only the ρ^{-1} term is used to express the tangential field. This means that with the source in the center of the chamber, the dimensions of a room must be greater than 2.24λ before accurate radiation measurements can be made in it. However, a room 2.24λ on a side will have an error in the incident field greater than one per cent, except very near the walls, unless the terms of higher order than ρ^{-1} are considered. When calculating the total field in such a chamber, the ρ^{-1} term is the only one needed to compute the reflected field. However, the complete expression, including higher powers of ρ , for E_θ given in Equation (1) should be used to compute the direct field of the source.

With the above restriction, the only significant component of the electric field at the surface of the walls is given by Equation (1)

$$E_\theta = \frac{-P_c \beta^2}{4 \pi \epsilon \rho} \sin \theta \exp(-i\beta\rho) = \frac{i 60 \pi I l}{\lambda \rho} \sin \theta \exp(-i\beta\rho), \tag{7}$$

since $\omega = \frac{2 \pi c}{\lambda}$ and $c \epsilon = \frac{1}{120 \pi}$.

DERIVATION OF EQUATIONS

In order that the problem may be more easily visualized, it will be transformed to one of diffraction through an aperture rather than one of reflection from plates. Such a transformation can be made on the basis of Babinet's principle, which states that the problem of transmission through an aperture is complementary to that of reflection from a plate, where the incident fields are also complementary.⁶ There-

⁶ C. J. Bouwkamp, "Diffraction Theory," *Reports on Progress in Physics*, The Physical Society, London, Vol. 17, p. 35, 1949.

fore, each wall will be replaced by an aperture in a perfectly absorbing screen of infinite extent. A perfectly absorbing screen will be defined as a perfectly reflecting screen with the reflected fields on the illuminated side of the screen being neglected. Image sources having amplitudes equal to $\alpha E_s e^{i\delta}$ will be located outside the apertures (walls). The magnitude of the reflection coefficient of the material is α , E_s is the magnitude of the source within the room, and δ is the phase angle of the absorbing material. α and δ are determined by slotted-line measurements on small samples of the material. If the correct phase angle, referred to the surface of the wall covering, is used, the image sources can be located outside the room at a distance equal to that of the true source from the wall inside the room.

Diffracted Field—In the past few years, many theories of diffraction have been presented in the literature.⁶ This study will be based primarily on Kirchhoff's theory, subject to the following restrictions:

1. The radial component of the electric field and the tangential component of the magnetic field in the aperture are the same as the respective values of the incident free-space field. That is, the value of the free-field components are not changed by the presence of the aperture.
2. Only linearly polarized sources will be considered; any cross-polarization component will be neglected.

Kirchhoff's scalar diffraction theory does not, in general, give a true solution of the diffraction of electromagnetic waves through an aperture since the values given on the shadow side of the screen are not consistent with Maxwell's equations. It is, therefore, necessary to introduce terms due to time-varying line charges along the edge of the aperture in order to account for this inconsistency. The complete expression for the field diffracted through the aperture shown in Figure 3 is then^{5, 6}

$$\underline{E}_P = -\frac{1}{4\pi} \int_S \left(\psi \frac{\partial \underline{E}}{\partial n} - \underline{E} \frac{\partial \psi}{\partial n} \right) dS + \frac{1}{4\pi} \int_{\Gamma_S} \psi (\underline{E} \times \underline{\tau}) dS - \quad (8)$$

$$\frac{1}{4\pi i \omega \epsilon} \int_{\Gamma_S} \nabla \psi (\underline{\tau} \cdot \underline{H}) dS$$

where $\psi = r^{-1} \exp(-i\beta r)$ is a solution of the wave equation on the surface S and represents the spherical wave front upon which Huygen's principle is based, and \underline{E} is the incident electric field; $\underline{\tau}$ is a unit vector

tangent to the boundary Γ_s between the illuminated and dark side of the screen, and \underline{n} is the unit vector normal to an area in the aperture.

The above equation is in MKS units and is true for periodic fields having the time factor $\exp(i\omega t)$.

The contributions due to the line integrals at a point on the axis of the aperture are zero^{5, 7} when the aperture is symmetrical about the z axis. However, the contribution due to the line charges at a point on a line parallel to the aperture must be given further consideration. Since these line charges make significant contributions only near the edge of the aperture and in the shadow region, and we are only concerned here with the field in the geometrically illuminated zone at distances greater than one wavelength, the contributions of the line integrals may be considered negligible. Furthermore, inasmuch as

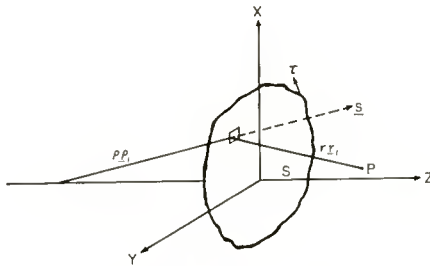


Fig. 3—The diffracted field.

the wall is highly absorbing, it is doubtful that there would be any significant charges collected on the boundary.

There is considerable experimental evidence in the literature to justify neglecting the contribution of the line integrals at distances greater than one wavelength. For example, Andrews reported on some measurements along the axis of a circular aperture illuminated by plane waves.³ He found this assumption could be justified as long as measurements were not made at distances less than a quarter wavelength from the aperture. Some similar measurements were made by H. K. Severin. His results are also published in Andrews' paper.³ It is interesting to note that in some regions where Andrews' experimental points were higher than the theoretical curve, those of Severin were lower.

If calculations are limited to that region in which the line integrals may be neglected, that is, field points in the region bounded by the

⁷ G. A. Woonton, D. R. Hay, and E. L. Vogan, "An Experimental Investigation of Formulas for the Prediction of Horn Radiator Patterns," *Jour. Appl. Phys.*, Vol. 20, p. 71, January, 1949.

geometric projection of the aperture along the z axis, the diffracted field can be written as the scalar equation.

$$u_p = -\frac{1}{4\pi} \int_S \left(\psi \frac{\partial u}{\partial n} - u \frac{\partial \psi}{\partial n} \right) dS, \tag{9}$$

where u represents the particular field component involved.

Wall Illumination—For a wall which is parallel to the short dipole source within the room, the image source is located parallel to the x axis at $(0, 0, -d)$ as shown by Figure 4. If the equation for the field of the source within the room at the wall surface is

$$E_\theta = \frac{i 60 \pi I l}{\lambda \rho} \sin \theta \exp(-i\beta\rho), \tag{7}$$

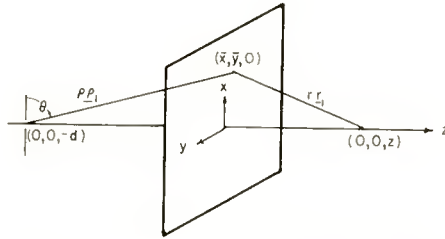


Fig. 4—Diffraction by a square aperture.

the field at the wall due to the image source located at the point $(0, 0, -d)$ can be modified in amplitude and phase to give

$$E'_\theta = \frac{i\alpha 60 \pi I l}{\lambda \rho} \sin \theta \exp(-i\beta\rho) \exp(i\delta). \tag{10}$$

The slotted-line measurements only give values of the reflection coefficient for normal incidence and parallel polarization. The reflection coefficient for large angles of incidence is greater than for normal incidence. However, no significant increase in the reflection coefficient occurs until the angle of incidence becomes greater than 30 degrees.⁸ For a cubical room the $\sin \theta$ term in Equation (10) will vary from 1.0 at the center of the wall to 0.707 at the edges. Since the reflection coefficient is greatest, although not by a large amount at the edges,

⁸ A. Hund, *Short Wave Radiation Phenomena*, McGraw-Hill Book Company, Inc., New York, 1952, pp. 285, 829.

little error will be introduced by allowing the $\sin \theta$ term of Equation (10) to assume a value of unity.

The top and bottom walls are oriented normal to the dipole source in the center of the room. In this case the polarization of the source is perpendicular to the wall and the magnitude of the $\sin \theta$ term is zero at the center of the wall. It increases to a value of 0.707 at the edges. In addition, the reflection coefficient for perpendicular polarization is smaller than for parallel polarization except for angles of incidence very nearly normal.⁸ The contribution of these walls is of the same order of magnitude as the decrease in illumination which was neglected in the case above. The accuracy of the solution will not be reduced by letting the $\sin \theta$ term equal zero for the walls normal to the dipole source, thus neglecting the contribution due to these walls.

It follows that the illuminating function for the walls parallel to the source can be written, by setting $\sin \theta = 1$ in Equation (10);

$$E_{\theta'} = \frac{i\alpha 60\pi Il}{\lambda\rho} \exp(-i\beta\rho) \exp(i\delta), \tag{11}$$

and the total contribution due to the walls normal to the source will be neglected.

Field Reflected from Walls—Using the value of $E_{\theta'}$ given by Equation (11), we find that⁵

$$\frac{\partial E_{\theta'}}{\partial n} = -\frac{i\alpha 60\pi Il}{\lambda\rho} \left[\frac{1}{\rho} + i\beta \right] \exp(-i\beta\rho) \exp(i\delta), \tag{12}$$

and with $\psi = r^{-1} \exp(-i\beta r)$, $\frac{\partial \psi}{\partial n} = r^{-1} (i\beta + r^{-1}) \underline{n} \cdot \underline{r}_1 \exp(-i\beta r)$

where $\underline{n} = \underline{s}$ and is normal to the elementary aperture $dxdy$ (see Figure 3). We find upon substitution in Equation (7) that the field on the shadow side of the aperture is

$$E_{\theta p} = \frac{i\alpha 15 Il \exp(i\delta)}{\lambda} \int_S \frac{i\beta \exp[-i\beta(r + \rho)]}{r\rho} (1 + \underline{n} \cdot \underline{r}_1) dS$$

$$+ \frac{i\alpha 15 Il \exp(i\delta)}{\lambda} \int_S \frac{\exp[-i\beta(r + \rho)]}{r\rho^2} dS +$$

$$\frac{i\alpha 15 Il \exp(i\delta)}{\lambda} \int_S \frac{\exp[-i\beta(r + \rho)]}{r^2 \rho} \underline{n} \cdot \underline{r}_1 dS. \quad (13)$$

Inasmuch as the higher order terms in ρ and r have been shown to be negligible, the last two integrals in Equation (13) are negligible and the diffracted field becomes

$$E_{\theta F} = \frac{-\alpha 30 \pi Il \exp(i\delta)}{\lambda^2} \int d\bar{y} \int \frac{\exp[-i\beta(r + \rho)]}{r \rho} (1 + \underline{n} \cdot \underline{r}_1) d\bar{x}, \quad (14)$$

where $d\bar{x}d\bar{y} = dS$.

The difference between this equation and the one which is normally used for such problems is that the differential area is taken normal to a ray from the source. This results in a value for $\underline{n} \cdot \underline{r}_1$ which is different from that usually given. This result comes about because the illuminating field cannot be assumed to be a plane wave since the source is at a distance from the aperture comparable to the dimensions of the aperture.

This expression will be used without further assumptions to determine the fields within an anechoic chamber.

It is now of interest to determine the contribution to the total field due to the walls normal to the principal axis of the room, since the actual calculations will be limited to that axis. From Figure 4 it can be seen that

$$\rho = (\bar{x}^2 + \bar{y}^2 + d^2)^{1/2} \text{ and } r = (\bar{x}^2 + \bar{y}^2 + z^2)^{1/2}. \quad (15)$$

The direction numbers of ρ are $a_1 = \bar{x}$, $b_1 = \bar{y}$, and $c_1 = d$. Those of r are $a_2 = -\bar{x}$, $b_2 = -\bar{y}$, and $c_2 = z$. Then $\underline{n} \cdot \underline{r}_1$, where \underline{n} is normal to the elementary area dS , is

$$\underline{n} \cdot \underline{r}_1 = \frac{zd - \rho^2 + d^2}{r\rho}. \quad (16)$$

If the above results are substituted in Equation (14) and all values are normalized with respect to the wavelength, then the field reflected from a wall normal to the axis of computation and parallel to the dipole source at the center of the room is

$$E_{\theta F} = \frac{-120 \pi Il \alpha \exp(i\delta)}{\lambda^2} \int_0^d d\bar{y} \int_0^d \left[\frac{r\rho + zd}{r^2 \rho^2} \right]$$

$$+ \frac{d^2 - \rho^2}{r^2 \rho^2} \Big] \exp[-i2\pi (r + \rho)] d\bar{x} = I_a (\bar{x}, \bar{y}, z). \tag{17}$$

If the origin of coordinates is shifted to the center of the room, the contribution to the total field within the room due to one of the walls normal to z will be

$$E_{\theta^1 P} = I_a (\bar{x}, \bar{y}, d + z), \tag{18}$$

and that due to the other wall normal to z will be

$$E_{\theta^2 P} = I_a (\bar{x}, \bar{y}, d - z), \tag{19}$$

where the room is $2d$ long.

In order to solve for the field reflected from the two side walls parallel to the z axis of the room, refer to Figure 5 where

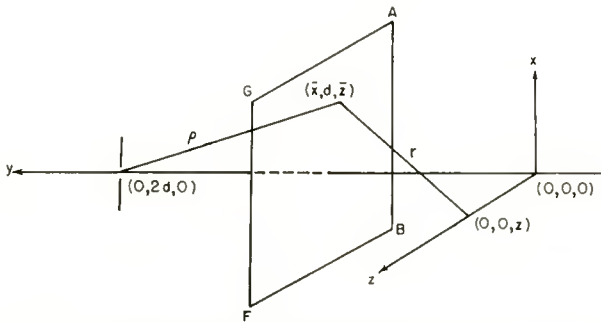


Fig. 5—Field along a line parallel to the aperture.

$$\rho = (\bar{x}^2 + d^2 + \bar{z}^2)^{\frac{1}{2}} \text{ and } r = [\bar{x}^2 + d^2 + (z - \bar{z})^2]^{\frac{1}{2}}.$$

The direction numbers of ρ are $a_1 = \bar{x}, b_1 = -d, c_1 = \bar{z}$; those of r are $a_2 = -\bar{x}, b_2 = -d,$ and $c_2 = z - \bar{z}$. Then,

$$\underline{n} \cdot \underline{r}_1 = \frac{2d^2 - \rho^2 + z\bar{z}}{r\rho}. \tag{20}$$

Again substituting in Equation (14) and normalizing with respect to the wave-length,

$$E_{\theta^3 P} = \frac{-\alpha 60 \pi I l \exp(i\delta)}{\lambda^2} \int_0^d d\bar{x} \int_{-d}^d \left[\frac{r\rho + 2d^2 - \rho^2 + z\bar{z}}{r^2 \rho^2} \right] \exp[-i2\pi (r + \rho)] d\bar{z} = I_b (\bar{x}, d, \bar{z}; z - \bar{z}), \tag{21}$$

and the contribution due to the opposite wall will be the same. The total reflected field within the room will be

$$E_x = I_a (\bar{x}, \bar{y}, d + z) + I_a (\bar{x}, \bar{y}, d - z) + 2I_b (\bar{x}, d, \bar{z}; z - \bar{z}) \quad (22)$$

and the direct field is given in Equation (1). If the room is large enough, the direct field can be written

$$E_0 = \frac{i 60 \pi I l}{\lambda^2 z} \exp(-i2\pi z), \quad (23)$$

where again all dimensions are normalized with respect to the wavelength. Therefore, the total field within the room is

$$E_t = E_x + E_0. \quad (24)$$

THEORETICAL RESULTS

The integrals of Equations (17) and (21) were evaluated numerically on an IBM Model 650 computer. The integration was performed by integrating along lines corresponding to fixed values of \bar{y} , for \bar{x} going from 0 to d . The Newton-Cotes numerical integration formulas were used for regularly spaced points. When the integrations on \bar{x} were completed for equally spaced \bar{y} from 0 to d , a single numerical integration of these results gave the value of the double integral. This process was repeated for each value of z which was plotted.

Inasmuch as the calculation of a double integral requires a large amount of machine time, it was necessary to perform rather extensive tests on the integrand in order to determine the largest increment of \bar{x} , \bar{y} , and \bar{z} which could be used to obtain the required accuracy in the shortest time. It was found that it was necessary to use an increment of $\bar{x} = \bar{y} = \bar{z} = 0.0625$ in order to obtain an accuracy of three significant figures.

Since the evaluation of the integrals of Equations (17) and (21) is extremely laborious, especially for large values of d , they have only been computed for a value of $d = 1.25$. This is the lowest value for which the theory can be expected to give reliable results. As has been pointed out earlier, the exact expression for E_θ given in Equation (1) must be used for E_0 in Equation (24) in the calculations of the fields in a room having dimensions as small as 2.5 wavelengths.

Figure 6 shows curves of the total field along the axis of a cubical

room 2.5 wavelengths on a side for several values of the power reflection coefficient α^2 . In these curves the reflection coefficient is expressed as a power ratio rather than a voltage ratio in order to comply with customary practice. If the room were larger, the increased path difference in wavelengths would result in more oscillations in the field in the room. However, the increased attenuation due to the greater distance which the reflected wave travels would result in oscillations of smaller magnitude, except very near the walls. Figure 7 is a curve showing the maximum deviation from free-space values to be found in a 2.5

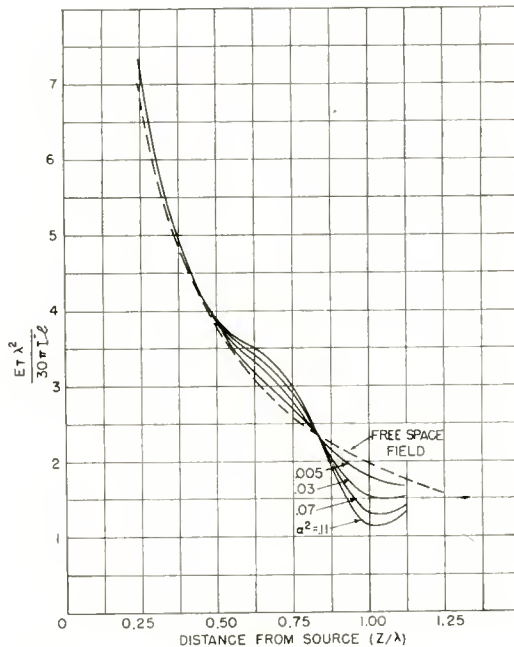


Fig. 6—Field along axis of a 2.5λ cubic room.

wavelengths cubic room as a function of the reflection coefficient of the walls. The data for Figure 7 was obtained from a series of curves like those of Figure 6. Inasmuch as a larger room will have reflections of lower magnitude, this curve represents the maximum error to be expected in a room having walls with a given reflection coefficient. The curve is shown as a broken line above $\alpha^2 = 0.10$ since beyond this point the magnitude of the energy reflected at the second incidence can no longer be neglected. Therefore, if the reflection coefficient of the walls is greater than 0.10 , the maximum error in the observed field will be greater than the value given in Figure 7.

When the room is to be used for antenna-pattern or other relative rather than absolute measurements, a constant loss of 2 or 3 decibels would have no effect on the data if the antennas were sufficiently small. If, however, the reflection coefficient were high, the maximum slope of the curve in Figure 6 would also be high and an exact determination of the error in the field at the point of measurement would be difficult or impossible.

EXPERIMENTAL RESULTS

The preceding theory was developed on the assumption that only first-order reflections need be considered. The total field within the room is made up of the direct wave from the source and the reflected field. The total reflected field along an axis of the room is expressed by two integrals, one for the field along a line parallel to a wall and

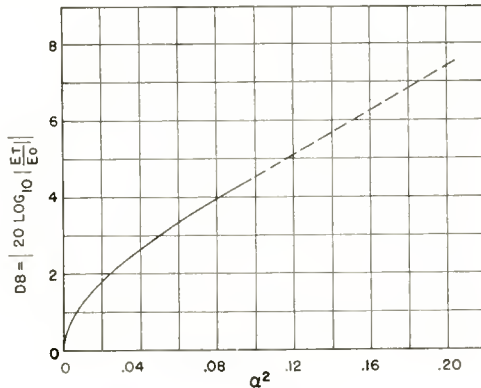


Fig. 7—Error in measured field in a 2.5λ cubic room versus reflection coefficient of walls.

another along a line normal to a wall. If these two integrals can be verified experimentally, the accuracy of the theory will have been proved.

The solid curves of Figures 8a, b, c, and d, were obtained by adding the results of the tabulation of Equations (17) and (21) to the value for E_θ given by Equation (1). The experimental points which are indicated by round dots were obtained by measuring the field in front of a wall 12 feet square. The transmitting and receiving antennas were vertically polarized dipoles. Two values for α were used. The curves marked $\alpha = -1$ were obtained by measuring the field in front of a 12-foot-square aluminum sheet. Those for $\alpha^2 = 0.02$ were obtained from measurements on a wall constructed of material which transmission-line

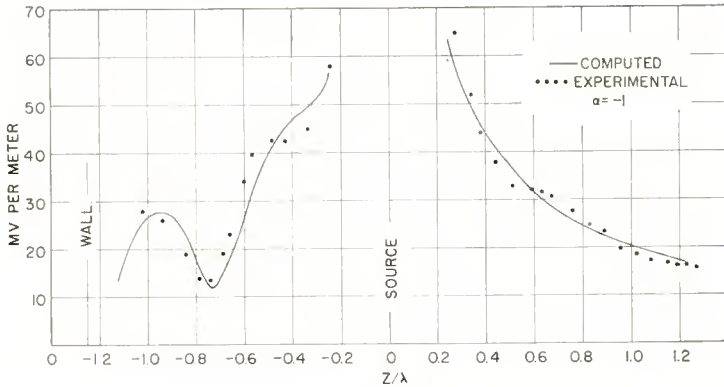


Fig. 8a—Field along a line normal to a perfectly conducting wall.

measurements showed had a reflection coefficient of two per cent. Note that experimental agreement with theory is good even for the perfectly conducting wall, indicating that Kirchhoff's equation is valid at distances as close as 0.25 wavelength from an aperture having dimensions comparable to a wavelength, provided no unjustified assumptions are made in order to evaluate the equations.

Unfortunately, in making the measurements there was no area available which was sufficiently clear of reflecting objects so that unwanted reflections from objects other than the wall could be completely ignored. The proximity of the earth and other good reflectors in the neighborhood could account for the minor oscillations which

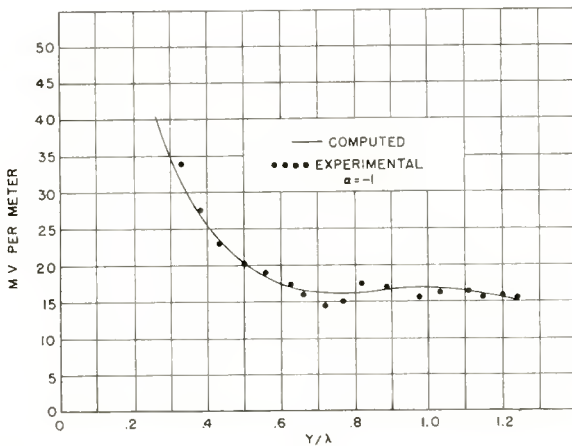
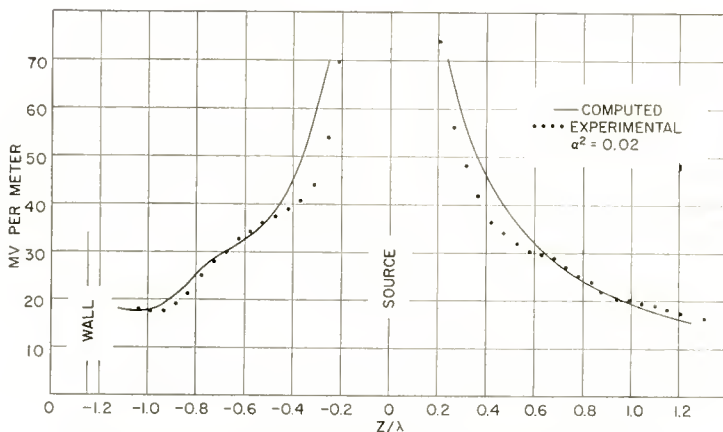


Fig. 8b—Field along a line parallel to a perfectly conducting wall.



8c—Field along a line normal to an absorbing wall.

are present in some of the curves. In view of the above and other experimental difficulties, the agreement with theory can be considered excellent.

CONCLUSIONS

A method has been developed which enables the performance of an electromagnetic anechoic chamber to be predicted from the results

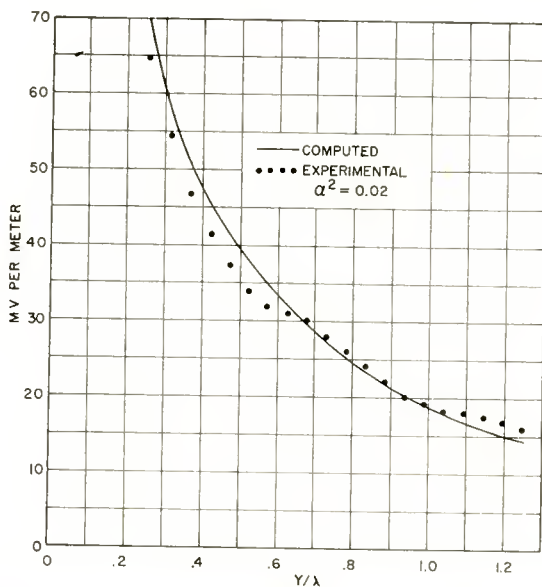


Fig. 8d—Field along a line parallel to an absorbing wall.

of transmission-line measurements on small samples of absorbing material. A curve is given to be used to compute the performance of a cubical room 2.5 wavelengths on a side from the transmission-line measurements. The theory which is used is basically that of Kirchhoff, except that some of the approximations which are usually made in order to simplify the calculations are not used. The resulting equations have been checked by making measurements of the field in front of a twelve-foot square wall. The measurements were made for a very high and for a very low reflection coefficient. This study has shown that Kirchhoff's diffraction theory is capable of predicting the near field of square apertures having dimensions as small as 2.5 wavelengths along lines which are either normal to the aperture or parallel to it and located in a plane of symmetry of the aperture. Care must be taken in evaluating the integrals and an accurate expression for the aperture illumination must be used.

ACKNOWLEDGMENTS

The sub-routine used to evaluate the double integrals was developed by Franz Edelman of RCA Laboratories, Princeton, N. J. The testing of the integrand and programming of the computer were done by Mrs. Rosemary Johnson of the RCA Victor Television Division, without whose assistance the integrals would not have been evaluated. The author wishes to express his appreciation to Robert Serrell of RCA Laboratories for his cooperation in making machine time available for calculating the results, and to M. S. Corrington of the RCA Victor Television Division, and Charles Polk of the University of Pennsylvania for their guidance in the preparation of this paper.

PERFORMANCE AND DESIGN OF LOW-NOISE GUNS FOR TRAVELING-WAVE TUBES

BY

R. C. KNECHTLI AND W. R. BEAM

RCA Laboratories,
Princeton, N. J.

Summary—This paper discusses qualitatively the factors determining the performance of low-noise guns in microwave beam amplifiers. The discussion is substantiated by systematic measurements on a three-region low-noise gun.

The main conclusions are: (1) That sharp potential discontinuities on the electron beam should be avoided in a low-noise gun. This is an argument against guns of the velocity-jump type. (2) That an exponential type of space-charge wave transformation is favorable because it minimizes such potential discontinuities. (3) That 3-region guns or, more generally, multi-region guns, represent good and mechanically simple approximations to such transformers. This explains the outstanding performance obtained for the last 3 to 4 years with this type of gun.

Based on these considerations and some empirical data obtained from successful low-noise traveling-wave tubes, directions are given for the optimum choice of the gun design parameters.

INTRODUCTION

ACCORDING to low-noise traveling-wave-tube theory^{1, 2} and to the transmission line analog³ of a modulated electron beam, the electron gun of a low-noise traveling-wave tube can be considered as a space-charge wave transformer matching the effective beam impedance $R_a = V_a/I_a$ at the potential minimum to the desired beam impedance Z_b at the helix input. This is illustrated by Figure 1. The terminating impedance R_a of this transformer is determined by the electron velocity and beam-current fluctuations at the potential minimum in front of the cathode. It is assumed that the r-f voltage V_a is that of Rack,¹ and the current I_a is full shot noise. The terminating

¹ S. Bloom and R. W. Peter, "A Minimum Noise Figure for the Traveling-Wave Tube," *RCA Review*, Vol. XV, p. 252, June, 1954.

² S. Bloom, "The Effect of Initial Noise Current and Velocity Correlation on the Noise Figure of Traveling-Wave Tubes," *RCA Review*, Vol. XVI, p. 179, June, 1955.

³ S. Bloom and R. W. Peter, "Transmission Line Analog of a Modulated Electron Beam," *RCA Review*, Vol. XV, p. 95, March, 1954.

⁴ A. J. Rack, "Effect of Space Charge and Transit Time on the Shot Noise in Diodes," *Bell Sys. Tech. Jour.*, Vol. 17, pp. 592-619, October, 1938.

impedance, normalized with respect to the beam's characteristic impedance, is then given by

$$r_a = 1.61 \times 10^{-9} R_c T_c^{1/4} \frac{f}{\sqrt{i_0}}, \tag{1}$$

where

- r_a = normalized impedance at potential minimum
- = ratio of terminating impedance R_a to characteristic beam impedance W_0 ,

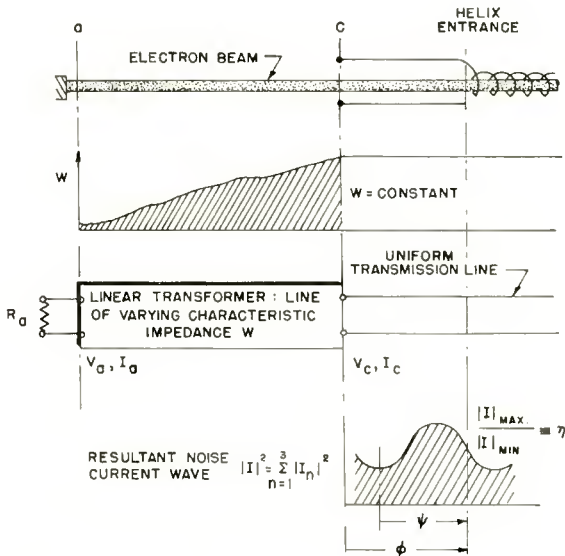


Fig. 1—Noise wave and optimization parameters.

i_0 = beam current density at potential minimum in amperes m^2 ,

T_c = cathode temperature in $^{\circ}K$,

f = signal frequency in cycles per second.

This relation is the same as that derived by Bloom and Peter.¹ The factor 1.61 of Equation (1) (instead of 1.52 as in Bloom and Peter's paper) arises from substituting $(\bar{v}_{0a})^2$ instead of $\overline{v_{0a}^2}$ in Equation (19) *et seq.* of Bloom and Peter. Numerical applications of this equation for typical microwave tubes indicate that r_a can be made to be nearly unity with reasonable cathode current densities.

The first-order theory of low-noise traveling-wave tubes shows that

minimum noise figure is obtained for relatively small standing-wave ratio (SWR) of noise current at the helix input. For practical values of Pierce's parameters QC and d , this SWR varies between approximately 1.5 and 3.5. Therefore (considering that one can make $r_a \cong 1$) the design of a low-noise gun can be reduced to that of a space-charge wave transformer bridging a large ratio of characteristic beam impedances with little mismatch. (For the definition of the characteristic beam impedance, the ratio of characteristic beam impedance at helix input to that at the potential minimum is found in practical cases to be several hundreds to one.) One attack on this problem is to change the characteristic beam impedance between the potential minimum and the helix input region smoothly and slowly. In the transmission line analog, this is equivalent to a transmission line transformer consisting of a transmission line whose impedance varies in the said smooth fashion. The exponential transmission line is a particular example of this as a transformer; it provides relatively good match for quite short electrical lengths.

The exponential space-charge wave transformer is defined as a region in which the characteristic beam impedance, W , increases exponentially with phase angle, ϕ ;

$$W = W_0 e^{k(\phi - \phi_0)}. \quad (2)$$

The phase angle is defined by the relation

$$\phi - \phi_0 = \int_{z_0}^z \frac{2\pi}{\lambda_p} dz, \quad (3)$$

where λ_p is the plasma wavelength of the beam, and z is the distance along the beam (z is defined as increasing from cathode to collector). Because of its mathematical simplicity, such an exponential transformer is readily amenable to analysis. This analysis and the basic properties of this type of transformer are presented in another paper.⁵ In particular, Reference (5) shows that mismatch introduced by a transformer with $k \leq 1$ gives an SWR ≤ 3 from a matched load.

From these considerations, one good way of producing a low-noise gun is to design it as an approximately exponential transformer, with a sufficiently small k , e.g., $k \leq 1$. To carry this out, one must compute

⁵ A. L. Eichenbaum and R. W. Peter, "An Exponential Low-Noise Gun for Beam Type Amplifier," to be published.

the d-c potential distribution required to produce along the beam an exponential increase of characteristic impedance of the type expressed by Equation (2). Such a computation presented in Reference (5), shows that the variation of d-c potential with distance (V_0 versus z) required to fit an exponential increase of characteristic beam impedance with ϕ in typical cases is not far from linear. This applies in the range of beam potentials from a few volts up to helix potential, if the latter does not exceed 1000 volts, for typical geometries. Such a quasi-linear potential distribution presents three important advantages:

1. It can readily be approximated by means of plane parallel apertured electrodes.
2. A linear potential distribution results in a minimum of electrostatic lens effects. Because of the undesirable noise increase caused by such effects,⁶ this quality is particularly valuable.
3. Numerical computations show that the physical length required to perform an exponential space-charge transformation between first-anode and helix potential³ is reasonably short. Assuming a first-anode potential not lower than 20 volts, a helix potential not higher than 1000 volts, and $k \leq 1$ one finds typical lengths of the order of $\frac{1}{2}$ inch.

Hence, between first anode and helix a nearly exponential impedance transformation meets the following needs of low-noise guns: low mismatch, short length, easy construction.

THE MULTI-REGION GUN

For the design of a complete low-noise gun, the above does not suffice. Indeed, in the vicinity of the potential minimum the shape of the potential distribution along the beam is determined essentially by space charge rather than by the externally applied potentials and, therefore, requires special attention. Furthermore, a certain amount of adjustability will also be required from a low-noise gun; this means that both the noise-current SWR and the position of the noise-current minima in the helix-input region should be adjustable by means of the gun potentials. A single exponential transformer between potential minimum and helix input (assuming this could be realized) does not satisfy this requirement. These considerations lead to the concept of the multi-region gun, exemplified by the three-region gun used with great

⁶ R. C. Knechtli, "Effect of Potential Discontinuities on Beam Noise," presented at "Conference on Electron Tube Research," Boulder, Colo., June, 1956.

success for the last 3 to 4 years. The basic idea is to cascade a number of separately adjustable transforming regions.

A typical multi-region gun is shown in Figure 2. It consists of a "triode section" followed by a number of plane parallel and properly spaced apertured electrodes. The triode section consists of the cathode, a beam-forming electrode (often called the grid) and an apertured positive electrode referred to as the first anode. The space between the cathode and the first anode is called the first region of the gun; the space between first and second anodes is the second region, etc.

It is evident, then, that each region from the second to the final region before the helix can be considered in first approximation as an exponential transformer since in first approximation, the beam potential increases linearly from one anode to the next. (This is not the case between cathode and first anode, hence the separate treatment of this region.)

The steepness of the exponential transformation (factor " k ") in

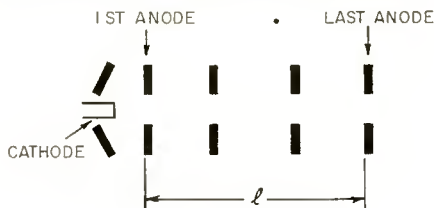


Fig. 2—Multi-region gun.

a given region is controlled by the potential difference between the two anodes limiting this region. When this difference of potential is increased while the mean potential of the regions remains nearly unchanged, the steepness of the transformation in this region increases. This can be seen by expressing k for the region considered, as follows:

$$k = \frac{\log \left(\frac{W_2}{W_1} \right)}{\bar{\beta}l} \quad (4)$$

Equation (4) results from Equations (2) and (3) if l is the length of the region considered, $\beta = 2\pi/\lambda_p$, and $\bar{\beta}$ is the *average value* of β in this region; W_1 and W_2 are the characteristic beam impedance at the beginning and at the end of this region. According to the definition³ of W ,

$$\frac{W_2}{W_1} = \frac{p_2}{p_1} \left(\frac{V_2}{V_1} \right)^{\frac{3}{2}}, \quad (5)$$

where p = plasma frequency reduction factor and V_1 and V_2 are the d-c beam potentials at the ends of the region. Let $[V_2 - V_1]$ increase but $\sqrt{V_1 V_2}$ remain about constant. Then V_2/V_1 and, though Equation (5), W_1/W_2 increase, while $\phi = \bar{\beta}l$ does not change appreciably when the mean potential $\sqrt{V_1 V_2}$ remains unchanged. It follows from Equation (4) that under these conditions k does increase (q.e.d.).

One may also predict how the position of a noise-current minimum in the helix region is affected by a change of anode potentials. For this purpose, one observes that the plasma wavelength, λ_p , increases with increasing beam potential. By raising the potential of any anode of the gun, the average potential of the gun as a whole is increased. This means, according to Equation (3), that the total phase angle from cathode to last anode is reduced. The cathode side corresponds to the termination of the space-charge wave transformer, and this termination remains unchanged when the anode potentials are varied if the beam current is held constant. Hence, a decrease of phase angle between cathode and last anode corresponds to a motion of the noise-current standing-wave pattern away from the gun and towards the collector. Under these conditions, increasing the potential of any anode in the multi-region gun must shift the noise-current minima in the helix region away from the cathode; conversely, decreasing any anode potential shifts the noise-current minima towards the cathode.

These remarks lead to a good understanding of the behaviour of all regions of a multi-region gun from the second on to the last one. It remains to examine the space-charge wave transformation in the first region. The first region or triode section of a multi-region gun is designed as a "Pierce gun" to insure uniform laminar flow. By letting the cathode protrude through the beam-forming electrode, the fields at the cathode surface can be given various degrees of divergence (or convergence), depending on the applied potentials, without introducing large distortions of flow near the cathode edge. This feature is found to be of considerable importance. For the case of parallel flow* in an infinite beam ($p = 1$), the transformation between potential minimum and first anode may be computed by means of the Llewelyn-Peterson equations. Such a computation shows that for beam potentials higher than a few volts, the space-charge wave transformation is a

* In this text, "parallel flow" means operation wherein the beam potential varies with distance in the same way as in a planar Child's-law diode.

steep exponential transformation whose factor " k " approaches a limiting value of 2.12. Such a steep transformation in the first region of the gun is undesirable because whatever the termination at the potential minimum (matched or mismatched), a considerable SWR appears at the first anode. From this point of view, convergent flow is even worse. Since a small SWR is needed at the helix input, the mismatch produced in the first region of the gun would have to be compensated by a corresponding mismatch or discontinuity in another part of the gun. This means another region of high k which would be rather critical in adjustment and would be obtainable only by use of very strong fields. Such fields produce electrostatic lens effects, which have been found undesirable because they increase the noisiness of the beam.⁶ The steep space-charge wave transformation obtained in the first region of the gun with the potential distribution corresponding to parallel or to convergent flow should therefore be avoided.

A closer examination of the variation of characteristic beam impedance with distance in the immediate vicinity of the potential minimum shows that this variation is initially very slow; the transformation obtained between the potential minimum and any plane of the beam at a d-c potential not higher than a few tenths of a volt is nearly equivalent to the transformation obtained by a drift space ($k \approx 0$). (This can be seen, e.g., from Figure 4 of Reference (3).) Therefore, there is no need to modify the potential distribution in the immediate vicinity of the potential minimum.* From potentials of a few tenths of a volt to the first-anode potential, however, the situation is different. For parallel flow, the characteristic beam impedance rises more and more steeply with increasing distance and d-c potential along the beam; this leads to the generally steep transformation characteristic of parallel flow. Consequently, in this latter part of the first region of the gun, the d-c potential distribution along the beam should be modified to produce a transformation less steep than that of perfect parallel flow. This is done by reducing the first-anode potential to a value lower than required for parallel flow, and increasing the potential of the beam-forming electrode to less negative values to keep the beam current constant. This process modifies only negligibly the potential distribution and space-charge wave transformation in the immediate vicinity of the potential minimum, mainly because the confining magnetic field at the cathode prevents excessive beam divergence. From a few tenths of a volt up to first-anode potential, however, this departure from perfect parallel flow conditions has

* Of course, the assumption that the single-valued velocity of the transmission line analog is applicable may be untenable in this region.

important beneficial effects. These effects may be analyzed as follows. On one hand, the rate of potential increase along the beam is reduced; according to the definition of the characteristic beam impedance, this leads to a less steep increase of characteristic beam impedance with distance away from the cathode. On the other hand, the general reduction of beam potential corresponds to a reduction of plasma wavelength and an increase of the phase angle $\phi - \phi_0$ (related to λ_p by Equation (3)) between any two given planes of this region. In summary, when the first-anode potential is depressed below its parallel flow value, the rate of increase of characteristic beam impedance with distance decreases, while the rate of increase of electrical length with distance increases. Hence, the rate of increase of characteristic beam

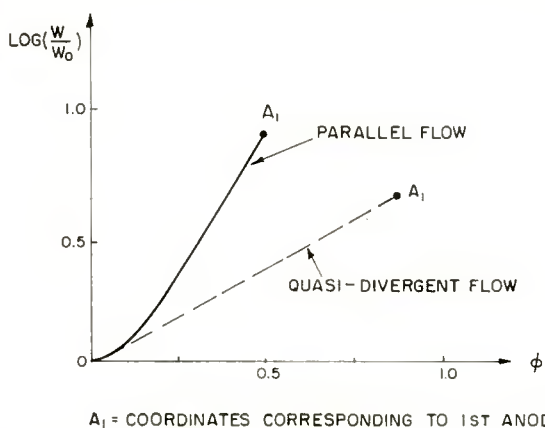


Fig. 3—Characteristic beam impedance versus phase angle in first region; qualitative representation.

impedance with electrical length is reduced even more when the first-anode potential is reduced at constant beam current. This is illustrated by Figure 3, and is precisely what is desired.

A lower first-anode potential and a higher beam-forming electrode potential (with respect to the values required for parallel flow) tend to produce a diverging beam. The focusing magnetic field at the cathode limits this divergence; however, it may produce spatial variations in beam diameter. It seems appropriate to call this condition "quasi-divergent flow." From the reasoning above, quasi-divergent flow appears desirable because it results in a less steep space-charge wave transformation and less mismatch in the first region of the gun.

This understanding of the space-charge wave transformation in the various regions of a multi-region low noise gun enables one to

visualize the performance of such a gun as follows. Starting from normal operating potentials which establish a smooth transformation and then raising the voltage of *one* intermediate anode will increase the k in one region, and decrease it in another. The effect of this will be a greater standing-wave ratio if the original value represented a matched condition between the potential minimum and helix input. At the same time, the electrical length of the transformer is decreased, because the average voltage is increased. This results in a *shifting of the standing wave* away from the cathode. A decrease of voltage will, for the same reason as before, cause an increase of SWR, while the standing wave will move towards the cathode. If one starts with only a slight mismatch at the potential minimum (by proper choice of the beam current density, as indicated by Equation (1)), SWR's almost down to unity can be attained readily in a gun of the type pictured, and adequate adjustability is achievable. Near-unity SWR's can be attained because the mismatch in all parts of the gun is kept small. In the first region this is done by applying potentials corresponding to quasi-divergent flow, and in the subsequent regions, by producing not too steep an exponential transformation. Flexibility results from the division of the gun into several separate regions. The fact that the 2 quantities of importance (noise current SWR and position of the noise current minima) are not adjusted independently by the electrode voltages presents little practical difficulty. Best operation is usually obtained with anode voltages not far from those giving a smooth exponential impedance variation.

This theory has demonstrated the advantages of multi-region guns for low-noise beam-type microwave amplifiers. This superiority is partly due to the advantages of exponential space-charge wave transformation. The advantages of multi-region guns are their ability to operate without sharp potential discontinuities, thereby avoiding lens effects; their flexibility, which permits electrical compensation for imperfections in tube construction; and their mechanical simplicity.

MEASUREMENTS AND PERFORMANCE OF A THREE-REGION GUN

The validity of the qualitative theory and its conclusions presented above on the performance of multi-region low-noise guns has been substantiated by a comprehensive set of noise current measurements performed with a standard type of three-region low-noise gun. The dimensions of this gun are shown in Figure 4. The measurements consist of recordings of noise current versus distance along the beam in a drift space following the third anode of the gun. (The noise current was measured automatically by means of a receiver described

in another paper.⁷ The first- and second-anode potentials V_{a1} and V_{a2} were systematically varied from one recording to the other. The potential of the beam-forming electrode was readjusted for each recording such as to maintain the beam current constant. The beam current, the potential of the drift space following the gun, and the focusing magnetic field were kept constant throughout the entire set of measurements. The third-anode potential V_{a3} also remained unchanged and equal to the drift-space potential.

The quantities of interest in these measurements are

1. The noise current SWR,

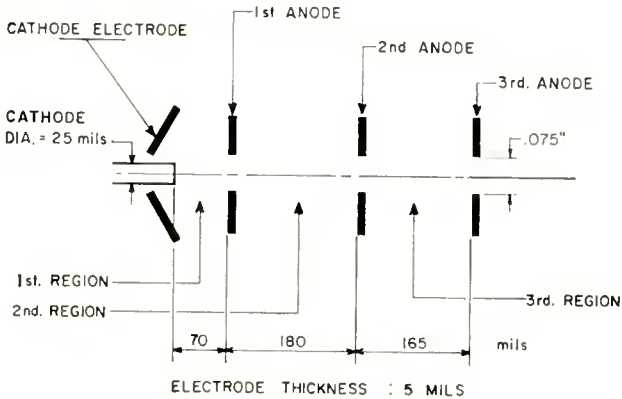


Fig. 4—Three-region low-noise gun.

2. The position of the noise current minima,
3. The noisiness of the beam.

As a consequence of higher-order space-charge wave modes,⁸ the successive minima or maxima of noise current in the drift space following the gun are not all equal. In order to obtain a consistent representation of gun performance, the noise current SWR was measured at the first pair of noise current extrema occurring on this recording as one moved away from the reference plane $z = 0$ (noise-measuring cavity closest to the gun) towards the collector. Two facts make this procedure legitimate:

⁷ W. R. Beam and R. C. Knechtli, "An Automatic Beam Noise Current and Noise Figure Measuring System for Traveling-Wave Tubes," to be published.

⁸ W. R. Beam and S. Bloom, "Minimum Noise Figure of a Traveling-Wave Tube, Including Higher Space Charge Wave Modes," to be published.

1. The noisiness computed by means of these two first extrema was found constant and within about 1 decibel of the first-order theoretical value, for all recordings.

2. From a practical standpoint, interest is in the SWR in the region where the helix input would be located in a normal traveling-wave tube; this is the vicinity of the reference plane $z = 0$, for our case.

The position of the noise current minima for all recordings is referred to the same fixed plane $z = 0$. This plane is located 1.7 inches from the third anode of the gun.

The results of these measurements are shown on the Smith chart of Figure 5. On this diagram, the reference plane $z = 0$ corresponds to the line from the center to the point R . The radial coordinate is a measure of the noise current SWR; the angular coordinate specifies the distance in plasma wavelengths from the reference plane to the first noise current minimum. Dashed lines correspond to constant first-anode potential, solid lines to constant second-anode potential.

These measurements bear out the following facts of significance:

1. By decreasing any of the anode potentials, the noise current minima move towards the cathode.

2. The minimum SWR is obtained with the lowest first-anode potential ($V_{a1} = 50$ volts) and with an approximately linear increase of potential from first to last anode, the d-c cathode current density corresponding in first approximation to near match.

The first fact verifies the theory concerning the effect of the average gun potential on the position of the noise current minima. The second fact verifies the theoretical prediction that low SWR is obtained when one starts with near match at the potential minimum, keeping the first-anode potential at a low value (quasi-divergent flow) to prevent appreciable mismatch within the first region, and proceeding from there to the helix with a smooth, gradual and approximately exponential space-charge wave transformation. As shown above, exponential transformation corresponds to nearly linear d-c potential increase along the beam. Thus, the smoothest transformation (minimum mismatch) should be obtained when the second anode has a potential producing such a linear potential distribution between first and third anodes: the second and third regions of the gun then transform with the same "steepness" (same factor k) resulting in the minimum mismatch. It is remarkable to observe that the second-anode potential, $V_{a2} = 275$ volts, for which minimum SWR is obtained (see Figure 5)

corresponds closely to this condition. It is also remarkable that departure from this condition either by decreasing or increasing the second-anode potential, V_{a2} , increases the noise current SWR, as predicted by the theory. Finally, the low first anode potential, $V_{a1} = 50$ volts, at which (together with $V_{a2} = 275$ volts) the minimum SWR has

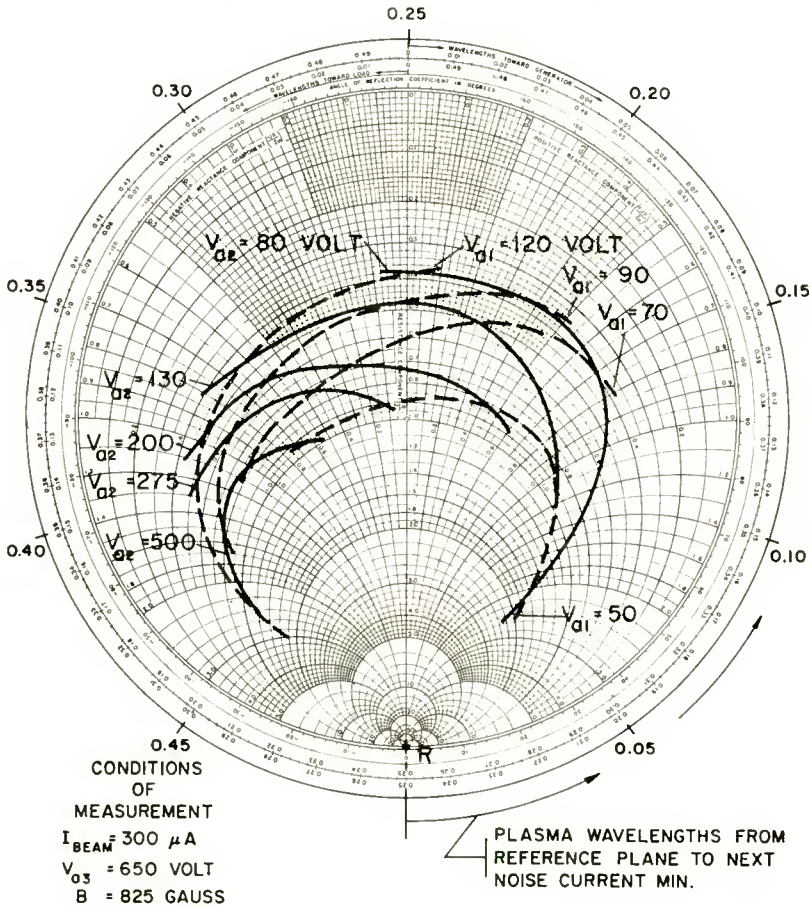


Fig. 5—Measurement of performance of three-region gun.

been obtained actually corresponds to quasi-divergent flow; in fact, $V_{a1} = 50$ volts corresponds to approximately half the first-anode potential required for parallel flow with the electrode spacings and beam current density used in the experiment.

The measurements described have satisfactorily substantiated the

theory of space-charge wave transformation in a multi-region low-noise gun. A further conclusion obtained by inspection of Figure 5 is that the three-region gun used in these measurements is quite flexible in adjustment. This means that noise current SWR and position of the noise current minima can be varied over an adequately wide range by simple changes of electrode potentials.

DESIGN OF MULTI-REGION GUNS

The information obtained thus far can be applied to a design procedure for low-noise guns of the type shown in Figure 2. Assuming that the helix potential and the beam diameter have been determined, the other gun parameters can be selected as follows:

1. *Cathode current density.* Its value is determined approximately by the requirement of near match at the potential minimum. This requirement, together with the condition of quasi-divergent flow, is aimed at keeping the noise current standing wave ratio at the first-anode reasonably small.

Once approximate match at the potential minimum is specified, the order of magnitude of the cathode current density is determined by Equation (1), when solved for the d-c beam current density i_0 .

Practically speaking, the requirements of cathode life and uniformity of emission may compel use of a smaller cathode current density than the value given by this equation. Empirical data show that quite low noise figures have been obtained with cathode current densities corresponding to a normalized impedance r_a as large as 2, while match requires $r_a = 1$.

2. *The number of regions* or anodes is theoretically specified by the requirement that both the SWR and the position of the noise-current minima in the helix-input region should be adjustable by means of the anode potentials. This requires a minimum of two independent anodes, not including the helix. Empirically, it has been found that two, or not more than three independent anodes provide sufficient versatility. More than three regions may be useful for the simultaneous optimization⁸ of more than one space-charge wave mode.

3. *The cathode-first anode spacing* should theoretically be as small as possible. Since the k in this region may be higher than elsewhere, this region should be short. In addition, keeping the first-anode potential low, gives greater latitude for the adjustment of the other anode potentials, and results in more flexibility.

The lower limit to this spacing is set by the field penetration from

the second anode through the first-anode aperture into the cathode region. A spacing equal to the diameter of the first-anode aperture has been found adequate.

4. *The total gun length* is theoretically determined by two contradictory requirements:

- a. It should be long, for flexibility.
- b. It should be short, to minimize the importance of possible growth of noise with distance away from the cathode.*

A compromise for the distance l between first and last (helix) anodes has been found empirically. It corresponds to an average factor k of exponential increase of the characteristic beam impedance approximately equal to unity. The relation between l and k_{avg} is given below. This does not include the length of a possible drift space between the gun and the helix-input.

$$l = \frac{\log \frac{W_2}{W_1}}{k_{\text{avg}} \beta_{\text{avg}}},$$

$$\beta_{\text{avg}} \cong \sqrt{\beta_1 \beta_2}; \quad \beta = \frac{d\phi}{dz} = \frac{2\pi}{\lambda_p},$$

l = distance between first and last anodes,

W_1 = characteristic beam impedance at first-anode potential,

W_2 = characteristic beam impedance at last-anode potential.

Empirical condition: $k_{\text{avg}} \cong 1$.

5. *The anode spacings themselves* are chosen to be approximately equal. This is justified by the fact that the potential distribution between first and last anodes for exponential transformation is approximately linear. Because the plasma wavelength increases with potential and the potential increases with distance from the cathode, more flexibility could possibly be gained by making the first-to-second-

* This effect is not actual noise amplification. It is caused by the contribution of higher-order space-charge wave modes of noise current to the total noise figure of the traveling-wave tube. The precise conditions of optimization of higher-order modes have been derived by Beam and Bloom.⁸ Practically, simultaneous optimization of the two first modes is probably obtained for an optimum gun length such that the total phase angle from potential minimum to helix input differs by approximately π radians between the first- and second-order modes.

anode spacing shorter than the second-to-third-anode spacing. It has been found empirically that a first-to-second-anode spacing between 80 and 100 per cent of the second-to-third-anode spacing gives satisfactory performance.

6. *The diameter of the anode apertures* is a compromise between two theoretical requirements:

- a. They should be large, to minimize electrostatic lens effects⁶ and mechanical imperfections.
- b. They should be small enough to prevent excessive field penetration from one region to the other, which would reduce the adjustability of the gun.

Empirically, aperture diameters equalling two to three times the cathode diameter have been found adequate.

7. *The first-anode potential* should, for initially divergent flow, be smaller than the value corresponding to perfect parallel flow. Empirical values 20 to 50 per cent below the parallel-flow value have been found suitable.

8. *The potentials of the other anodes* cannot be predicted easily or accurately. A linear increase of potential with distance will minimize the undesirable electrostatic lens effects.⁶ Practically, the potentials are adjusted to produce minimum noise figure in the tube. This adjustment, as well as the choice of the helix position, is an experimental, but straightforward, process.

CONCLUSIONS

1. The operation of multi-region guns has been explained, based on an exponential transformation of space-charge waves. This explanation has been substantiated by experiments employing a three-region gun.

2. It has been shown that multi-region guns offer several advantages, namely, their ability to operate without sharp potential discontinuities, their flexibility, and their mechanical simplicity.

3. A design procedure for low-noise multi-region guns has been established. This design procedure is based on the present understanding of the operation of these guns, and on the results of noise measurements. Empirical data obtained from various experimental low noise tubes has been used where it was required to define the design parameters more precisely.

IMAGE ORTHICON FOR PICKUP AT LOW LIGHT LEVELS

BY

A. A. ROTOW

RCA Tube Division,
Lancaster, Pa.

Summary—The performance of standard image orthicons at low light levels is limited by noise and time lag. It is shown that signal-to-noise ratio is a direct function, and time lag an inverse function, of the beam modulation, i.e., the ratio of signal current to beam current. It is also shown that the beam modulation may be increased by an increase in the spacing between the glass target and mesh screen.

An image orthicon incorporating relatively large target-to-mesh spacing has been designed. In this tube, which is usable at light levels as low as 10^{-4} foot-lambert, noise and time lag have been substantially reduced by the use of a target-to-mesh-screen spacing of 0.150 inch.

INTRODUCTION

EXPERIMENTS conducted by several investigators during the last few years have shown that television pickup systems are inherently capable of higher sensitivity than even the best dark-adapted human eye. It has been shown by Strum and Morgan¹ that at the light levels encountered in roentgenoscopy (10^{-4} to 10^{-2} foot-lambert) the resolving capability of the eye becomes a small fraction of that at normal light levels (10 to 100 foot-lamberts). A standard 5820 image orthicon used with lens systems of $f = 0.85$ to $f = 1.3$ was able to reproduce scenes having brightness ranging from 10^{-2} to 10^{-3} foot-lambert with more information than could be derived from the same scenes by a dark-adapted eye.

It is highly desirable that the usefulness of television pickup systems be extended to light levels as low as 10^{-4} foot-lambert. At these low light levels, however, noise and time lag become very objectionable. Camera tubes other than the image orthicon have fixed noise levels which do not decrease when the tubes are operated at low light levels. The noise of a properly operated image orthicon, on the other hand, decreases with the square root of the highlight level. Consequently, of all known television pickup tubes, only the image orthicon

¹ Ralph E. Strum and Russel H. Morgan, "Screen Intensification Systems and Their Limitations," *American Journal of Roentgenology and Radium Therapy*, Vol. LXII, No. 5, November, 1949.

inherently possesses sufficient over-all sensitivity for use at very low light levels.

The signal-to-noise ratio, S/N , of an image orthicon is given by the expression

$$\frac{S}{N} = K \sqrt{i_s M},$$

where K is a constant, i_s is the signal current at the target, and M is the "beam modulation," which will be defined later. The noise, N , is given by

$$N = K_1 \sqrt{\frac{i_s}{M}},$$

where K_1 is a constant.

If M were constant, the noise would decrease with the square root of the signal current. However, M decreases with the signal current, and at low light levels becomes very small. The resulting curves of noise and signal as a function of illumination are shown on an arbitrary scale on Figure 1.

The new tube was designed to provide the highest possible M at low light levels to improve the signal-to-noise ratio and decrease the time lag. It was found that M could be increased by an increase in the target-to-mesh spacing. Although the new tube is extremely useful for applications involving very low light levels, it is not well suited for use at the light levels normally encountered in television broadcast service.

DESCRIPTION OF THE NEW IMAGE ORTHICON

The new tube differs from the standard image orthicon only in the use of a greater spacing between the glass target and the target mesh screen. Its method of operation, which is identical with that of a standard tube,² will be briefly summarized with emphasis on the charge-discharge cycle of the target because an understanding of this cycle is essential for understanding of low-light-level operation.

All image orthicons, regardless of their target spacing or other characteristics, employ photosensitive surfaces of the photoemissive type, targets which operate as storage elements, and low-velocity scan-

² A. Rose, P. K. Weimer, and H. B. Law, "The Image Orthicon — A Sensitive Television Pickup Tube," *Proc. I.R.E.*, Vol. 34, p. 424, July, 1946.

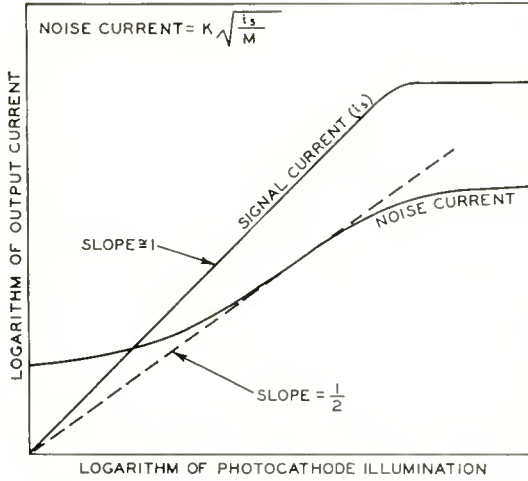


Fig. 1—Noise characteristics of image orthicon.

ning beams. These terms will be clarified by reference to Figure 2, which is a schematic drawing of the image orthicon from which all parts not pertinent to the present discussion have been omitted.

A real image of the object (*O*) to be televised is projected by means of the lens (*L*) upon the semitransparent photocathode (*PC*) formed on the inner surface of the glass faceplate (*F*). Illuminated areas of the photocathode emit electrons (hereafter referred to as “photoelectrons”). The number of photoelectrons emitted at any point of the photocathode is proportional to the intensity of the illumination at that point.

These photoelectrons are electrostatically accelerated and electromagnetically focused on the target-mesh assembly. This assembly consists of a very thin glass target (*a*) and a metal mesh screen (*b*) which is located between the target and the photocathode at a distance δ from the target. The photocathode is maintained at a negative potential of about 400 to 500 volts, and the mesh screen (*b*) at a positive potential of about 0 to 2 volts, with respect to the grounded thermionic cathode (*C*) of the gun. Consequently, the photoelectrons (current i_1) strike the glass target with an energy of 400 to 500

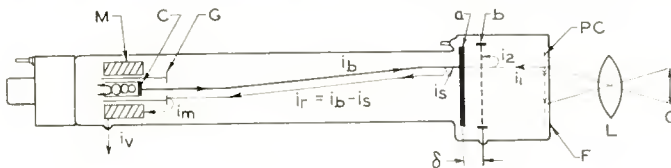


Fig. 2—Schematic diagram of image orthicon.

electron-volts, displacing secondaries from the glass (current i_2) in the ratio of 4 to 5 secondary electrons for each photoelectron. These secondary electrons are collected by the mesh screen (b). The glass target (a) is scanned on the gun side (opposite the photocathode) by the scanning beam (current i_b). Because the target assembly is only slightly positive with respect to the gun cathode, the scanning-beam electrons land on the glass target with a very low axial component of velocity. During the short time that the scanning beam dwells on an elemental area of the glass target, it drives the area to a potential determined by the axial velocity distribution of the beam electrons. Because the number of photoelectrons which land on the target element during this very short time is negligible, this potential is called the "dark potential" (V_d). It has a value of approximately -0.25 volt. The mesh (b) is held at a positive potential of 2 volts (plus the algebraic sum of all the contact potentials encountered between the gun cathode and the mesh screen) with respect to the dark potential. Consequently, the glass target and the mesh form a parallel-plate capacitor which is charged by the beam to a potential of approximately two volts, the glass target being the negative electrode. Photoelectrons striking the target during a frame time change the potential of this capacitor by an amount V_s (called the "potential swing"). The scanning beam (i_b), therefore, deposits on the target a signal current, i_s , given by

$$i_s = i_2 - i_1. \quad (1)$$

The beam returning to the gun, i_r , is given by

$$i_r = i_b - i_s. \quad (2)$$

This return beam is intensity- (amplitude-) modulated by the signal current, i_s . The return beam strikes the grid (G) and displaces secondaries from its surface. The current i_m represented by these secondaries is directed into the ring-shaped electrostatic multiplier (M), where it is amplified 300 to 1,000 times. The amplified current, i_r , represents the video output signal of the tube and is applied to the video pre-amplifier.

Signal-to-Noise Ratio as a Function of Beam Modulation

It is apparent from the preceding discussion that the video signal is carried by the beam returning from the target. Because the useful video signal, i_s , at the target is subtracted from the scanning beam, i_b , the video output signal, i_r , is negative (i.e., maximum signal

represents black and minimum signal white). The shot noise carried by the return beam into the multiplier, however, increases with the return beam current. Consequently, the signal-to-noise ratio of the image orthicon increases with the ratio $M = i_s/i_b =$ signal current developed at the target/scanning-beam current.

The ratio M is called the "beam modulation" of the image orthicon. The signal-to-noise ratio can be described in terms of M as follows:

$$\frac{S}{N} = \sqrt{\frac{i_s M}{eB}}, \quad (3)$$

where e is the charge of the electron and B is the bandwidth of the video amplifier.

At low light levels, the maximum value of the signal current, i_s , is fixed by the amount of light available. The signal-to-noise ratio at these light levels can, therefore, be improved only by an increase in the beam modulation, M .

Time Lag As a Function of Beam Modulation

It can be shown that the beam modulation, M , is a function of the potential swing, V_s , of the target during its charge-discharge cycle. The function $M = f(V_s)$ has the general appearance shown in Figure 3. For small values of V_s , such as those developed at low light levels, this curve is strongly concave towards the positive direction of the M -axis.

The potential swing, V_s , is proportional to the illumination, and the charge stored on the target in one frame time decreases linearly with V_s . Because of the curvature of the characteristic $M = f(V)$, however, the modulation, M , decreases much faster than the value of the stored charge. Consequently, at very low light levels the scanning beam cannot discharge the picture in one frame time. Unless special measures (such as those described in this paper) are taken, several frame times may be required for complete discharge of the picture, and an image of a televised object will persist for some time after the object has been removed. This effect, which may become very objectionable at low light levels, is called "time lag."

DESIGN OF IMAGE ORTHICON FOR OPERATION AT LOW LIGHT LEVELS

The beam modulation, M , increases with the potential swing, V_s , to which the target is charged by the photoelectrons during its charge-

discharge cycle in each frame time. This relationship is given by the following equations:

For $V_s \leq V_d$ (V_d = dark potential)

$$M = \epsilon^{-11.05V_d} \left[\frac{11.05V_s - (1 - \epsilon^{-11.05V_s})}{1 - \epsilon^{-11.05V_s}} \right]$$

($\epsilon = 2.718 \dots$)

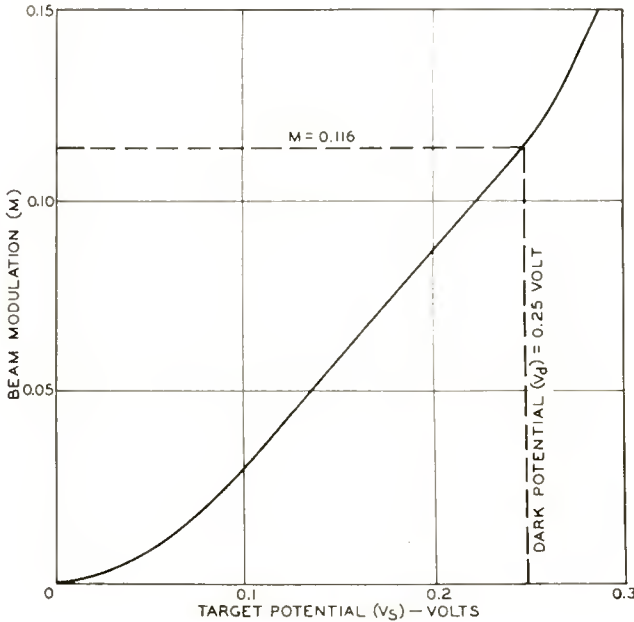


Fig. 3—Beam modulation characteristic.

For $V_s > V_d$

$$M = \frac{V_s}{V_s + A}$$

where A is a constant given by

$$A = V_d \left[\epsilon^{11.05V_d} \left(\frac{1 - \epsilon^{-11.05V_d}}{11.05V_d - 1 + \epsilon^{-11.05V_d}} \right) - 1 \right]$$

The value of the function $M = f(V_s)$ is shown in Figure 3 for $V_d = -0.25$ volt.

It is seen that M increases when V_s increases. These equations have been derived for an "ideal" beam having a rectangular cross

section and uniform current-density distribution. In practical tubes, the beam has a circular cross section and its current density decreases from its axis outward. As a result, the absolute magnitude of M for a given V_s is smaller in practical tubes than in the ideal case, but the general form of the curve $M=f(V_s)$ is similar to that shown in Figure 3. To increase M it is necessary to increase V_s . It is shown below that V_s can be increased by an increase in the spacing between the glass target and the mesh. The new tube was, therefore, designed to have a very large target-to-mesh-screen spacing.

EFFECT OF TARGET CAPACITANCE

It has been shown that signal-to-noise ratio and time lag can be improved by increasing the potential swing, V_s , of the target during its charge-discharge cycle.

For a given target capacitance, C , the potential swing is

$$V_s = \frac{Q}{C}. \quad (4)$$

For a given illumination and photocathode sensitivity, the electric charge, Q , stored by the target during one frame time is perfectly defined and cannot be changed. Consequently, if V_s is to be as large as possible for a given Q (corresponding to a given light level of the scene), the target capacitance, C , must be decreased.

If we consider the target-mesh assembly as a parallel-plate capacitor having as plates the glass target (a) and mesh (b) spaced at a distance δ (Figure 2), then C can apparently be decreased and V_s increased by increasing δ .

However, Rose, Weimer, and Law² have shown that this assumption is not correct insofar as the target capacitance available for maximum charge storage is concerned. They show that the maximum stored charge will decrease as δ increases only until δ becomes about 1 mil. For values of δ greater than 1 mil the maximum stored charge remains constant at a value corresponding to the total "free-space" capacitance of all picture elements of the glass target. This capacitance evidently is not a function of δ .

Operation of the tube can be explained as follows: (a) The maximum charge which can be stored on a picture element of the glass target depends on the capacitance between this element and the rest of the universe. Here, the "universe" is the rest of the tube, and this "free-element capacitance" does not depend on the target-to-mesh spacing unless the mesh screen is very close to the glass (1 mil or

less) (b). Because the potential swing of the target, V_s , is measured with respect to the mesh, its value depends on the integral over the total mesh area of the flux of the electric field vector of the target picture element divided by the capacitance between this element and the mesh screen. V_s will, therefore, depend on the target-to-mesh-screen spacing and will be greater when this spacing is greater.

The simple parallel-plate capacitance relations will be valid, however, only if a large area of the photocathode is uniformly illuminated. If a pattern of alternate dark and light areas is projected on the photocathode, the relation becomes much more complicated. In such a case, the effective capacitance, C , will be increased by the capacitance between the individual elements of the glass target. This inter-element capacitance is responsible for the "white-edge" effects in the 5820 image orthicon at transitions from black to white areas. These effects are illustrated in Figure 4. In this figure, c_1 , c_2 , and c_3 represent the capacitances between elements of the glass target and the corresponding elements of the mesh screen, and C_1 , C_2 , and C_3 the capacitances between adjacent elements of the glass target.

If the entire target is uniformly charged, then C_1 , C_2 , and C_3 are not charged and c_1 and c_2 are charged in parallel and constitute a single large parallel-plate capacitor. If, however, zone I (to the left of the line A-B) is uniformly dark (uncharged) and zone II (to the right of A-B) is uniformly illuminated (charged), then points a and b on the mesh will have equal charges corresponding to the equal capacitances c_4 and c_5 . Point o, adjoining the transition from black to white, however, will carry a charge corresponding to the capacitance c_3 plus the capacitances c_2 and C_2 in series with each other and in parallel with c_3 . Consequently, the total charge stored at point o will correspond to a capacitance

$$c = c_3 + \frac{c_2}{1 + c_2/C_2}. \quad (5)$$

For close-spaced tubes such as the 6474/1854, $c_2 = c_3 > C_2$, and the fractional corrective term in Equation (6) becomes insignificant. For a 5820 tube in which $c_2 = c_3 < C_2$, the corrective term makes $c > c_3$, and, if sufficient light is available so that operation is over the "knee" of the tube characteristic, a white edge appears at the transition from black to white. If the target-mesh spacing is increased so that $c_2 \ll C_2$, then $c_2/C_2 \ll 1$ and

$$c = c_3 + c_2. \quad (6)$$

Consequently, the value for the capacitance C which must be used

in Equation (4) can have a maximum value equal to twice the parallel-plate capacitance of the target assembly when a sufficiently fine raster of alternate black and white bars is projected on the photocathode. Therefore the potential swing V_s in Equation (4) will be increased by increasing the target-to-mesh spacing.

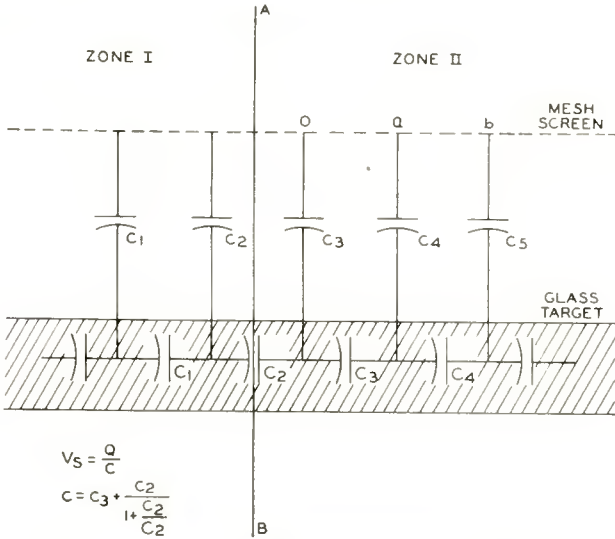


Fig. 4—Target capacitance equivalent circuit.

CHARACTERISTICS AND APPLICATIONS OF THE NEW
IMAGE ORTHICON

The photocathode used in the new tube is exactly the same as that used in the standard image orthicons, types 5820 and 6474/1854, and so its spectral response is the same as that of the standard tubes. Its "transfer characteristic," however, differs substantially from that of standard tubes, and is shown together with that of the type 5820 in Figure 5. This figure shows the output (signal) current of the tube as a function of photocathode illumination.^{3,4} The curves shown were derived from measurements made on large numbers of tubes of both types and represent average performance. The characteristic of the 5820 image orthicon starts at an illumination level of approximately 0.0001 foot-candle, which is, on the average, the lowest value at which

³ Otto H. Schade, "Electro-Optical Characteristics of Television Systems," *RCA Review*, Vol. IX, 1948.

⁴ R. B. Janes and A. A. Rotow, "Light-Transfer Characteristics of Image Orthicons," *RCA Review*, Vol. X, p. 364, September, 1950.

signal-to-noise ratio and time lag are small enough to provide a picture containing useful information. The characteristic of the 5820 then rises linearly with a gamma very close to unity until a photocathode illumination in the vicinity of 0.01 foot-candle is reached. At this illumination level, the number of photoelectrons emitted is sufficient to charge the target-to-mesh capacitance to the full target potential of 2 volts. Consequently, in this region of the characteristic (the "knee"), a further increase in illumination does not result in an appreciable increase in signal output current. However, as the illumination is further increased the inter-element capacitance of the glass target

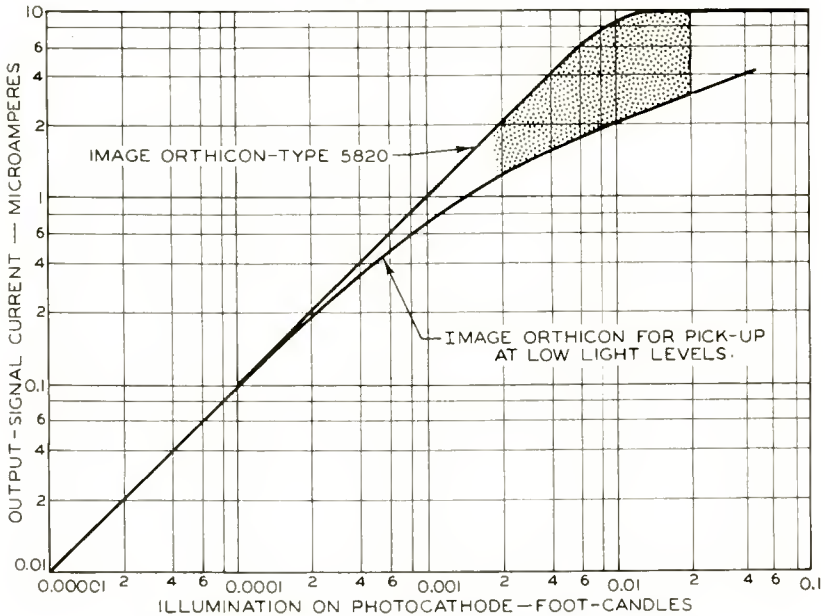


Fig. 5—Transfer characteristic of image orthicon.

becomes noticeable, as explained above, and the characteristic rises again and reaches a second "knee" (not shown in Figure 5). The target-to-mesh-screen spacing in the new tube is substantially greater than in the 5820; therefore, the knee in its characteristic is located at lower light levels and is much less pronounced than in the 5820. The transfer characteristic for the new tube starts at a light level approximately one tenth of the minimum for the 5820.

For very low light levels ($B = 0.00001$ to 0.00015 foot-candle on the photocathode), both tubes would have substantially the same signal output. The new tube, however, due to its higher beam modulation,

has a better signal-to-noise ratio and less time lag than type 5820 at such low light levels. This feature extends the useful low-light-level range of the new tube. At the relatively high light levels currently used in television broadcasting (the shaded area in Figure 5), the new tube, because of its small target-to-mesh capacitance, cannot utilize the whole amount of light available, and its signal output is much lower than that of the 5820. Consequently, the new tube is not recommended for use at the light levels normally encountered in television broadcast. It is the only tube known, however, which is capable of transmitting useful information at photocathode illumination levels of less than 0.0001 foot-candle. The source of the illumination or type of scene to be picked up is immaterial; the scene may be anything from the image of a star projected by a telescope to a scene illuminated by moonlight or starlight.

ACKNOWLEDGMENTS

The author wishes to thank E. E. Spitzer, F. S. Veith, R. G. Neuhauser, B. H. Vine, and T. N. Chin of the RCA Tube Division for their aid and encouragement in the preparation of this paper. Special thanks are also due to R. G. Neuhauser and B. H. Vine for proof-reading the manuscript.

RCA TECHNICAL PAPERS†

Second Quarter, 1956

Any request for copies of papers listed herein should be addressed to the publication to which credited.

"Colorimetry, Film Requirements and Masking Techniques for Color Television," H. N. Kozanowski and S. L. Bendell, <i>Jour. S.M.P.T.E.</i> (April)	1956
"Color-TV Receiver Servicing," R. C. Janzow, <i>Service</i> (June)	1956
"Compression and Dialog Equalization in Motion Picture Sound Recording," E. P. Ancona, Jr., <i>Audio</i> (June)	1956
"Contact Arcing Factors to 100,000 Feet," M. R. Alexy, <i>Electrical Manufacturing</i> (June)	1956
"Correction Circuits for Color TV Transmitters," K. E. Mullenger and R. H. McMann, Jr., <i>Electronics</i> (April)	1956
"Effect of Magnetic Deflection on Electron Beam Convergence," P. E. Kaus, <i>RCA Review</i> (June)	1956
"Electroluminescence from Boron Nitride," S. Larach and R. E. Shrader, <i>Phys. Rev.</i> (April 15) (Letter to the Editor)	1956
"Electrolytic Transport Phenomena in the Oxide Cathode," R. H. Plumlee, <i>RCA Review</i> (June)	1956
"The Electron Donor Centers in the Oxide Cathode," R. H. Plumlee, <i>RCA Review</i> (June)	1956
"Equivalent R-Z Chart," H. E. Goldstine, <i>Electronics</i> (Reference Sheet) (June)	1956
"Galvanomagnetic Effects in a Semiconductor with Two Sets of Spheroidal Energy Surfaces," M. Glicksman, <i>Phys. Rev.</i> (June 15)	1956
"Graphic Arts Techniques in the Deposition of Phosphor Screens for Color Television Tubes," H. Rosenthal, <i>Proceedings of the Eighth Annual Meeting of the Technical Association of the Graphic Arts</i> (May)	1956
"How to Convert Color TV Receivers for Video Drive," E. R. Klingeman, <i>Broadcast News</i> (June)	1956
"Incidence of an Electromagnetic Wave on a 'Cerenkov Electron Gas'," M. A. Lampert, <i>Phys. Rev.</i> (April 15)	1956
"Increasing the Sensitivity of a Commercial Spectroradiometer," A. E. Hardy and G. P. Kirkpatrick, <i>Rev. Sci. Instr.</i> (Notes) (June)	1956
"Intensity Markers Aid Television Alignment," L. W. Dixon, <i>Electronics</i> (Production Techniques) (April)	1956
"Kinescope Electron Guns for Producing Noncircular Spots," R. C. Knechtli and W. R. Beam, <i>RCA Review</i> (June)	1956
"Ligand Field Theory and the Stability of Transition Metal Compounds," D. S. McClure and co-authors, <i>Jour. Chem. Phys.</i> (June) (Letter to the Editor)	1956

† Report all corrections or additions to RCA Review, RCA Laboratories, Princeton, N. J.

“Luminescence Properties of Zinc-Inter-Chalcogenides. I. Zinc Sulfo-Telluride Phosphors,” S. Larach, W. H. McCarroll, and R. E. Shrader, <i>Journal of Physical Chemistry</i> (May)	1956
“Mobile Unit for Color TV Broadcasting,” H. H. Klerx, <i>Tele-Tech & Electronic Industries</i> (June)	1956
“A Mobile Unit for Color Television Broadcasting and Closed-Circuit Applications,” H. H. Klerx, <i>Broadcast News</i> (April)	1956
“Modern Turntable Design Considerations,” E. J. Meehan, <i>Broadcast News</i> (June)	1956
“New Lightweight Weather-Mapping Radar,” G. Daggy, <i>Broadcast News</i> (June)	1956
“New RCA Automatic Turntable,” R. H. Barnaby, <i>Broadcast News</i> (June)	1956
“Pedestal Processing Amplifier for Television Studio Operation,” R. C. Kennedy, <i>RCA Review</i> (June)	1956
“Principal Electron Donors in the Oxide Cathode,” R. H. Plumlee, <i>Jour. Appl. Phys.</i> (Letter to the Editor) (June)	1956
“Recent Improvements in the 21AXP22 Color Kinescope,” R. B. Janes, L. B. Headrick, and J. Evans, <i>RCA Review</i> (June)	1956
“Servicing Printed-Wiring TV Chassis,” A. Lytel, <i>Service</i> (April) ..	1956
“Spectral Distribution of Photoconductivity,” H. B. DeVore, <i>Phys. Rev.</i> (April 1)	1956
“Toroidal Transformers Pass Video Bandwidths,” G. W. Gray, <i>Electronics</i> (May)	1956
“Transistor Circuits for Digital Computers,” D. E. Deutch, <i>Electronics</i> (May)	1956
“Transistorized Intercom,” A. L. Cleland, <i>Rad. and Tele. News</i> (April)	1956

AUTHORS

WALTER R. BEAM—(See *RCA Review*, Vol. XVII, No. 1, March 1956, p. 135.)



MAURICE ARTZT received the B.S. degree in Electrical Engineering from the University of Texas in 1925 and the M.S. degree in Electrical Engineering from Union College in Schenectady in 1929. From 1925 until 1930 he was in the Radio Test Department and the Radio Engineering Department of the General Electric Company in Schenectady. He was a member of the engineering staff of the RCA Manufacturing Company in Camden, New Jersey from 1930 until 1942, where he was engaged chiefly on the design and development of facsimile equipment. In 1942 he transferred to the RCA Laboratories at Princeton, New Jersey where he has continued to work on facsimile and allied devices. Mr. Artzt is a member of Tau Beta Pi and of Sigma Xi.

HAROLD E. HAYNES received the B.S. degree in Electrical Engineering from the University of Nebraska in 1939. During 1940, he was an instructor in Electrical Engineering at the South Dakota State School of Mines. Since 1940 he has been engaged in development work at RCA, starting in Camden, N. J., transferring to Indianapolis, Ind., in 1941, and returning to Camden in 1946. He is at present a member of the Commercial Electronic Products Advanced Development section. He has been engaged in work on electronic scanning systems, bandwidth saving techniques for picture transmission, infrared devices and systems, facsimile, and audio circuits. Mr. Haynes is a Senior Member of the Institute of Radio Engineers, and a member of the Optical Society of America and of Sigma Xi.



WILLIAM D. HOUGHTON graduated from the RCA Institutes in 1939. He joined the Research and Advanced Development group of RCA Communications, Inc. in 1940 and was transferred to the RCA Laboratories in 1942. From 1942 to 1950 he specialized in time-division multiplex research at the Rocky Point, N. Y. laboratory of RCA. In 1950 Mr. Houghton was transferred to the David Sarnoff Research Center in Princeton, N. J. where he has been actively engaged in the color television development program and on systems for video recording on magnetic tape. Mr. Houghton is a Member of Sigma Xi and The Institute of Radio Engineers.

RONALD C. KNECHTLI—(See *RCA Review*, Vol. XVII, No. 2, June 1956, p. 309.)



ROBERT F. KOLAR received the B.S. degree in Electrical Engineering in 1949 at Purdue University and the M.S. degree at the University of Pennsylvania in 1956. He joined the Advanced Development Section of the RCA Victor Television Division in 1949 and since that time has been working primarily on television receiving antenna development and other radiation problems. Mr. Kolar is a member of Eta Kappa Nu, Tau Beta Pi, and the Institute of Radio Engineers.

ADOLPH R. MORGAN received the B.S. degree in Electrical Engineering from the University of California in 1931. In the same year he joined the RCA Manufacturing Company in their Student Training Activities and in 1933 became a research engineer. In 1942 he transferred to RCA Laboratories Division in Princeton, N. J., where he has been engaged in recording and acoustic research problems. Mr. Morgan is a Member of the Acoustical Society of America, Tau Beta Pi, Eta Kappa Nu, Sigma Xi, and Phi Beta Kappa.



HARRY F. OLSON received the B.S. degree in 1924, the M.S. degree in 1925, the Ph.D. degree in 1928 and the E.E. degree in 1932 from the University of Iowa. From 1928 to 1930 he was in the Research Department of Radio Corporation of America; from 1930 to 1932, in the Engineering Department of RCA Photophone; from 1932 to 1941, in the Research Division of RCA Manufacturing Company; since 1941, with the RCA Laboratories. Dr. Olson is a member of Tau Beta Pi and Sigma Xi. He is a Fellow of the Society of Motion Picture and Television Engineers, the American Physical Society, the Institute of Radio Engineers, the Acoustical Society of America and the Audio Engineering Society. He is a past president of the Acoustical Society of America.

ALEXANDER A. ROTOW received the B.S. degree in Electrical Engineering and in Physics from the University of Belgrade, Yugoslavia, and the M.S. degree in Physics from Franklin and Marshall College, Lancaster, Pennsylvania. He was employed by the Ikarus airplane factory in Yugoslavia as Manager of the Physical Laboratories. During World War II he was a reserve lieutenant in the Yugoslav Royal Air Force and later a civilian engineer with the United States Army. In 1948 he came to the United States and has since been employed by the Radio Corporation of America, working on camera-tube development. Mr. Rotow is a Senior Member of the Institute of Radio Engineers and a member of the American Association for the Advancement of Science and of Sigma Pi Sigma.





LOUIS SHAPIRO received the B.S. degree in Physics-Music from the City College of New York, and the M.S. degree in Physics-Mathematics from Washington University in St. Louis, and has done graduate work at New York University and the University of Pennsylvania. After serving as a civilian instructor in communications and radio navigation for the Air Force, he joined the Naval research cosmic ray team at Washington University. He then joined the faculty of the University of Missouri, and in 1948 he joined the Polytechnic Research and Development Company. Since 1952 he has been with the

Radio Corporation of America in Camden, N. J. where he has been engaged in work on the color correction system. Mr. Shapiro is a member of Phi Beta Kappa and the Institute of Radio Engineers.

J. G. WOODWARD received the B.A. degree from North Central College in 1936, the M.S. degree in Physics from Michigan State College in 1938, and the Ph.D. degree in Physics from the Ohio State University in 1941. He held Graduate Assistantships at Michigan State College from 1936 to 1939 and at the Ohio State University from 1939 to March 1941. In March 1941 he joined the Research Division of the RCA Manufacturing Company at Camden, N. J., and later that year transferred to the RCA Laboratories Division at Princeton, N. J. where he has been engaged in research in acoustics. Dr. Woodward is a member of the Acoustical Society of America and Sigma Xi, and is a Fellow of the American Association for the Advancement of Science.



JOSEPH A. ZENEL received the B.S. degree in Electrical Engineering from Bucknell University in 1949, and the M.S. degree from Princeton University in 1956. Upon graduation, he joined RCA Laboratories in Princeton, N. J. where he is now engaged in work on magnetic recording. He served with the U. S. Army from 1942 to 1945. Mr. Zenel is a member of Tau Beta Pi, Pi Mu Epsilon, American Institute of Electrical Engineers, the Acoustical Society of America, and Sigma Xi.

